Technical quality control in the Norwegian Breast Cancer Screening Program with focus on radiation doses

Ingrid Helen Ryste Hauge

Department of Physics

Faculty of Mathematics and Natural Sciences

University of Oslo

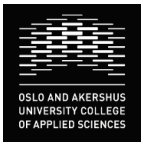

Series of dissertations submitted to the
Faculty of Mathematics and Natural Sciences, University of Oslo
No. 1461

ISSN 1501-7710

Cover: Inger Sandved Anfinsen.
Printed in Norway: AIT Oslo AS.

Produced in co-operation with Akademika Publishing.
The thesis is produced by Akademika Publishing merely in connection with the thesis defence. Kindly direct all inquiries regarding the thesis to the copyright holder or the unit which grants the doctorate.

Table of contents

Acknowledgement

The work presented in this thesis was conducted at the Department of Radiography and Dental Technology, Faculty of Health Sciences, Oslo and Akershus University College of Applied Sciences (HiOA). I would like to thank former Assistant Dean/Head of Studies Agnes Vinorum for granting me the 4-year doctoral scholarship at the Department of Radiography and Dental Technology in 2009, and for encouraging me to study at the University of Salford for two months. Also, I would like to thank the present constituted Assistant Dean, Trude Myhrer, for showing an interest in my work, and for your faith in me.

My sincere gratitude goes to Dr. Hilde Olerud, Head of Section at the Norwegian Radiation Protection Authority (NRPA) and Associate Professor at the Department of Physics, University of Oslo (UiO), for taking on the role as my supervisor, and for granting me a 4-year leave of absence from 2009 to 2013 from my position at the NRPA in order to work on this PhD. Thank you very much for giving me this opportunity to grow and develop my knowledge in the field of mammography, and for your valuable feedback on Paper I, Papers III-V, and the thesis as a whole.

Further, I would like to thank my co-supervisors Professor Solveig Hofvind, at HiOA and the Cancer Registry of Norway, and Dr. Audun Sanderud, at HiOA, for giving me this opportunity. I have cherished this time at HiOA, and I am sincerely grateful for this opportunity. Professor Solveig Hofvind has in addition given a lot of input in writing Paper I and Paper V in this thesis, and I would like to thank you for all of the time you have put into working with these two papers, for your enthusiasm, and belief in me.

Many thanks also go to my co-supervisor Professor Eli Olaug Hole, at the Department of Physics, UiO. Thank you for taking on the role as university-associated co-supervisor for my PhD, and thank you for your support and valuable introduction to the field of radiation

dose and risk of radiation-induced cancers. Your input helped me tremendously in writing Paper V.

In the fall of 2010 I got the opportunity to go to the University of Salford in Greater Manchester and do a study in collaboration with Professor Peter Hogg, Head of the Directorate of Radiography, University of Salford. This collaboration resulted in Paper II in this thesis. I would like to offer my sincere thanks to Professor Peter Hogg for his great enthusiasm, kindness, dedication, great ideas, determination, and belief in the project. I am also forever grateful to Professor Peter Hogg and his wife Dianne Hogg for inviting me to their house on several occasions and making my stay in Salford, Greater Manchester, so enjoyable.

I would like to thank my colleagues at the Department of Radiography and Dental Technology for their warm welcome, and especially I would like to thank Vanja Hårsaker for your help with my lectures in the basic physics courses that are a part of my mandatory work as a PhD student. Also, I would like to thank Randi Føleide for your kindness and for being so helpful.

To all other co-authors: Your important contributions are highly appreciated. Also, I would like to thank all of the radiographers who were involved in collecting data for the papers included in this thesis. Your contribution is greatly appreciated.

I would like to thank my present colleagues at the NRPA for being such great colleagues: Kristin Pedersen, Tore Istad and Silje Flatabø. Also, I would like to thank my colleague, Kirsti Bredholt, for the collaboration that resulted in Paper IV and for your friendship.

When I started this PhD, radiographer Metta Hauge collected a lot of data for me together with other radiographers working at that time in Sandvika. The data ended up not being used, but I would like to extend my great appreciation for all of your help and interest in my work.

I have to thank all of my friends, and especially, Synne Margrethe Egset, for your friendship and positive spirit. Also, I want to thank Robin Lee Hammond, who works as a radiographer in the Norwegian Breast Cancer Screening Program (NBCSP), for your friendship and faith in me.

Last, I would like to thank my parents, my sister and my brother for believing in me.

Abbreviations

AEC	Automatic exposure control
Ag	Silver (Z=47)
Al	Aluminium (Z=13)
ASR	Age-standardized, or age-adjusted, (world) incidence rate
BEIR	Biologic Effects of Ionizing Radiation
CC	Craniocaudal
CI	Confidence interval
CNR	Contrast-to-noise ratio
DDREF	Dose and dose-rate effectiveness factor
DNA	Deoxyribonucleic acid
DRL	Diagnostic reference level
DQE	Detective quantum efficiency
EAR	Excess absolute risk
ERR	Excess relative risk
FFDM	Full-field digital mammography
FOM	Figure-of-merit
GE	General Electric (GE Medical Systems, Buc, France)
Gy	Gray
ICRP	International Commission on Radiological Protection

ICRU	International Commission on Radiation Units & Measurements
HVL	Half value layer
Kerma	Kinetic energy released per unit mass
keV	Kiloelectron-volt
kV	Kilovolt
kV_p	Kilovolt peak
LNT	Linear no-threshold model
LSS	Life Span Study
MGD	Mean glandular dose
MLO	Mediolateral oblique
Mo	Molybdenum (Z=42)
NBCSP	Norwegian Breast Cancer Screening Program
NRPA	Norwegian Radiation Protection Authority
OD	Optical density
PMMA	Polymethyl methacrylate
RERF	Radiation Effects Research Foundation
Rh	Rhodium (Z=45)
SFM	Screen film mammography
Sv	Sievert
UNSCEAR	United Nations Scientific Committee on the Effects of Atomic Radiation
W	Tungsten or wolfram (Z=74)

List of publications

Paper I

Patient doses from screen-film and full-field digital mammography in a population based screening programme

Hauge IH, Pedersen K, Sanderud A, Hofvind S, Olerud HM. *Radiation Protection Dosimetry,* January 2012, Vol. 148, No. 1, pp. 65–73. Published online before print 17 February 2011.

Paper II

The readout thickness versus the measured thickness for a range of screen film mammography (SFM) and full-field digital mammography (FFDM) units

Hauge IH, Hogg P, Szczepura K, Connolly P, McGill G, Mercer C. *Medical Physics*, January 2012, Vol. 39, No. 1, pp. 263-271.

Paper III

Uncertainties involved in the estimation of mean glandular dose for women in the Norwegian Breast Cancer Screening Program (NBCSP)

Hauge IH, Olerud HM. *Radiation Protection Dosimetry,* June 2013, Vol. 155, No. 1, pp. 81-87. Published online before print 27 November 2012.

Paper IV

New diagnostic reference level for full-field digital mammography (FFDM) units

Hauge IH, Bredholt K, Olerud HM. *Radiation Protection Dosimetry,* December 2013, Vol. 157, No. 2, pp. 181–192. Published online before print 14 June 2013.

Paper V

The risk of radiation-induced breast cancers due to biennial mammographic screening in women aged 50-69 years is minimal

Hauge IH, Pedersen K, Olerud HM, Hole EO, Hofvind S. *Acta Radiologica,* accepted for publication 1 November 2013. Published online before print 5 December 2013.

The above publications will in the following chapters be referenced by their roman numerals.

In chapter 9 the original papers have been reproduced with kind permission of the following publishers:
Radiation Protection Dosimetry (Papers I, III and IV)
Medical Physics (Paper II)

1 Introduction and objectives

Breast cancer is the most common cancer in women worldwide, both in terms of number of new cases, (23% out of all cancers) and malignancy (14% of all cancer deaths) (1, 2). In Norway breast cancer among women comprises more than 20% of all female cancer cases, and it is the third most common cause of cancer death (3). In 2008 the age-standardized (world) incidence rate (ASR) for breast cancer was 72.9 per 100 000 person-years for women in Norway (year 2010: 73.0) (4). The ASR for breast cancer worldwide for women was 39.0 per 100 000 person-years, ranging from 19.3 per 100 000 person-years for women in Eastern Africa to 89.9 per 100 000 person-years for women in Western Europe (2). The cancer incidence in Norway is thus high compared to many other countries.

Mammography is an x-ray examination of the breast and has been conducted for a 100 years (5). Further, mammography is the only proven method capable of screening, i.e. to identify non-palpable breast cancer in women without clinical signs who may be at increased risk of early stage breast cancer (6-8). In Norway an organized screening program, the Norwegian Breast Cancer Screening Program (NBCSP), which is part of the public health care system in Norway, started up as a trial project in 1995/1996, and was gradually implemented in the time period 1996-2005. All women in Norway aged 50-69 years are invited to a screening examination biennially, and this has resulted in an increase in the number of mammography examinations of 70% (9). The program complies with the principles of early disease detection set by the World Health Organization (WHO), and the main goal is to reduce disease-specific morbidity and mortality through early detection (10-17). The mortality reduction is 16-36% (Europe: 25-31%) in invited versus non-invited women in service screening programs, while in screened versus non-screened women the reduction in mortality is 24-48% (Europe: 38-48%) (18-20). In the NBCSP a mortality reduction of 43% has recently been reported (21), in other words in accordance with other screening programs. The reduction in mortality is mainly the result of early detection of subtle soft-tissue masses and microcalcifications, which may be early signs of breast cancer, and improved treatment (22, 23). Early detection, as can be achieved with

mammographic screening, thus, is important, and screening as a method seems to work presuming high quality standards in every part of the program.

Overall, mammography is one of the most technically challenging of all radiographic examinations (24-26). Thus quality control is of the utmost importance in order to obtain adequate image quality and keep the radiation doses "as low as reasonably achievable" (ALARA principle). In 1993 the European Commission published the first guidelines for quality assurance in mammography screening, and these guidelines has improved the quality of breast screening, the diagnosis and treatment of breast cancer, and reduced the differences in the quality of care of breast disease among member states of the European Union (27, 28). Further, it contributed immensely to the success of the breast screening projects in Europe. In connection with the start-up of the NBCSP a quality assurance manual was published and later revised (1998 and 2003) (25). It has been implemented in all 16 breast clinics in the NBCSP. The manual is based on the European Guidelines, the WHOs 10 principles of early disease detection, policies, and experiences from randomized trials (16, 27-32).

Prior to the start-up of the trial project the Norwegian Radiation Protection Authority (NRPA) had acquired expertise in the field of technical quality control in mammography (33-37). With the start-up of the NBCSP the NRPA was given a special mandate: the NRPA was to conduct technical quality control, be responsible for optimization of image quality/radiation dose and be responsible for training in technical quality control, image quality and radiation principles in mammography. In the NBCSP the NRPA conduct annual technical quality controls, so-called status controls, and through these annual technical quality controls data on technical performance, radiation dose and image quality are collected (25, 38). In addition, dose surveys for the women attending the NBCSP have been conducted in accordance with the mandate given to the NRPA, which is stated in the quality assurance manual for the NBCSP (25).

The NRPA base its radiological protection on the three principles of the International Commission on Radiological Protection (ICRP): Limitation, optimization, and justification (39). The principle of optimization implies that all exposures shall be as low as reasonably achievable with respect to radiation dose. In order to fulfill this criterion surveys of the

radiation dose for the women examined in the NBCSP have been conducted (40-42). With the change from screen film mammography (SFM) to full-field digital mammography (FFDM), which took place in the time period 2000-2011, it was necessary to examine how different manufacture/models of SFM and FFDM systems operate in a population-based screening programme with respect to the mean glandular dose (MGD). And if there are differences, can they be explained by differences in technology and/or exposure factors? Further, after the transition from SFM to FFDM it was necessary to establish a new diagnostic reference level (DRL) for the FFDM units. The DRL is a pragmatic tool used for optimizing radiation doses for radiologic examinations (43, 44). In the regulations it is demanded that a DRL is established in order to serve as a comparison between different units used for the same type of examination (45). That said, optimization is not only a question about optimizing the radiation dose, but also about optimizing the image quality (46). Therefore, when establishing a new DRL it was also of interest to evaluate the image quality for the units of different manufacture/models to see if any differences occur, and in addition investigate how the image quality and MGD relate to each other for different manufacture/models. Further, the parameters that are used to estimate the MGD are encumbered with uncertainties. It was needed to address these uncertainties in order to estimate the uncertainty inflicted for the estimated MGD.

The principle of justification implies that no practice involving exposure to ionizing radiation shall be adopted unless it produces a net benefit. The reduced mortality from the disease and breast conserving treatment, instead of mastectomy, are considered the main benefits from breast cancer screening (14, 19, 20, 47-54). Another advantage is the improved quality assurance of the diagnostic chain (54). The disadvantages are a) the false positives (a woman receiving a positive test result from screening, when in fact the result was negative), b) the interval cancers (a cancer that occurs between two screening rounds), c) the overdiagnosis (the diagnosis of "disease" that will never cause symptoms or death during a patient's lifetime), and d) the potential risk of developing cancer caused by the radiation dose. In addition to an evaluation of the breast mortality reduction, it is also important to evaluate the other pros and cons listed above. Ionizing radiation is a risk factor for breast cancer (55). It is therefore important to evaluate the potential risk of radiation-induced breast cancers due to an organized mammographic screening program as

performed in Norway, in order to weigh the pros and cons in a cost-benefit analysis and in order to examine if the operation of the NBCSP can be justified.

The overall objective of this thesis is to study the trends and possible dose savings in the transition from analogue to digital mammography in a screening setting, refine the dosimetric method and assess the uncertainties in an assessment of mean glandular dose to women, examine technology differences between different manufacture/models that make a common national DRL less feasible, identify an image quality parameter that can be used along with dose to assess performance for the different manufacture/models and to establish well founded risk estimates as an input in the cost-benefit discussion in a screening program.

2 Scientific background

2.1 Dosimetry

2.1.1 Definition of kerma and absorbed dose

Kerma ("kinetic energy released per unit mass") is defined as the initial kinetic energy of all secondary charged particles liberated per unit mass at a point of interest by uncharged particles (56). If ψ (J m^{-2}) is the energy fluence of monoenergetic photons passing normally over an area in an absorber, then for a polyenergetic x-ray beam the air collision kerma can be written as

$$K_{c,air} = \int_0^\infty \left(\frac{\mu_{en}}{\rho}\right)_{air} \psi_{hv} d(hv) = \left(\overline{\frac{\mu_{en}}{\rho}}\right)_{air} \psi \qquad (1)$$

where the mass energy absorption coefficient in air is averaged over all photon energies in the x-ray spectra, $\left(\overline{\frac{\mu_{en}}{\rho}}\right)_{air}$ (57).

For low atomic number materials (such as air) the production of bremsstrahlung is negligible, and the mass energy transfer coefficient, which is the fraction of the mass attenuation coefficient which contributes to the production of kinetic energy in the charged particles, $\left(\frac{\mu_{tr}}{\rho}\right)$, is equal to the mass energy absorption coefficient, $\left(\frac{\mu_{en}}{\rho}\right)$ (58).

The energy deposited per unit mass of the medium is known as the absorbed dose. It is a very useful quantity for the prediction of biological effects and is the basic physical quantity in radiation biology, radiology and radiological protection (59). Further, it is used for all types of ionizing radiation. The absorbed dose, D, is defined in International Commission on Radiation Units and Measurements (ICRU) Report 60 as

$$D = \frac{d\bar{\varepsilon}}{dm} \quad (2)$$

where $d\bar{\varepsilon}$ is the mean energy imparted to matter of mass dm after interaction with ionizing radiation. The SI unit of absorbed dose is J/kg and this unit has been assigned the name gray (Gy).

For a given material (for instance tissue or air) and radiation field, absorbed dose and kerma are numerically equal, when secondary electron equilibrium is established. At the low energies used in mammography, charged particle equilibrium is fulfilled in both the dosemeter and the absorbing medium (56, 60).

The absorbed dose in tissue, D_{tissue}, is related to the absorbed dose in air, D_{air}, by (58):

$$D_{tissue} = D_{air} \frac{\left(\frac{\mu_{en}}{\rho}\right)_{tissue}}{\left(\frac{\mu_{en}}{\rho}\right)_{air}} \quad (3)$$

where $\left(\frac{\mu_{en}}{\rho}\right)_{tissue}$ and $\left(\frac{\mu_{en}}{\rho}\right)_{air}$ are the mass energy absorption coefficients in tissue and air, respectively.

In mammography the air kerma free-in-air on the central axis of the x-ray beam at a specific distance from the focal spot is measured, employing a calibrated ionization chamber and electrometer, and can be used to evaluate the entrance dose (entrance surface air kerma (ESAK)) (28, 60). The chamber should have a flat energy response for the kV range applied in mammography (60).

2.1.2 Definition of equivalent dose and effective dose

The probability of cancer incidence is found to depend not only on the absorbed dose, but also on the type and energy of the radiation depositing the dose (61). The ICRP therefore

recommends that for radiological protection purposes the organ dose should be weighted for the radiation quality. Equivalent dose is defined by the ICRP as absorbed dose multiplied by a unitless radiation weighting factor (w_R) that accounts for differences in biologic effectiveness between different types of radiation. The unit of equivalent dose is J/kg and this unit has been assigned the name sievert (Sv) (for x-rays: 1 Gy = 1 Sv = 1 J/kg). Effective dose, which is also measured in Sv, is defined by the ICRP as the equivalent dose multiplied by a unitless tissue weighting factor (w_T) that accounts for inherent differences in tissue radiosensitivity, and then summing the contributions for all specified tissues. Effective dose is used to compare the impact of different exposure situations from a radiation protection point of view. Risk estimates, however, should be based on the absorbed dose in the organ (62).

2.1.3 Monte Carlo simulations and mean glandular dose (MGD)

It is of interest to estimate the average dose to the breast tissue rather than the entrance dose. It is the amount of radiation dose delivered to the proliferative tissue or stem cells within the terminal ductolobular units that is of importance, since this tissue is considered to be the most sensitive to radiation (63-66). As a result, there is agreement that the average dose to the glandular tissue (MGD) is the most appropriate dosimetric quantity to predict the risk of carcinogenesis (66, 67).

Some assumptions are made in order to determine the MGD: a) that compression is applied, b) that there is an outer layer of adipose tissue surrounding the breast, and c) that the breast contains a uniform mix of adipose and glandular tissue (68). The dose to the whole breast strongly depends on: a) the x-ray spectrum, b) the breast composition and c) the breast thickness (60). The MGD cannot be measured directly, but needs to be estimated from the measured incident air kerma multiplied by conversion coefficients, based on simulations of photon transport in tissue; so-called Monte Carlo techniques (60, 67-69). In the dose estimations that are included in Papers I-V the method and conversion factors used proposed by Dance et al. have been applied (41, 42, 70).

Different conversion coefficients have been published throughout the years, but the model that is currently used when estimating the MGD in the NBCSP is the one published by Dance et al. (41, 66, 70-73):

$$MGD = K_{a,i} gcs \quad (4)$$

Here $K_{a,i}$ is the incident air kerma on the compressed female breast. The factors g, c and s are conversion factors: g is the conversion coefficient from air kerma to MGD (41), c is the correction factor for any difference in breast composition from 50% mammographic density (42) and s is the correction factor for any difference in the x-ray spectrum from that produced by an x-ray tube with a Mo target and a Mo filter (42, 70).

In order to estimate the conversion factors a compressed breast phantom is used (42). The phantom has the shape of a cylinder of semicircular cross section, a diameter of 16 cm, a 0.5 cm thick adipose surface layer, and a central region. Originally, conversion factors were obtained through simulations of a central region composed of 50% adipose and 50% glandular tissues by weight (50% glandularity) (41). The conversion factors were then extended to breasts of varying breast thickness (2-11 cm), varying glandularity (varied between 99.9% adipose tissue/0.1% glandular tissue (0.1% glandularity) and 100% glandular tissue (100% glandularity) in steps of 25% glandularity) and for a wider range of mammographic x-ray spectra (42). The radiation dose within the breast decreases rapidly with increasing depth (60).

A Monte Carlo program simulated each photon that started at the focal spot of the x-ray tube and followed its path from region to region through the model until all the energy of the photon was absorbed or it left the system (74). All of the energy deposited in each region of the model was recorded. The energy deposited in the central region of the breast was divided between adipose and glandular tissues in accordance with the interaction probabilities in the two tissue types. Because the technical parameters and imaging protocols have changed over the years, new conversion factors have had to be established (41, 42, 66, 70, 71, 75-78).

2.2 Image quality

In mammographic screening high image quality at a low dose to the breast is crucial, and therefore the technique needs to be optimized (60, 79, 80).

2.2.1 Efficacy of diagnostic imaging

A hierarchical model of the efficacy of diagnostic imaging was proposed by Fryback and Thornbury in 1991 (81, 82). Level 1 concerns technical quality of the images, Level 2 addresses diagnostic accuracy associated with interpretation of the images, Level 3 focuses on whether the information produces change in the referring physician's diagnostic thinking, Level 4 concerns effect on the patient management plan, Level 5 measure effect of the information on patient outcome, and at Level 6 analyses examine societal costs and benefits of a diagnostic imaging technology. These can be used as a guiding principle in the evaluation of medical imaging systems (83). Increases in technical image quality (Level 1) will not guarantee improvements at higher levels due to improvements in technical image control (for instance patient outcome) (81). Estimations of the dose and estimation of the image quality, as conducted in Papers I-IV, are part of Level 1 in this hierarchy of six levels of diagnostic efficacy.

2.2.2 Contrast

Both low and high contrast resolution is a requirement for the visualization of tumor masses and characterization of microcalcifications, respectively (84). From a technical point of view low and high contrast resolution can be measured by noise characteristics and use of contrast detail phantoms (84).

Given a tissue of thickness t (Figure 1) and linear attenuation coefficient μ_1 (the background signal) containing an embedded block of "target" tissue of thickness x (the attenuating object) and linear attenuation coefficient μ_2. The contrast C is defined in terms of the image distribution functions I_1 and I_2, which give the energy absorbed per unit area

of the receptor in the background and in the attenuating object (85, 86). The contrast can be defined as (86):

$$C = \frac{I_1 - I_2}{I_1} = \frac{(1 - exp[(\mu_1 - \mu_2)x])}{1 + R} \quad (5)$$

where R is the scatter-to-primary ratio.

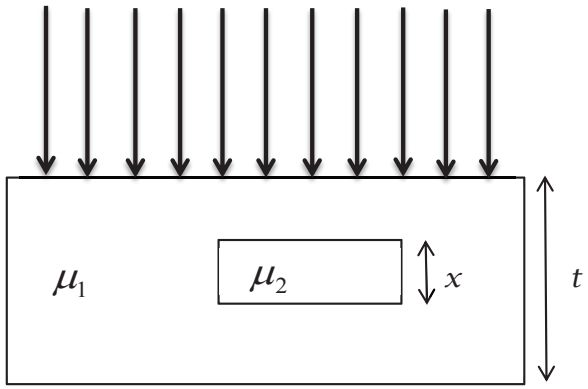

Figure 1. Simple model used for the estimation of contrast. Given a tissue of thickness t and linear attenuation coefficient μ_1 (the background signal) containing an embedded block of "target" tissue of thickness x (the attenuating object) and linear attenuation coefficient μ_2.

The x-ray attenuation coefficients of normal breast tissue and cancer are similar, and therefore the differences in transmission are small (Figure 2). This causes difficulties when it comes to separating normal breast tissue from cancer tissue. As the energy increases the inherent contrast for both tumors and microcalcifications falls. The small difference in x-ray attenuation between glandular tissue and cancer tissue calls for dedicated equipment, dedicated exposure parameters, quality control, and optimization regimes.

In order to discriminate between very similar soft tissues (fat, parenchyma etc.), low kV x-rays are required in mammographic examinations (87). This will result in an increased radiation dose, mainly higher skin doses, but at the same time higher subject contrast is

achieved (88). Dedicated x-ray tubes for mammography are operated at 28 kV_p or less, where the photoelectric cross section dominates over the Compton cross section, and makes the largest contribution to the total cross section (60, 84, 89). Due to the fact that the energy transfer from scattering processes in the mammographic energy range is small, the photoelectric cross section also provides the difference between the mass energy absorption coefficients for adipose and glandular tissue (60). The major factors which emphasize photon absorption differences in tissue (subject contrast) are kV, linear attenuation coefficient, and tissue thickness.

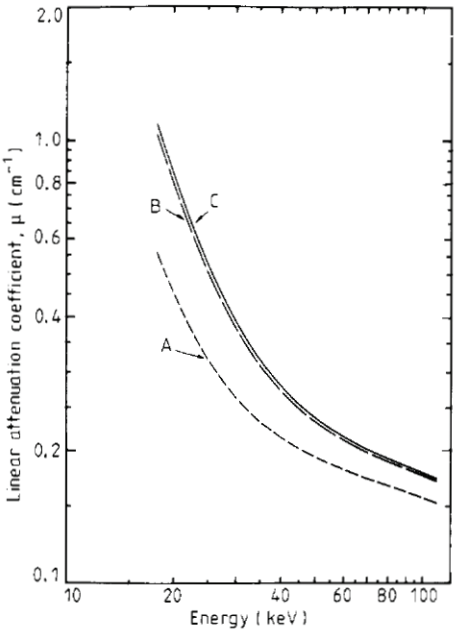

Figure 2. Mean values of the linear attenuation coefficients (μ) of fat (adipose tissue (A)), fibroglandular tissue (B) and tumor (infiltrating ductal carcinoma (C)) in the breast as a function of photon energy (measured in kiloelectron-volt (keV)). The linear attenuation coefficient describes the attenuation properties of a specific material at a specific x-ray energy (58). Figure reproduced from Johns and Yaffe (90) with permission.

2.2.3 Noise

The two major contributors to noise in the radiographic image are statistical fluctuations in the number of x-ray photons detected per unit area (quantum noise), and fluctuations due to the properties of the image receptor and display system. The quantum noise arises from fluctuations in the energy absorbed by the receptor. A total of three components are assumed to make up the noise: a) electronic noise, b) quantum noise, and c) structural noise. The standard deviation in the image is given as

$$\sigma = \left(\sigma_e^2 + \sigma_q^2 + \sigma_s^2\right)^{0.5} \quad (6)$$

Where σ_e, σ_q and σ_s are the standard deviation terms representing the electronic noise, quantum noise and structural noise, respectively (91). Electronic noise is an additive source, independent of x-ray exposure, and may be written as $\sigma_e = e$. Quantum noise scales with the square root of the air kerma, and may be written as $\sigma_q = qK^{0.5}$, where q is some coefficient. Structured noise results from factors specific to a given detector, and the signal from the different structured noise sources is amplified by the x-ray signal used and is therefore written as $\sigma_s = sK$.

2.2.4 Signal-to-noise ratio (SNR)

Diagnostic information should be obtained with the minimum possible absorbed dose (88). The aim is to predict the x-ray energy which gives the highest signal-to-noise ratio (SNR) for the least amount of absorbed dose. SNR is defined as

$$SNR = \frac{\langle n_d \rangle}{\sqrt{\langle n_d \rangle}} \quad (7)$$

where $\langle n_d \rangle$ is the average number of x-rays used to form the image by interacting with the detector, and this number will fluctuate from location to location with a standard deviation of $\sigma = \sqrt{\langle n_d \rangle}$ (92). This fluctuation is referred to as quantum noise. SNR indicates the quantum noise limited region of operation (93). Maximum SNRs per unit mean absorbed

dose ranges from 16-23 keV, and therefore suitable filters should be in the range 18-25 keV, which is the case for Mo and Rh as shown in Figure 3.

2.2.5 Signal-difference-to-noise ratio (SDNR)

For SFM contrast is used to rank the image quality, while for FFDM systems the signal-difference-to-noise ratio (SDNR) is used as figure-of-merit (FOM) for physical image quality (93, 94). SDNR quantify the detector behaviour over time and exposure ranges using an arbitrary object as proxy, but does not in itself indicate how well a system can perform imaging tasks. However, it is a simple measure that can indicate trends. The SDNR is used to characterize the quality of the image in terms of potential detectability of structures in the breast, such as a calcification or a tumor (92). The SDNR[1] is the ratio of the signal difference (using the detected rather than the incident number of x-rays):

$$SDNR = \frac{n_{Ad} - n_{Bd}}{\sigma_{tot}} \quad (8)$$

where $n_{Ad} = \eta n_A$ and $n_{Bd} = \eta n_B$ are the actual number of x-rays that will be detected for paths A and B, which are two different regions of differing signal intensity, respectively, and η is the quantum detection efficiency, which describes the fraction of the x-rays incident on the detector that interact with the detector and producing some signal (92, 95). The noise variance, σ_{tot}, is the total noise variance for paths A and B.

2.2.6 Detective quantum efficiency (DQE)

The detective quantum efficiency (DQE) is defined as the degradation in information (SNR) caused by the detector relative to the information in the incident beam (91). DQE is given by (86):

$$DQE = \frac{(SNR_{out})^2}{(SNR_{in})^2} \quad (9)$$

[1] The SDNR is a display-independent parameter that can give equivalent information to the contrast-to-noise ratio (CNR=Contrast/Noise). The SDNR is a unitless quantity, while CNR has units of inverse noise. CNR and SDNR can be shown to be equivalent if the objects being compared are displayed at the same intensity.

DQE gives the efficiency of a detector in converting incident x-ray energy into an image signal. An ideal detector extracts all the information in the beam (DQE=1), although, a partially absorbing detector may be more efficient (provide a higher SNR) than a detector that absorbs all the radiation (96).

2.2.7 Modulation transfer function (MTF)

The DQE and modulation transfer function (MTF) are quantitative measurements of the detector performance. MTF is the two-dimensional Fourier-transform amplitude, as a function of spatial frequency, of the point spread function (PSF) (97). In short, the MTF is the transfer of information at each spatial frequency (86). The MTF has been used to characterize the resolution properties of SFM systems (98). However, the MTF's for FFDM systems need to be interpreted carefully due to the aliasing effect, which is caused by discrete data sampling. For all real imaging systems there is a loss of spatial-frequency information at high spatial frequencies, which is parameterised by the MTF. The MTF, DQE and normalized noise power spectrum (NNPS) are used to assess the detector performance (91). The DQE can be expressed as (in the 1-dimensional case):

$$DQE(u) = \frac{MTF^2(u)}{q_0 \times K \times NNPS(u)} \quad (10)$$

where q_0 (SNR_{in}^2) is the integrated x-ray photon spectrum normalized for the air kerma to give photons per unit air kerma per mm^2 for the x-ray beam (the density of incident x-ray quanta), K is the air kerma for the uniformly exposed images and u is the spatial frequency variable in cycles per mm (28, 91). The true q_0 values depend on the properties of the actual x-ray spectrum for a given system, and the q_0 values used by Marshall et al. and others are therefore only approximate.

2.3 X-ray units dedicated for mammography

2.3.1 X-ray spectrum

The spectrum shape is determined by the target material, the applied x-ray tube voltage and the added filtration of the beam. Further, the spectrum should be narrow-band in order to

attenuate the low-energy x-rays, which only produce high skin doses, and to attenuate the high energy photons, which reduce the contrast (88, 99). Image contrast and dose reduction improvement in mammographic x-ray imaging can be obtained by using narrow energy band x-ray beams in the 16–24 keV range (100).

The x-ray spectrum consists of polyenergetic radiation. An improvement in the diagnostic potential of mammography can be achieved by using monochromatic or quasi-monochromatic x-rays (85). More monochromatic radiation will also result in a reduction in the radiation dose. This provides a better contrast of breast lesions and a relevant reduction of dose to the patient. The improvement is comparable with the improvement expected with scanning slit devices over conventional antiscatter grids. The optimum x-ray spectrum is a compromise between image contrast, radiation dose, and the statistical noise in the image (101). The main factor that affects the performance of a given x-ray spectra is the compressed breast thickness (73, 102, 103).

A combination of bremsstrahlung and characteristic x-ray processes occurs and are used by x-ray tubes (85). Characteristic radiation is the radiation emerging when beam electrons collide with the inner orbital electrons (K-shell and L-shell). The collision creates orbital vacancies which are filled, and this is accompanied by the emission of characteristic radiation. The ratio of characteristic to bremsstrahlung intensity is approximately 25% of the fluence of the x-ray beam from a molybdenum (Mo) target. The K-edge describes a sudden increase in the attenuation coefficient (μ) of photons occurring at photon energies just above the binding energy of the K-shell electron of the atoms interacting with the photons. The sudden increase in attenuation is due to photoelectric absorption of the photons. This is shown as a peak in the curves in Figure 3. The K-absorption edges effectively define the upper edges of the “window” of x-ray energies transmitted by these filters (88). Energies just below the K-edge filter will to a large extent pass through the filter, while x-rays with energies just above the K-edge will to a large extent be attenuated. X-rays below the optimum energy band are strongly attenuated, the effect being that both the low- and high-energy x-rays are removed to bring their mean-energy nearer to the calculated optimum. A partial energy window is created just below the absorption edge with an enhanced transmitted spectrum. In a study where a Monte Carlo code and a breast

model as proposed by Hammerstein et al. was used it was shown that filters with K-absorption edges slightly higher than the optimum energy are the most suitable filters, with respect to both image quality and dose (67, 104). Such an optimum combination of the K-edge filter and tube potential produces spectra with a large proportion of photon energies that lie within, or close to, the monoenergetic optimum range (88).

Mo anode and Mo filter has been regarded as the "standard" for mammography (99). Compared to the tungsten (W) anode, which is commonly used in the majority of radiographic procedures, the Mo anode produce softer x-rays (105). The softer x-ray beams allow improved visualization of low contrast masses and microcalcifications. Mo emits K-characteristic x-rays at 17.5 and 19.5 keV in addition to a rich bremsstrahlung spectrum between 15 and 20 keV (84, 106) (Figure 3). The target/filter combination Mo/Mo is an optimal compromise between low-energy and high-energy spectrum, when operated at a tube potential of 24-32 kV (84). For thin to average compressed breast thicknesses the Mo characteristic radiation is transmitted through the breast and provides high-contrast mammograms (107). For the thick or dense breast the target/filter combinations Mo/Rh and Rh/Rh achieved contrast comparable to or better than Mo/Mo at a lower dose (101, 106). Rh has a higher K-absorption edge (23.2 keV) and higher K-characteristic x-rays than Mo, but just like the Mo anode, the Rh anode provide soft x-rays (71, 106, 108). The higher K-absorption edge of a Rh filter allows bremsstrahlung of a higher energy (range: 20-23 keV) (106). At a given kV_p the target/filter combination Rh/Rh will be a more penetrating beam than in turn a combination of Mo/Rh and Mo/Mo will be (106).

There has been an increase in the use of W anode, especially with full-field digital mammography detectors that produce noise-limited images. The shift from Mo to W x-ray tube target implies more high-energy photons, the characteristic radiation line spectra for W occur at roughly 58 and 69 keV (67-69, 87). W anode provide harder x-rays, seem to provide poorer contrast, but do provide lower doses (105). Filters with K-edges above 20 keV are chosen in order to create relatively narrow band of energies for the W anode (107). The target/filter combination W/Rh (Figure 3 c) performs better than Mo/Mo for all thicknesses, although the difference is small for the smallest phantom thicknesses (109).

For the thicker breasts, both target/filter combinations tungsten/aluminium (W/Al) and tungsten/silver (W/Ag) has shown to provide optimum x-ray spectra (88, 110).

Increasing the filter thickness will increase the percentage of x-rays in the optimum bands, making the x-ray beam more penetrating. For the Mo/Mo target/filter combination contrast and dose changes little with filter thickness, while the tube loading changes significantly with a change in the filter thickness (99).

a)

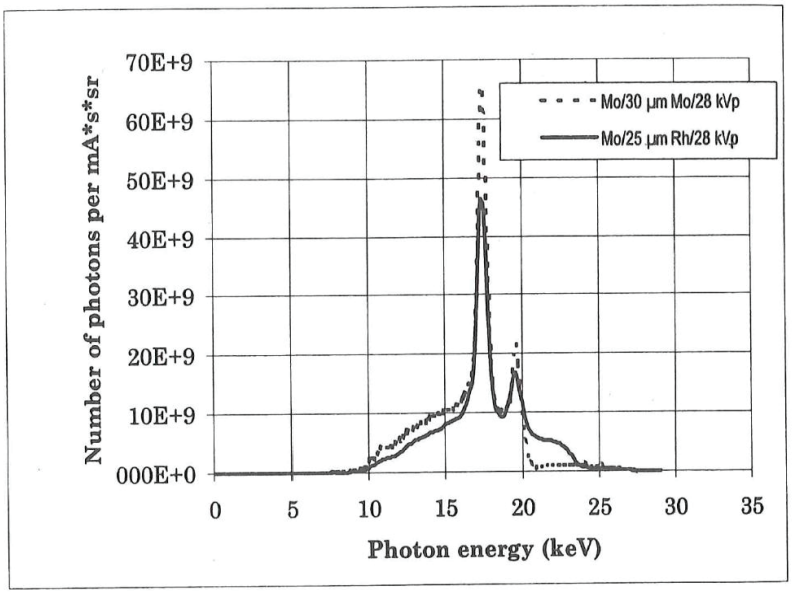
70E+9
60E+9
50E+9
40E+9
30E+9
20E+9
10E+9
000E+0
Number of photons per mA*s*sr
0
5
10
15
20
25
30
35
Photon energy (keV)
Mo/30 µm Mo/28 kVp
Mo/25 µm Rh/28 kVp

b)

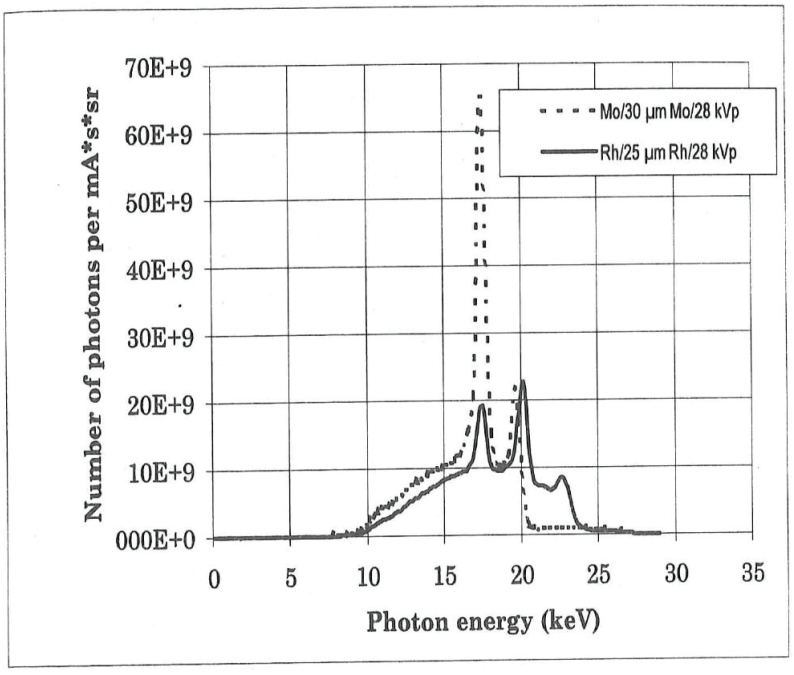
70E+9
60E+9
50E+9
40E+9
30E+9
20E+9
10E+9
000E+0
Number of photons per mA*s*sr
0
5
10
15
20
25
30
35
Photon energy (keV)
Mo/30 µm Mo/28 kVp
Rh/25 µm Rh/28 kVp

c)

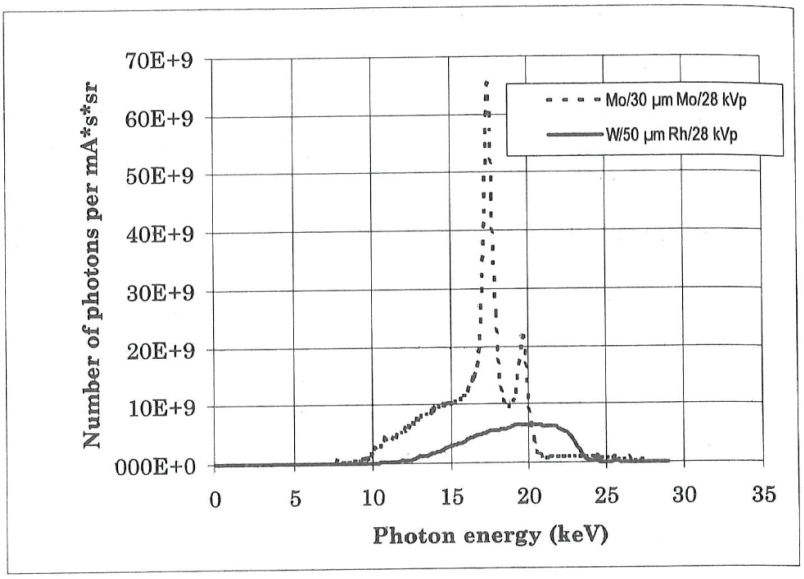

Figure 3. Measured absolute (normalized) x-ray spectra at 28 kV a) for the target/filter combinations Mo/Mo and Mo/Rh from Siemens Mammomat 3000 and General Electric Senographe DMR (the spectra from the two units were inseparable), b) for Mo/Mo and Rh/Rh from General Electric Senographe DMR, and c) for Mo/Mo and W/Rh from Siemens Mammomat 3000. The x-ray spectrum is presented as the number of photons in each photon energy interval (0.1 keV) normalized to the same tube current (mA), total exposure time (s) and solid angle (sr). X-ray photon energy distributions were measured using a Compton scattering spectrometer. The K-peaks are broadened due to the measurement procedure. Figure reproduced from Thilander-Klang et al. (111) with permission. The x-ray spectrum is only valid for a given filter thickness. Varying the filter thickness will result in a different x-ray spectrum.

2.3.2 Half value layer (HVL)

The half value layer (HVL) is defined as the thickness of high purity Al (≥99.9%) given in mm Al which attenuates the air kerma of non-monochromatic x-ray beams by half (29).

HVL is used to describe the radiation quality (target, filter, kV and the output from the generator). An increase in HVL results in a lower radiation dose (101), and a lower image contrast (69). The HVL can be assessed by adding thin Al filters to the x-ray beam and measuring the attenuation for all target/filter/kV combinations in use for a given mammography unit (29).

For 28 kV Mo/Mo the HVL must be over 0.30 mm Al equivalent, and is typically <0.40 mm Al (112). The HVL varies for different target/filter combinations and choice of tube output (kV) (Table 1).

Table 1. Typical values for the HVL (mm Al) for different choices of target/filter combination and choice of tube output (kV). The data are from Table A5.3 in the "European protocol for the quality control of the physical and technical aspects of mammography screening" and Table A5.3 in "Supplement to the European Guidelines" (112, 113). The HVL is measured for tube outputs in the range 25-37 kV.

Target/filter combination	**HVL range (mm Al)**
Mo/30 µm Mo	0.32±0.02-0.40±0.02
Mo/25 µm Rh	0.38±0.02-0.47±0.02
Rh/25 µm Rh	0.37±0.02-0.47±0.02
W/50 µm Rh	0.50±0.03-0.62±0.03
W/0.45 µm Ag	0.51±0.03-0.67±0.03
W/0.5 mm Al	0.34±0.03-0.53±0.03
W/ 0.7 mm Al	0.50±0.03-0.62±0.03

2.3.3 Anti-scatter grids

In mammography the x-rays may pass through the breast without interaction, be absorbed or scatter in the breast and escape (7). The x-rays that pass through the breast without interacting, versus the x-rays which are absorbed, are carriers of diagnostic information and form the image. Incoherent or coherent scatter on the other hand will just blur the image. In mammography low energies are used, but still x-rays scattered in the breast and recorded by the image receptor contribute greatly to degrade the contrast in the image (7, 84). The amount of scattered radiation towards the imaging system for an average breast may amount to as much as 70% of the number of directly transmitted x-rays (7, 114).

The traditional way of rejecting scattered radiation is by placing a grid between the breast and the detector. In order to avoid the presence of grid lines in the image, the grid has to move during the exposure. Mammography anti-scatter grids transmit 60-75% of the primary x-rays, and absorb 75-85% of the scattered radiation (115-118). By reducing the scatter-to-primary ratio the radiation dose has to increase in order to maintain the same amount of primary photons for SFM, which are the carriers of diagnostic information, as without a grid. The factor (Bucky factor) by which the tube current (mAs) must be increased for SFM is in the order of 2.5-3 (84). Due to a larger dynamic range for FFDM systems the reduced exposure to the detector due to the grid does not necessarily imply an increase in dose (94).

The shortcomings of anti-scatter grids are that a large fraction (15-25%) of the primary radiation is absorbed by the grid, and that scattered radiation can still traverse the grid (25-40%). All systems used for mammography in the NBCSP have anti-scatter grids, with the exception of multislit scanning digital systems, due to their high efficiency in rejecting scattered radiation (94).

2.3.4 Automatic exposure control (AEC)

The AEC is an x-ray exposure termination device, and consists of a sensor located beyond the image detector. When the sensor has received a predetermined amount of radiation the exposure discontinues. The ALARA principle on dose administered to the patient urges the

use of an AEC system to ensure the optimal exposure of the image receptor compensating for breast thickness and composition (119).

For the SFM systems included in Paper I from General Electric (GE), Instrumentarium[2] and Siemens different approaches to automation of exposures are employed. Siemens and Instrumentarium determine the exposure values based on compressed breast thickness. For GE the detector is used as the AEC sensor, as detector operation entails separate acquisition and image-read phases (44, 120), and a short pre-exposure is given in order to find the correct choice of target/filter/kV_p/mAs. In Paper I-V FFDM systems from GE, Siemens, Hologic and Philips were included. The FFDM systems from GE and Siemens have similar AEC set-up as the SFM systems. Hologic has a similar AEC as GE, basing exposure on registered breast thickness and signal recorded during a brief pre-exposure (121). Philips on the other hand permits instantaneous AEC sensor operation during image acquisition using the leading edge detector (122).

2.3.5 Compression

Compression is important in mammography, and should be applied slowly and gently (123-125). It serves several purposes: a) spreading out the tissue and thereby reducing superposition, b) reducing the scatter-to-primary ratio (126), c) reducing the dose since a thinner breast is more easily penetrated, d) causing less image blurring and reducing the degree of geometric magnification, since all parts of the breast will be closer to the imaging system (84), e) decreasing the breast thickness, and f) resulting in improved breast contrast, due to decreasing relative intensity of scatter and a reduction of beam hardening (126).

Flat paddles with an abrupt 90-degree flange at the chest wall are widely used now, since these paddles grip the posterior breast and achieve more uniform compression compared to curved paddles (126). It has been revealed that variability between and within practitioners do exist (127), and that compression plates have an unsuitable pressure distribution (128, 129).

[2] Now owned by GE.

2.3.6 Screen film mammography (SFM)

Mammographic images are produced with a single intensifying screen used as a back screen in combination with a single-emulsion film (130). The mammographic screens incorporate phosphors containing metals from the lanthanaide series, and may incorporate light absorbed in the phosphor in order to increase sharpness. All radiologic images contain random fluctuation, or noise, due to the statistics of x-ray quantum absorption (131). Film granularity is a major noise source (132).

In the NBCSP the two screen film combinations Kodak Min-R 2190/Kodak Min-R 2000 and Kodak Min-R EV 190/Kodak Min-R EV were in use in the time period 2006-2008. The characteristic curve of the screen film system Kodak Min-R EV 190/Kodak Min-R EV provides the highest contrast over the widest optical density (OD) range compared to Kodak Min-R 2190/Kodak Min-R 2000 (Figure 4). The Kodak Min-R EV 190/Kodak Min-R EV screen film combination is the newest of the two and has a) a comparable sensitivity, b) a better contrast, c) a higher MTF, d) slightly better resolution, and e) an equivalent noise level to Kodak Min-R 2190/Kodak Min-R 2000, although the Kodak Min-R 2000 film is the noisiest film (133, 134). For the Kodak Min-R EV system the glandular part of the breast should be imaged at a higher OD than usual (for example: 1.0–1.2), requiring the AEC system to be set to a higher range, i.e. 1.8–2.0 instead of 1.4–1.6. This shift in OD would increase the entrance dose compared to the screen film combination Kodak Min-R 2190/Kodak Min-R 2000.

Radiographic film is limited by the fact that the gradient of the characteristic curve varies with exposure level. Successive doubling of the exposure does not give a constant increase in the density, i.e. the opacity is not proportional to the exposure. The central region of the characteristic curve is called the "linear" or "straight-line" portion, the underexposed part is called the "toe", and the overexposed region is called the "shoulder". In mammography the AEC has a very important role when it comes to improving the consistency of film OD, contrast and radiation exposure (118).

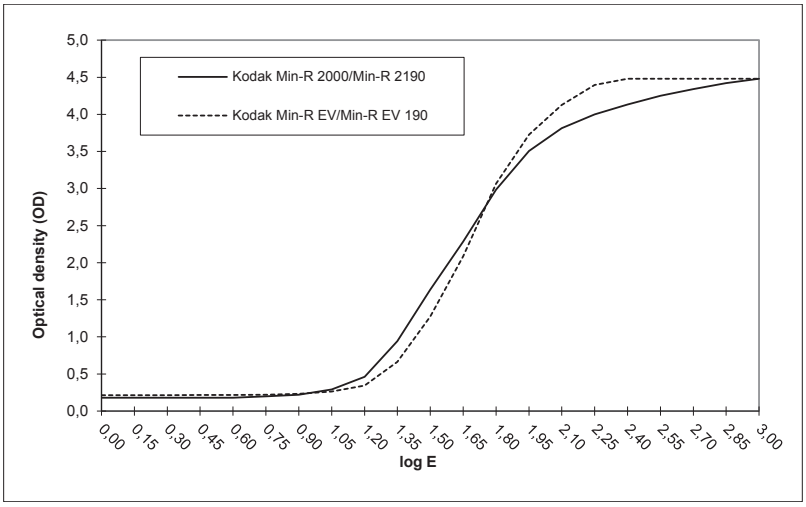

Figure 4. The characteristic curve, which is a plot of film density (log of opacity) versus the log of exposure, for the screen film combinations Kodak Min-R 2190/Kodak Min-R 2000 and Kodak Min-R EV 190/Kodak Min-R EV. The sensitometer had a maximum reading of approximately 4.5 for the optical density (OD).

2.3.7 Full-field digital mammography (FFDM)

The processes of image acquisition, image display, and storage are separated in digital mammography, in contrast to SFM. This allows for optimization of each of these processes separately (120). The FFDM systems included in Paper I-V utilizes different kinds of digital technology: a) selenium flat-panel digital detector, b) flat-panel phosphor digital detector, c) and photon counting scanning-slit detector (135). a) and c) are so-called direct and b) is an indirect systems, respectively (Figure 5).

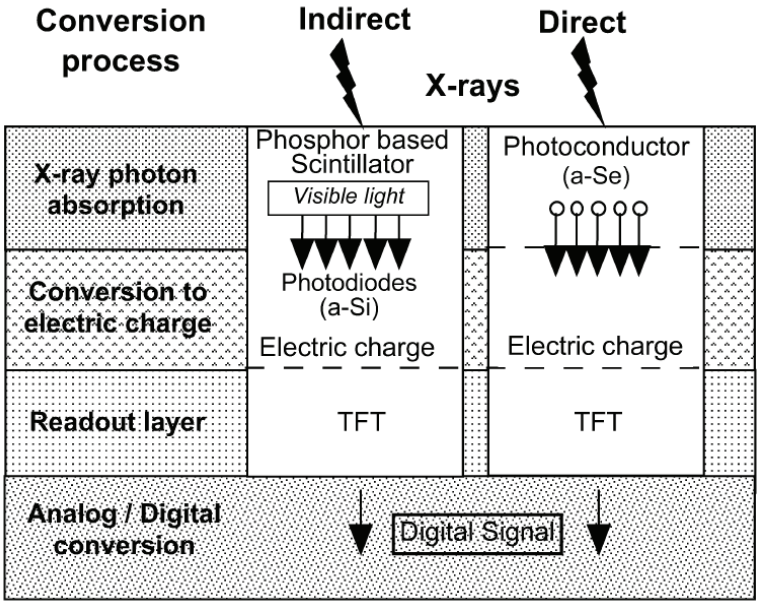

Figure 5. Signal conversion principle for direct and indirect detectors. Figure reproduced from Noel and Thibault (136) with permission.

Selenium flat-panel digital detector is a direct conversion detector; the x-ray energy is converted directly into electric charge using a photoconductive detector. The x-rays interact with an amorphous selenium (a-Se) photoconducting layer and an electric charge is liberated in the material in the form of electron-hole pairs. Electrodes are placed on the upper and lower surfaces of the selenium, and an electric field is applied between the electrodes. The electric charge is collected by a matrix of electrodes. The advantages of this system are a) a high DQE and b) a high MTF (137). Measurements for the DQE and MTF published by Marshall et al. showed that the peak DQE for GE Senographe 2000D, GE Senographe DS, GE Essential, Hologic Selenia, Sectra MDM (in the scan direction), and Siemens Inspiration were 0.41, 0.40, 0.59, 0.48, 0.81, and 0.44, respectively, while the MTF at 5 mm^{-1} were 0.27, 0.28, 0.16, 0.44, 0.22 and 0.48, respectively (91). The MTF for the newer GE Essential detector is lower than for the older generation detectors GE Senographe 2000D and GE Senographe DS. Siemens Inspiration and Hologic Selenia both have a-Se based detectors, and for these the difference in MTF was small (0.44 versus 0.48).

Flat-panel phosphor digital detector is called indirect-conversion detector; the x-ray energy is first converted to light by an x-ray scintillator (cesium iodide is a common scintillator), which in turn is converted to an electric signal. The electric signal is transferred to be stored as a charge on the large-area detector. An advantage of phosphor flat-panel systems is that the images can be obtained in a short period of time (138). The pixel size of the detector elements of the phosphor flat-panel systems is 100 μm, the selenium-based systems has a pixel size of 70-85 μm and the pixel size of the photon counting scanning-slit detector from Philips is 50 μm.

A special type of a direct detection radiography system is the individual counting of each interacting x-ray photon (119). One photon produces exactly one count regardless of its energy. The detector is a multi-slit scanning system that uses an array of silicon wafers to detect the x-rays (94, 139). This way the electronic noise is reduced, and by utilising a high energy spectrum and not applying a standard grid design this reduces the patient dose by 55-65% (135, 140, 141). While the flat-panel systems operate with sophisticated systems for automatic optimization of the radiation parameters, the scanning system determines exposure based only on the breast thickness (119).

2.3.8 Technological development: Transition from screen film mammography (SFM) to full-field digital mammography (FFDM)

SFM has remained in use for a long time, and was close to being fully optimized when FFDM first came into use (142). The reason why SFM has been in use for such a long time, even though FFDM has been available is a) the concern of a lower spatial resolution in digital systems, b) concern about using soft-copy reading (143), and c) the cost, FFDM being more expensive than SFM (144, 145). However, since all other modalities in the radiology departments (x-ray, computed tomography (CT), magnetic resonance imaging (MRI) and ultrasound) were developing towards digital equipment and picture archiving and communication system (PACS), mammography was pushed in the same direction (119, 142), which improved the information flow in the hospitals. From the 1990s onward, digital mammography has become increasingly available (146), and is gradually replacing

SFM (147, 148). The main difference between SFM and FFDM is the separation of the image acquisition, processing and display (142).

The advantages of SFM are: a) low cost, FFDM costs 1.5-4 times more (149), and b) SFM is superior to FFDM when it comes to spatial resolution (142). An important limitation with SFM, however, is the contrast resolution (142). The limitations of SFM are partly due to the detector, and to the image acquisition geometry (inefficiency of scatter rejection) (131). The SFM detector has: a) shorter dynamic range (the range of light intensities that can be captured simultaneously) (Figure 6), b) restricted exposure latitude (the extent to which a light-sensitive material can be overexposed or underexposed and still achieve an acceptable result), c) restricted contrast, d) lack of detection efficiency, and e) presence of film-granularity noise.

Many of the limitations of conventional mammography could be effectively overcome with a FFDM imaging system in which image acquisition, display, and storage are performed independently, allowing optimization of each of them separately (131). The advantages with FFDM are among others: a) a wider dynamic range, b) linear relationship between dose and signal intensity, c) higher cancer detection rate, d) dose savings for women with larger breasts, and e) the possibility of image processing (142, 143, 150). The wider dynamic range gives FFDM a clear advantage over SFM. With SFM parts of an image might be under- or overexposed, but this is avoided with FFDM. Further, for SFM the limited dynamic range results in difficulty in detecting soft-tissue lesions in dense glandular tissue (142). A higher cancer detection rate for FFDM is obtained in younger women with denser breasts due to FFDMs ability to selectively optimize contrast in areas of dense parenchyma (138). Dose savings for women with larger breasts is obtained by switching to a higher energy beam spectrum (151, 152). The image may be processed after the image is obtained by changing the dynamic range of the breast tissue.

Early dose studies for FFDM showed a reduction in glandular dose of 25-35%, depending on breast thickness (119, 138, 151). Studies comparing radiation doses from one FFDM with one or more SFM systems have found that FFDM systems are capable of providing lower radiation doses than SFM systems (151, 153-155).

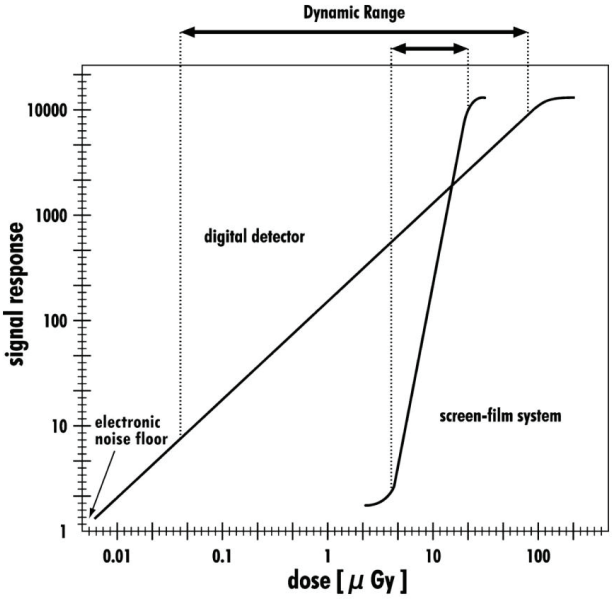

Figure 6. The dynamic ranges for screen-film systems and digital detectors. Screen film systems have a limited tolerance for radiation exposure, while digital detectors cover a wider range. Therefore, an optimal signal response will occur over a wider exposure range with digital detectors than with screen film systems. Figure reproduced from Korner (156) with permission.

In the diagnosis of microcalcifications, FFDM is equivalent or superior to SFM (143, 157-163). GE's Senographe 2000D was used in most of these studies, although other systems (FFDM: Fischer, Lorad, Hologic and Sectra; CR technology) were represented as well (143). Objects with size smaller than the pixel size of a digital detector will be displayed as a) larger than they actually are and b) with a lower contrast (138, 159, 164). This could be a worry in the detection and characterization of microcalcifications, but seems to be irrelevant. The lower spatial resolution of FFDMs is more than compensated for by other characteristics leading to an enhanced detection of microcalcifications (119).

When it comes to the detection and characterization of masses, FFDM seems to perform at least equivalent to SFM (119). However, when it comes to detecting cancer, FFDM is superior to SFM only in younger women (<50 years) (165). Although, as long as only

women aged 50-69 years is screened in the NBCSP, this last finding is not of importance as of now for the women invited in the NBCSP. Digital systems have higher DQE, and therefore lower noise. Due to this, digital systems can compensate for the relative loss of contrast via appropriate windows settings.

Overall, studies conducted on different FFDM systems (Fischer (SenoScan), Fuji (CR system), GE (Senographe DS and Senographe 2000D), and Hologic (a digital mammography system and Lorad Selenia)) have shown that FFDM is just as accurate as SFM (144, 149, 166). However, one disadvantage was found for FFDM in that recall rates were higher compared to SFM (166).

2.4 Radiological protection and risk of radiation-induced cancer

Ionizing radiation is defined as radiation that has sufficient energy to remove orbital electrons from an atom or molecule (87). In the human body, ionizing radiation can be absorbed and damage DNA (167). The mechanism of DNA damage can be either direct or indirect. Direct damage comes from an ejected electron, and indirect damage through the production of free radicals, such as hydroxyl radicals from water. The hydroxyl radicals can then go on to damage DNA. The indirect effect is the predominant effect from x-rays.

2.4.1 Definition of risk: Absolute and relative risk

After the discovery of x-rays, it was revealed that radiation exposure causes acute tissue damage and cancer, particularly leukemia (168). The health effects consequent to exposure to ionizing radiation are divided into two categories: a) tissue reactions (previously referred to as ‘deterministic effects’) and b) stochastic effects (62). Acute skin reactions in the most heavily radiated area are a major concern for patient safety especially in interventional radiology (56). Dose responses for radiation-induced tissue reactions in adults and children seem to have dose thresholds, which result in the absence of risk at low doses (62).

Stochastic effects consist of cancer in the exposed individual and hereditary disease in the descendants of the exposed individual. Cancer induction is generally considered to dominate the overall risk for the exposed person after radiological imaging (56). The stochastic nature of radiation carcinogenesis is the basis for the ALARA principle (169).

Epidemiological studies conducted in the past 6 decades have attempted to document the health consequences of exposure to low levels of ionizing radiation (170). There are four categories of data sources: a) atomic bomb survivors in Hiroshima and Nagasaki (Radiation Effects Research Foundation (RERF) data, Japan), b) persons exposed to medical radiation, c) workers in radiation and nuclear industries, and d) populations exposed to environmental radiation (including accidents in nuclear plants). The Japanese atomic bomb survivor life span study (LSS) cohort data, which is an ongoing study, is the major source when it comes to evaluating health consequences from ionizing radiation (62, 171, 172). The latest report in a series of periodic general reports on mortality in the LSS cohort of atomic bomb survivors concludes that the risk of all causes of death was positively associated with radiation dose (173). Most of the other population studies have shown no or much smaller health effects due to radiation exposure than the RERF data (171).

For the RERF data extrapolations are difficult due to differences in cancer incidence between the population of Japan and other populations and differences in exposure from an atomic bomb and medical imaging.

Risk is defined as the probability for an individual to develop a specified disease over a specified interval of time. It is assumed that the individual is alive and disease-free at the start of the time period. There are two essential components of risk assessment: a) measure of exposure (absorbed dose from ionizing radiation) and b) measure of disease occurrence. Evaluation of the association between exposure and disease occurrence is aided by the use of statistical models.

Absolute risk is defined as the probability that a person who is disease-free at a specific age will develop the disease at a later time in life following exposure to a risk factor. For example: the probability of cancer induction following exposure to radiation. In the excess absolute risk (EAR) model ionizing radiation is assumed to induce cancers at some fixed number above the natural incidence, and it is defined as (170):

$$EAR = R_e - R_u \quad (11)$$

where R_e are the incidence rates in an exposed population and R_u are the rates in an unexposed population. The EAR is expressed per population and time period (e.g. per 10 000 person-years). The excess relative risk (ERR) is expressed as a fraction or multiple of the naturally occurring risk:

$$ERR = \frac{R_e}{R_u} - 1 \quad (12)$$

R_u is often referred to as the baseline risk. The ERR is the excess risk expressed relative to the background risk. The ERR model assumes that exposure to ionizing radiation increases the natural incidence of a cancer at all ages proportional to spontaneous background rates (predicts a larger number of induced cancers in old age). This value is always greater than 1 (unless the radiation is assumed to produce a beneficial effect). The risk in the exposed population may be expressed as:

$$Risk\ in\ exposed = Baseline\ risk + EAR \quad (13)$$

$$Risk\ in\ exposed = Baseline\ risk\ (1 + ERR) \quad (14)$$

Risk factors from the EAR and ERR models are incorporated into a final risk model, the lifetime attributable risk (LAR) model to compute a risk estimate for the likelihood of radiation-induced cancer over the lifetime of individuals exposed to ionizing radiation. This approach is applied by United Nations Scientific Committee on the Effects of Atomic Radiation (UNSCEAR), in the report of the 7th committee of the Biologic Effects of Ionizing Radiation (BEIR VII) commissioned by the U. S. National Academy of Sciences, and by ICRP for estimating the likelihood of radiation-induced cancer (62, 171, 174). UNSCEAR has converted ERR into LAR in a way that differs from the ICRP procedure (175).

The radiogenic risk varies with the different x-ray procedures and to differing degrees depending on which body organ that has been irradiated (176). Further, it varies

significantly with the patient`s age and sex. In children the risks of radiation-induced stochastic health effects are estimated to be higher (by a factor of ≤4) than in adults, while for people ≥70 years the risks are lower (by a factor of ≥10) compared to younger people (176). Within the LSS, the ERR decreases with increasing age at exposure, while the EAR does not (174).

2.4.2 The dose-response relationship

Epidemiology is the study of the distribution and determinants of disease in human populations, and the relationship between an outcome (disease) and an exposure is studied (dose-response relationship).

For doses above 100 mGy the relationship between radiation dose and radiation related cancer risk is found to be linear (170, 177-185). Further, there is consensus that for doses in the range 0.2 to 3 Gy the so called linear no-threshold (LNT) dose-response model describes well the relation between the radiation dose and carcinogenic effect (186). The LNT model predicts that the excess risk of cancer is directly proportional to the dose of radiation received.

Radiation risk at low doses (<100 mSv) is commonly extrapolated from the risk at high doses (187-189). Different extrapolations can be conducted: a) linear extrapolation (LNT), b) linear quadratic model, c) threshold linear model, and d) hormesis model (Figure 7) (190). In the threshold model very small radiation doses are considered to be harmless. The hormetic model argues that radiation at very small doses can even be beneficial. For the LNT model it is considered that the sum of several very small exposures have the same effect as one larger exposure and the implication is that no dose of radiation is safe. For low doses, however, the risk is too small to be distinguishable from cancer incidence due to all causes, and an increased incidence of cancer has been difficult to identify with any degree of statistical confidence (168, 170, 187).

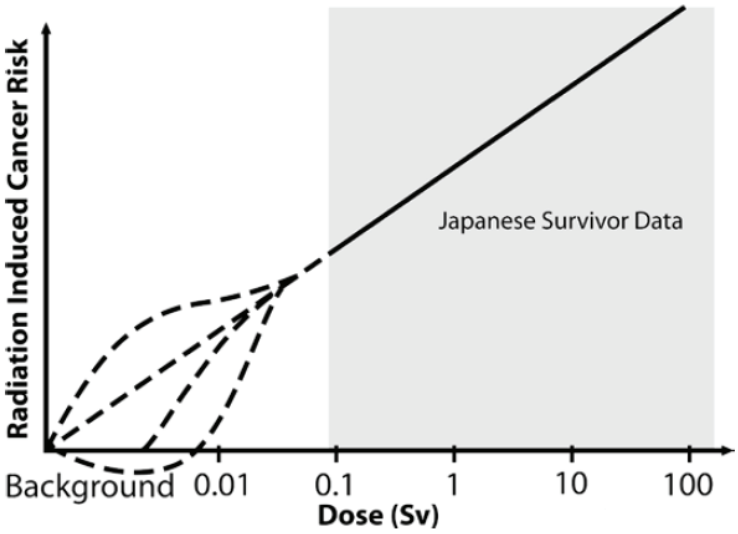

Figure 7. Different models (dashed straight lines) for extrapolating from the LNT model (straight line) applied at high doses (>100 mSv) to low: a) supra-linearity (downward curving curve) b) linear extrapolation (LNT), c) linear no-threshold model, and d) hormesis model. The linear-quadratic model would be between the linear no-threshold model and the hormesis model, with an upward curving curve and no positive effect at low doses. Figure reproduced from Hendee and O'Connor (170) with permission.

Assuming a hypothetical dose-response curve with a linear approximation for low doses (the tangent of the curve at dose zero, with slope s_L), and a linear approximation based on risk at some high dose (with slope s_H), the dose and dose-rate effectiveness factor (DDREF) is the slope at high dose (s_H) divided by the slope at the smaller dose (s_L) (171). If the DDREF is known, it can be used to convert a risk estimate (EAR) from the high dose (EAR_H) to the low dose (EAR_L) (171):

$$EAR_L = \frac{EAR_H}{DDREF} \quad (15)$$

The ICRP uphold the recommendation of applying a DDREF of 2 to correct for a lower effect at low doses and low dose-rate, while BEIR VII use a DDREF of 1.5, and UNSCEAR use a DDREF of 1 (62, 171, 191).

The LNT model is first and foremost used due to its simplicity and conservative approach (170, 192). When estimating the radiation risk, an LNT model is normally assumed, although the application of the LNT model at low doses, such as for mammography, is heavily debated (170, 189, 192, 193). Expert advisory bodies are divided in their view of the LNT model (194). One of the reasons being that the LNT theory fails to differentiate between low doses delivered at low dose-rates, high doses delivered at high dose-rates, and the effects of these. BEIR VII and ICRP support the hypothesis of the LNT relationship between exposure to ionizing radiation and the development of cancer in humans at low doses (171, 195). The French National Academies of Science and Medicine on the other hand concluded that the LNT model lacks justification for low doses (<100 mGy), and even more for very low doses (<10 mGy) (186). Either, because there is no effect, or the effect is too small to be detected by such studies. They base this decision partly on radiobiological evidence from epidemiological studies (194). They argue that the LNT model is not based on scientific data, and that the LNT model should only be used as a tool for regulatory purposes (186).

From a radiation protection point of view a conservative model that overestimates risk is preferred over a model that underestimates risk. The ICRP maintains that it is better to err on the side of caution (62). The LNT theory lays the foundation for current radiation protection philosophy (194). However, the LNT model was originally used to provide an upper limit estimate of the risk, with zero being the lower limit, of low level irradiation, since the dose-response curve could not be determined at low dose levels (196). The evidence supporting linearity for radiation was limited and not based on low doses (197). For low doses, in general, there are large statistical fluctuations (62, 190). For instance, no statistically significant increase in cancer risk was found in two areas with high background radiation (198, 199). In order to obtain statistical precision, the sample size must increase approximately as the inverse square of the dose (187); a sample size of approximately 5 million people would have to be included for a 10 mGy dose (200, 201). In 2007 the ICRP stated that “the long standing question on the true validity of the LNT model may well prove to be beyond definitive scientific resolution and that “weight of evidence” arguments and practical judgments are likely to continue to apply in the foreseeable future” (62).

2.4.3 Radiation effects on the female breast

Radiation exposure of the female breast from mammography from 1960 to the present shows that glandular tissue doses have decreased from an average of about 12 mGy to about 2 mGy (146). In the NBCSP dose surveys have been conducted by the NRPA since the start of the trial project (40, 202, 203). In the dose surveys the conversion factors of Klein et al., Wu et al. and a revised model of Dance et al. were applied when estimating the MGD (41, 42, 66, 71, 76). The MGD for the CC and MLO projections were no higher than 1.5 mGy (range: 1.17-1.38 mGy), while the MGD per examination was in the range 2.5-3.0 mGy.

Radiation effects on female breast cancer rates have been widely studied (181, 182, 204-210). The reason for this is that breast tissue appears to be relatively radiosensitive and because breast cancer is the most common cancer among women (174).

The atomic bomb survivor cohort (LSS) consists of a population that was primarily exposed to high energy, low (<1 keV μm^{-1}) linear energy transfer (LET) gamma radiation, while mammography x-rays are low energy exposures (photon energies about 30 keV) with higher LET (>1 keV μm^{-1}) compared to gamma rays (211, 212). The relative biological effectiveness (RBE), which is the ratio of biological effectiveness of one type of ionizing radiation relative to another, given the same amount of absorbed energy, is lower for x-rays, gamma rays, beta rays, and muons than for neutrons, protons, charged pions, alpha particles, nuclear fission products, and heavy nuclei. RBE is represented in regulations by the radiation weighting factor. Thus, the difference in RBE makes it difficult to compare the atomic bomb victims and exposures from medical imaging. *In vitro* studies on double-strand breaks (DSB) have shown that more clustered DNA damage is produced with mammography x-rays compared to gamma rays (211). These are more difficult to repair. Further, a RBE (for malignant transformation of human cells *in vitro*) of 4 for mammographic x-ray energies relative to higher energy x-rays has been found (212-214). If an RBE of 4.0 is assumed for mammography x-rays, there is no impact on the detection to induction ratio for women aged 50-70 years, and thus mammography still

remains a low risk procedure (212). There exists controversy regarding the RBE of low energy x-rays applied for mammography (212, 214, 215).

In the LSS an EAR per 10^4 woman-years per Gy of 2.3 (95% CI: 1.0-3.8) was found for breast cancer (173). The EAR was estimated for women exposed at age 30 years, having attained age 70 years. For Canadian tuberculosis patients given chest fluoroscopies the data were most consistent with a linear dose-response relationship, and this was confirmed in a follow-up study as well (209, 216). They found a standardized mortality ratio of 1.14 (95% CI: 1.02-1.27) for women exposed to a cumulative dose <100 mGy, which they defined as the unexposed group. Women exposed to a cumulative dose ≥100 mGy of radiation had a relative risk of death from breast cancer compared to the unexposed group of 1.36 (95% CI: 1.11-1.67) (216). However, it was concluded that the risk of breast cancer associated with radiation decreases sharply with increasing age at exposure. Further, it was concluded that even a small benefit to women of screening mammography would outweigh any possible risk of radiation-induced breast cancer. Overall, the studies seem to show a linear correlation, although age and radiation dose included in the studies are not the same as those that are applied in the NBCSP.

2.4.4 The principles of the International Commission on Radiological Protection (ICRP)

Modern radiological protection is based on the three principles of the ICRP, which were published in Publication 26 in 1977 (39):

- Principle of justification: no practice involving exposure to ionizing radiation shall be adopted unless it produces a net benefit.
- Principle of optimization: all exposures shall be as low as reasonably achievable, economic and social factors taken into account.
- Principle of limitation: exposure of radiation workers and members of the public must not exceed dose limits.

Their practical implementation requires procedures and methods for the quantification of exposures to ionizing radiation (217). In a screening setting and from a radiation protection point of view the radiation doses have to follow the ALARA principle (170).

3 Aims of the individual papers

Paper I

With FFDM units it is anticipated that the dose level will decrease compared to using SFM units. In the time period 2006-2008 a gradual shift from SFM to FFDM was taking place in the NBCSP, and a dose survey was conducted in order to evaluate the MGD for the screening units operating in the NBCSP.

Paper II

The estimation of MGD is based on the compressed breast thickness. Previous studies have shown that the readout[3] thickness of mammography machines is inaccurate, and some of these studies have proposed methods which may provide a better estimate of the compressed breast thickness (218-222). Some of the methods are quite accurate, although cumbersome to perform (221, 222). We therefore wanted to come up with an easy method to measure the difference between the displayed and real (measured) compressed breast thickness. Further, we wanted to estimate the difference between displayed and real (measured) compressed breast thickness for a range of SFM and FFDM units in clinical use.

Paper III

The uncertainty due to difference between the displayed and real (measured) compressed breast thickness will lead to uncertainties in the estimated MGD. The aim in this paper was to compare the uncertainties in compressed breast thickness with uncertainties in other parameters, such as HVL, glandularity, kerma, and s-factor, in order to estimate the total uncertainty in MGD.

[3] Displayed by the mammography machine

Paper IV

Given that a complete transition from SFM to FFDM had taken place by August 2010, it was needed to establish a new DRL in the NBCSP, since FFDM in general provide lower MGDs than SFM (Paper I). We wanted to estimate both the 75^{th} and 95^{th} percentile for the different manufacture/models. Further, we wanted to investigate if potential differences in MGDs for the different manufacture/models could be explained by variations in image quality (SDNR and low contrast detectability). And if this was the case, would it then render the use of different DRLs for the different manufacture/models.

Paper V

The aim was to estimate the risk of radiation-induced breast cancers for the women in the NBCSP, which offers women aged 50-69 years two-view mammography every two year. Yaffe and Mainprize described a scheme for estimating the risk of radiation-induced breast cancers, breast cancer deaths, the number of lives lost, and lives saved for a variety of mammography screening scenarios (223). However, biennial screening for the age group 50-69 years, as recommended by the European guidelines for breast cancer screening and diagnosis, was not included in their estimates. We wanted to apply the scheme developed by Yaffe and Mainprize to estimate the risk for the age range of the women that are invited in the NBCSP.

4 Material and methods

4.1 Material: Mammography units

For Paper II units in use clinically in Lancashire, Greater Manchester and Cheshire counties in England, United Kingdom (UK), in 2010 were included.

For Paper I, III, IV and V mammography units used for screening in the time period 2006-2011 in the NBCSP were included. For the trial project, which started up in 1995/1996, four SFM units were used (three Siemens Mammomat 300 and one were used Siemens Mammomat 3000) (40). The NBCSP was gradually expanded, and more SFM units were added to the program. In year 2000, the first FFDM unit was taken into use in the NBCSP, a GE Senographe 2000D unit. Since then there has been a gradual increase in the number of FFDM units used for screening in the NBCSP (Figure 8). Since August 2011 only FFDM units are used for screening in the NBCSP. Available target/filter combination(s) for the different SFM and FFDM units included in Papers I-V are shown in Table 2 and Table 3, respectively.

The SFM units included in the study in Paper I were manufactured by GE (GE Medical Systems, Buc, France), Instrumentarium and Siemens (Siemens Healthcare, Erlangen, Germany). All SFM units had screen film detector systems delivered by Kodak (Rochester, NY, USA)[4]. The FFDM units included in the studies in Paper I-V were manufactured by GE, Hologic (Hologic Inc., Bedford, MA, USA), Philips (Philips healthcare, Best, The Netherlands) and Siemens.

[4] Kodak has changed name to Carestream Health Inc. (Rochester, NY, USA).

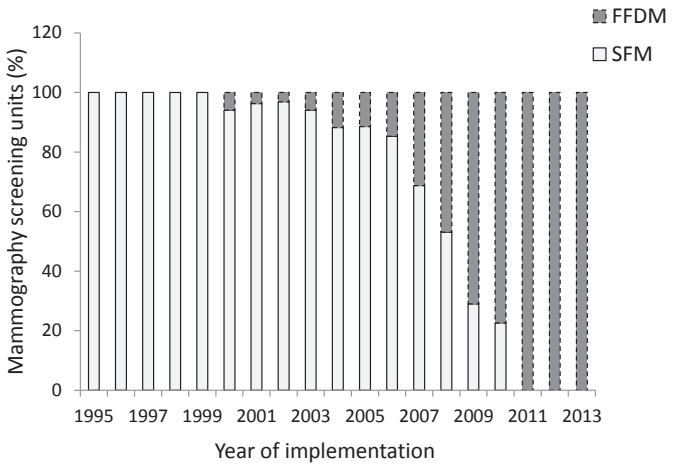

Figure 8. Screen film mammography (SFM) systems and full-field digital mammography (FFDM) systems used for screening in the Norwegian Breast Cancer Screening Program (NBCSP) since the beginning of the program in 1995/1996. The distribution between SFM and FFDM is given in percent (%).

Table 2. Available target/filter combination(s) for the different screen film mammography (SFM) units included in Paper I, II and IV.

Manufacturer	**Model**	**Available target/filter combination(s)**
GE	Senographe 800T	Mo/Mo, Mo/Rh
GE	Senographe DMR	Mo/Mo, Mo/Rh, Rh/Rh
Instrumentarium[1]	Alpha	Mo/Mo, Mo/Rh
Instrumentarium[1]	Diamond	Mo/Mo, Mo/Rh
Siemens	Mammomat 300	Mo/Mo
Siemens	Mammomat 3000/3000Nova	Mo/Mo, Mo/Rh, W/Rh

[1]: Now owned by GE.

Table 3. The available target/filter combination(s) used for the different full-field digital mammography (FFDM) units included in Papers I-V.

Manufacturer	Model	Available target/filter combination(s)
GE	Senographe 2000D	Mo/Mo, Mo/Rh, Rh/Rh
GE	Senographe DS	Mo/Mo, Mo/Rh, Rh/Rh
GE	Senographe Essential	Mo/Mo, Mo/Rh, Rh/Rh
Hologic	Lorad Selenia	Mo/Mo, Mo/Rh, W/Rh[1], W/Ag[1]
Hologic	Selenia Dimensions	W/Rh, W/Ag[2]
Philips[3]	MicroDose Mammography D40	W/Al
Philips[3]	MicroDose Mammography L30	W/Al
Siemens	Mammomat Novation DR	Mo/Mo[4], Mo/Rh[4], W/Rh
Siemens	Mammomat Inspiration	Mo/Mo[4], Mo/Rh[4], W/Rh

[1]: For the study published in Paper I the target/filter combinations Mo/Mo and Mo/Rh were applied, while for the study published in Paper IV the Mo anode had been replaced by a W anode and the target/filter combinations W/Rh and W/Ag were used.

[2]: In the user manual for Hologic Selenia Dimensions the target/filter combination W/Al is also listed, although this combination was not applied in this study.

[3]: The scanning multislit system was developed by Sectra. Royal Philips Electronics (Best, The Netherlands) bought Sectra's (Linköping, Sweden) mammography-modality operations worldwide (except for New Zealand and Australia), and took over the modality operation September 1, 2011.

[4]: Only the target/filter combination W/Rh was used.

4.2 Material: Patient population

All women aged 50-69 years are invited to biennial screening in the NBCSP. The women included in Paper I, III and IV were chosen at random. The women are invited by a

personal letter to have a two view (CC and MLO) mammographic screening biennially (Figure 9).

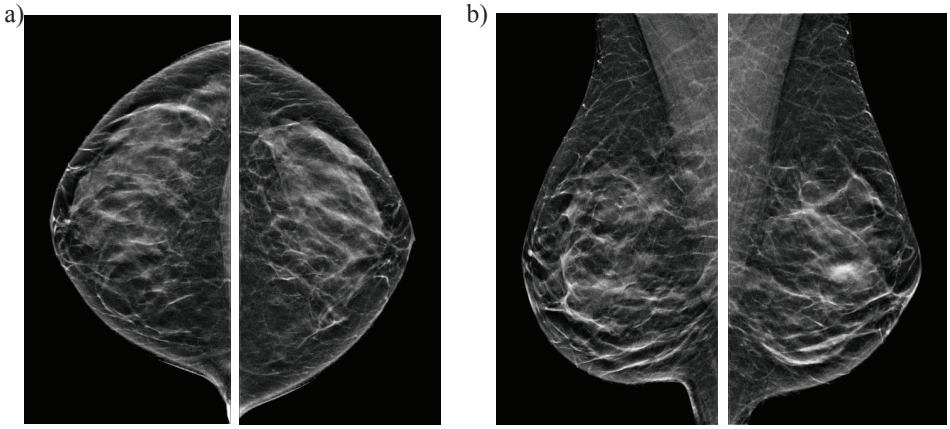

Figure 9. Two view screening examination in the Norwegian Breast Cancer Screening Program (NBCSP) is generally made up of one a) CC and one b) MLO of the left and right breast, respectively. Pictures: courtesy of Oslo University Hospital.

4.3 Method: Estimation of the mean glandular dose (MGD) in the NBCSP

The MGD is normally estimated per projection (craniocaudal (CC) and mediolateral oblique (MLO)), and per examination, where one examination consists of one projection of each breast.

When estimating the MGD in this papers that are part of this thesis, the method and conversion factors used proposed by Dance et al. have been applied (41, 42, 70).

The incident air kerma, $K_{a,i}$, was measured with a Radcal Ion Chamber Model 10x5-6M connected to a Radcal Electrometer/Ionchamber Model 9060 and Radcal Radiation Monitor Controller Model 9010 (Radcal Corporation, Monrovia, CA, USA) (Figure 10). Radcal Ion Chamber Model 10x5-6M is a dedicated mammography chamber. Calibration was conducted in 2008, 2010 and 2012. Until 2008 the Radcal ionization chamber was calibrated at the Radiological Protection Centre (RPC) (location: London, UK), but since 2010 it has been calibrated at the Secondary Standard Dosimetry Laboratory (SSDL) at the NRPA (location: Østerås, Norway). The calibration factors from the calibration certificate are applied when estimating the air kerma.

The incident air kerma, $K_{a,i}$, was measured for all applied target/filter and tube voltages for each mammography screening unit. When conducting the measurements, the ionization chamber was positioned 45 mm above the breast support table on a line extending from the tube focus to a point on the mid-line of the breast support table, 6 cm from the chest wall edge, and in contact with and below the compression paddle. The inverse square law was applied in order to estimate the $K_{a,i}$ at any other compressed breast thickness:

$$K_{a,i} = d_{FSD}^{-2} Y Q \qquad (16)$$

Where Q is the tube current-exposure time product (mAs) for an individual image and Y is the x-ray tube output (mGy/mAs) for the relevant radiation quality, i.e. target/filter combination and tube voltage for a specific mammography unit (224). The focal point-to-(breast) surface distance, d_{FSD}, is the difference between the distance from the focus to breast support table minus the compressed breast thickness (224).

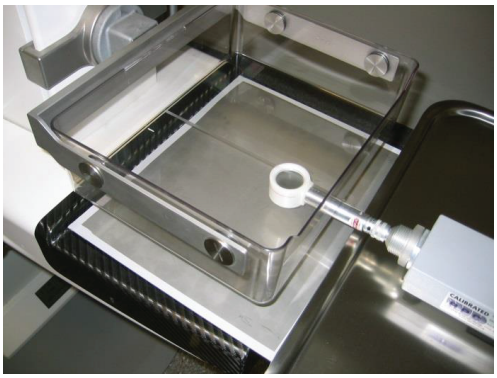

Figure 10. The ionization chamber used in the measurement of incident air kerma (Radcal Ion Chamber Model 10x5-6M connected to a Radcal Electrometer/Ionchamber Model 9060 and Radcal Radiation Monitor Controller Model 9010 (Radcal Corporation, Monrovia, CA, USA)). Photo: Norwegian Radiation Protection Authority (NRPA).

4.3.1 Diagnostic reference level (DRL)

DRL is one of the most efficient and pragmatic tools used for optimization of radiological examinations locally in hospitals (62, 225-227). DRL is defined by the ICRP as “a form of investigation level, applied to an easily measured quantity, usually the absorbed dose in air, or tissue-equivalent material at the surface of a simple standard phantom or a representative patient" (228), and by the European Commission as the “dose levels in medical radiodiagnostic practices or, in the case of radiopharmaceuticals, levels of activity, for typical examinations for groups of standard-sized patients or standard phantoms for broadly defined types of equipment” (225).

The purpose of a DRL is to trigger the first step in the optimization of patient doses (226). Complete optimization is concerned with maximization of risk/benefits, where the diagnostic outcome is relevant (229). Justification should be based upon accuracy of diagnosis as well as dose considerations.

It has been recommended to use the third-quartile values, the 75th percentile, of the distributions of the mean doses observed on a sample of standard-sized patients examined in each x-ray room as a simple indication of abnormally high doses when establishing a national DRL (NDRL) (226). The DRL is a useful tool in the optimization of mammography units, as well, and it has been proposed by a joint working party in the UK to base the DRL on the average MGD of MLO views for breasts with a compressed breast thickness of 55±5 mm (226). Further, the working party has proposed to apply a percentile closer to the top end of the distribution, because in mammography it is expected that the doses fall within a limited range. A 95th percentile has been applied in a study in Belgium (for SFM units) and Ireland (for FFDM units) (230-232).

4.4 Method: Assessing the image quality

4.4.1 Low contrast detectability

In mammography it is essential to distinguish between objects with very small contrast and diameter. Threshold contrast tests are a common means of assessing image quality for noise limited imaging systems (233). An analysis of contrast detail, i.e. detecting very low contrast and detecting very small details, for SFM and FFDM systems is performed by using the CDMAM 3.4 phantom (Artinis Medical Systems B.V., PW Elst, The Netherlands) (Figure 11) (234-236).

The image quality standard is based on contrast-detail measurements and a minimum standard is chosen to ensure that FFDM systems are as good as or better than current SFM systems (237). Software that automatically reads the phantom recordings is used (238-240). A contrast detail curve relating object size and contrast at some fixed detection threshold is plotted.

The CDMAM 3.4 phantom consists of an aluminium base with gold discs (99.99% pure gold) of varying thickness (0.03-2.00 μm) and diameter (0.06-2.0 mm) (241). The gold

discs are arranged in a matrix (16 rows by 16 columns). The disc diameter does not vary within a row, while the thickness increases (partly) logarithmically. Within a column the thickness of the discs is constant and the diameter increases logarithmically. Each square contains two discs with the same thickness and the same diameter. One is placed in the centre and the other in a randomly chosen corner. Easily recognizable patterns have been avoided. The matrix is rotated 45 degrees and the corners of the matrix are skipped. There are two reasons for this: a) getting a better focus on the interesting part (low contrast, small diameter) and b) making the recognition of the patterns more difficult. The matrix grid is silkscreen printed with x-ray contrasting paint.

The aluminium base (0.5 mm thick Al 1050, 99.5% pure aluminium) is attached to a Plexiglas® cover (5 mm, PMMA). When exposing the CDMAM phantom at “normal” conditions (Mo anode, 30 mm Mo filter, 28 kV), the aluminium base and PMMA cover together have an equivalent PMMA thickness of 10 mm. The phantom is delivered with 4 PMMA plates (each with 10 mm thickness) which are used for the simulation of different breast thicknesses.

Contrast-detail phantoms which show objects on a uniform background may not be ideal to predict the performance of a system in clinical practice (138).

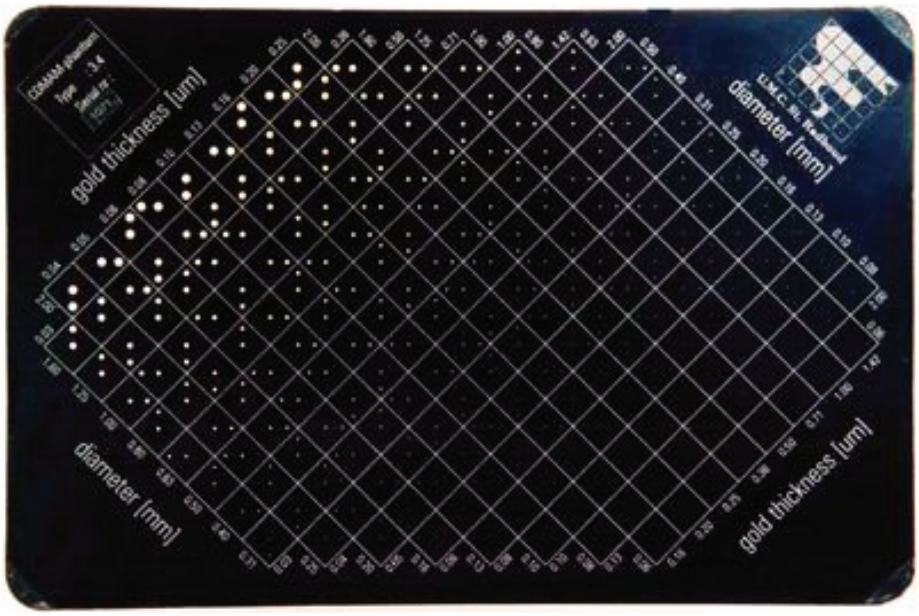

Figure 11. Photograph of the CDMAM 3.4 phantom (Artinis Medical Systems B.V., PW Elst, The Netherlands) consists of an aluminium base (0.5 mm thick Al 1050, 99.5% pure aluminium) attached to a Plexiglas® cover (5 mm, PMMA). Gold discs (99.99% pure gold) of varying thickness (0.03-2.00 μm) and diameter (0.06-2.0 mm) are arranged in a matrix (16 rows by 16 columns). Each square contains two discs with the same thickness and the same diameter. One is placed in the centre and the other in a randomly chosen corner.

4.5 Method: Dose-risk estimates

In the hierarchical model of efficacy proposed by Fryback and Thornbury cost-benefit analyses and an evaluation of number of lives saved are part of Level 6, societal efficacy (81). Dose-risk estimates seem to fall under Level 6 in the hierarchical model of efficacy.

In 2002 Preston et al. analyzed data from eight cohorts of irradiated women, and based on these data published an EAR model to assess the risk of radiation-induced breast cancer (180-182, 204-207, 242). The women included in the cohorts had been exposed to radiation doses ranging from 0.2 to 5.8 Gy delivered both at low and high dose-rates. Preston et al. stated that their analysis did not provide evidence against a linear dose-response model in the low-dose region, for which data was missing. Their EAR model has subsequently been widely used to estimate the risk of radiation-induced breast cancer due to mammography and mammographic screening (223, 243, 244). An ERR model was used by Berrington deGonzales in order to estimate the potential risk of radiation-related cancer from screening in the UK (179), although ICRP and BEIR VII recommends using an EAR model when estimating the risk for the organ breast (62, 171). In 2011 Yaffe and Mainprize described a scheme for estimating the risk of radiation-induced breast cancers, breast cancer deaths, the number of lives lost, and lives saved for a variety of mammography screening scenarios based on Preston et al.'s model (180, 223, 242). In Paper V this model is applied in order to estimate the correlation between dose and risk of radiation-induced breast cancer.

5 Summary of publications

Paper I

Patient doses from screen-film and full-field digital mammography in a population based screening programme.

Hauge IH, Pedersen K, Sanderud A, Hofvind S, Olerud HM. *Radiation Protection Dosimetry,* January 2012, Vol. 148, No. 1, pp. 65–73. Published online before print 17 February 2011.

Purpose

The aim was to compare the MGD per exposure from different manufacture/models of SFM and FFDM systems.

Materials and methods

In total, 31 screening units in the NBCSP were included (24 SFM and 7 FFDM). Six different FFDM models from four different manufacturers (GE, Hologic, Philips and Siemens) were included: GE Senographe 2000D, GE Senographe DS, GE Senographe Essential, Hologic Lorad Selenia, Philips MicroDose Mammography D40, and Siemens Mammomat Novation DR. Technical parameters from approximately 50 women from the screening units were collected in the study period September 2006 – October 2008. Based on the technical parameters the MGD was estimated for the 1567 women examined at the 31 screening units.

Results

The average MGD per examination was 2.84±0.08 mGy for the 24 SFM units and 2.49±0.08 mGy for the FFDM units. The MGD per exposure was significantly lower for FFDM compared with SFM (CC: 1.19 versus 1.27 mGy, respectively; MLO: 1.33 versus 1.45 mGy, respectively), but the MGD varied between manufacture/model and not all of the FFDM units provided lower doses than the SFM units. With the exception of the thinnest compressed breast thicknesses (20-29 mm), the FFDM unit Philips MicroDose

Mammography D40 provided the lowest MGD per exposure out of all (n=31) screening units.

Conclusion

One argument for changing from SFM to FFDM systems has been that FFDM provide a lower radiation dose to the screened women. Previous studies had shown that FFDM systems are capable of producing lower doses compared with SFM systems, but this study shows that changing from a SFM to a FFDM unit of any manufacture/model unit does not guarantee a lower MGD per exposure than SFM.

Paper II

The readout thickness versus the measured thickness for a range of screen film mammography (SFM) and full-field digital mammography (FFDM) units.
Hauge IH, Hogg P, Szczepura K, Connolly P, McGill G, Mercer C. *Medical Physics*, January 2012, Vol. 39, No. 1, pp. 263-271.

Purpose

This study aimed to develop a simple, clinically adaptable and accurate method to measure the difference between the readout and measured compressed breast thickness.

Materials and methods

A breast thickness measuring device (TMD) was constructed. The method was comprised of three stages. First, a clinically realistic breast phantom and backing plate with the creation of a rigid torso was tested. Second, the TMD was designed and tested. Finally, using the TMD, the breast phantom with its backing plate was used to assess several mammography units/paddle combinations. The measurements were performed on different mammography units from three different manufacturers (GE, Hologic and Siemens). Both SFM and FFDM were included. This selection is representative of machines that were in clinical use at the time of the study. A compression of 60 and 100 N were applied. Both flexible and nonflexible paddles of two different paddle sizes, standard size (approximately: 18 cm x 24 cm (18x24)) and large size (approximately: 24 cm x 30 cm (24x30)), were included in the study.

Results

The difference in the readout thickness and the measured thickness varies between units of the same model and between manufacturers. Both an over- and underestimation was found.

Conclusion

Individual correction factors for the readout compressed breast thickness may need to be established for each unit, paddle selection and applied compression force.

Paper III

Uncertainties involved in the estimation of mean glandular dose for women in the Norwegian Breast Cancer Screening Program (NBCSP).

Hauge IH, Olerud HM. *Radiation Protection Dosimetry,* June 2013, Vol. 155, No. 1, pp. 81-87. Published online before print 27 November 2012.

Purpose

In Paper II a difference in readout and measured compressed breast thickness was found for the different units. In Paper III the impact of the uncertainty in the compressed breast thickness on the MGD was examined. In addition, uncertainties in HVL, glandularity, kerma, and s-factor on the estimated MGD were also examined in order to obtain a broader view of the uncertainties in MGD.

Materials and methods

Estimation of MGD has been conducted by applying the method of Dance et al. (1990, 2000, 2009).

Results

The largest contributions to the overall uncertainty in MGD are uncertainties in the air kerma (+12 %), underestimation of the thickness of +13 mm (-10.7 %), change in HVL by -0.05 mm (-9.0 %), overestimation of the thickness of 28 mm (+8.7 %), and changing the glandularity to an age-dependent glandularity distribution (+8.4 %). Uncertainties in thickness of approximately ±10 mm adds uncertainties in the MGD of approximately ±10% and uncertainty in the mammographic density of ±10% will lead to an uncertainty in

the MGD of ±4%. The inherent uncertainty in the air kerma, given by the European protocol on dosimetry will add an uncertainty of 12%.

Conclusion

The total uncertainty in the MGD is estimated to be approximately 20%, taking into consideration uncertainties in compressed breast thickness (±10%), the air kerma (12%), change in HVL by -0.05 mm (-9.0%), uncertainty in the s-factor of ±2.1%, and changing the mammographic density to an age dependent mammographic density distribution (+8.4%).

Paper IV

New diagnostic reference level for full-field digital mammography (FFDM) units.

Hauge IH, Bredholt K, Olerud HM. *Radiation Protection Dosimetry,* December 2013, Vol. 157, No. 2, pp. 181–192. Published online before print 14 June 2013.

Purpose

In the NBCSP all units are now FFDM, and the establishment of a new DRL is called for. Systematic differences between categories of manufacture/models were investigated with respect to MGD and FOM.

Materials and methods

The 75^{th} and 95^{th} percentile were estimated for the distribution of mean MGDs for 26 FFDM units (84%) operating in the NBCSP in 2010/2011 for the compressed breast thickness range 55-65 mm with the intention of establishing a national DRL.

Results

A large spread in MGD for the different manufacture/models is found. As national DRL the value 2.0 mGy is proposed, which is the 95^{th} percentile of the dose distribution of all units, while the 95^{th} percentile should be used to determine which units can be accepted for use for diagnostic purposes. In addition, to identify the need for optimization, we propose a set of manufacture/technology specific DRLs based on the 75^{th} percentile values of the respective dose distributions; the value of 1.4 mGy may serve as DRL for both the GE Senographe Essential and Siemens Mammomat Inspiration models.

Conclusion

The results in this study do however indicate that the DRL is not sufficient as a tool to identify units in need of optimization. The image quality, by means of FOM, defined here as SDNR squared divided by the MGD, should be considered as well, especially when new manufacture/models are introduced on the market.

Paper V

The risk of radiation-induced breast cancers due to biennial mammographic screening in women aged 50-69 years is minimal.

Hauge IH, Pedersen K, Olerud HM, Hole EO, Hofvind S. *Acta Radiologica,* accepted for publication 1 November 2013. Published online before print 5 December 2013.

Purpose

The main aim of mammographic screening is to reduce the mortality from breast cancer. However, use of ionizing radiation is considered a potential harm due to the possible risk of inducing cancer in healthy women. The aim of the study was to estimate the potential risk of radiation-induced breast cancers due to organized mammographic screening as performed in Norway.

Materials and methods

We used a previously published EAR model which assumes a dose-response relationship in accordance with the LNT model. The estimates were calculated for 100 000 women aged 50-69 years, a screening interval of two years, and a follow-up until age 85 or 105 years. Radiation doses of 0.7, 2.5, and 5.7 mGy per screening examination, a latency time of 5 or 10 years, and a DDREF of 1 or 2 were applied.

Results

The total lifetime risk of radiation-induced breast cancers per 100 000 women was 10 (95% CI: 4-25) when the women were followed from age 50 to 85, for a dose of 2.5 mGy, a latency time of 10 years, and a DDREF of 1. For the same parameter values the number of radiation-induced breast cancer death was 1 (95% CI: 0-2).

Conclusion

The risk of radiation-induced breast cancer and breast cancer death due to mammographic screening is minimal. Women should not be discouraged from attending screening due to fear of radiation-induced breast cancer death.

6 Discussion

Here the shift in dose level when changing from SFM to FFDM, differences in exposure factors for different manufacture/models, accuracy of MGD estimates, establishment of a DRL, and the radiation dose in the NBCSP in a dose-risk perspective will be discussed.

6.1 Transition from SFM to FFDM in mammography

In Paper I the transition from SFM to FFDM was studied to see the impact on the dose level. The ideal set-up would have been to conduct a study when only SFM units operated in the organized screening program, and then after the transition to FFDM, do a similar study with only FFDM units. Since the transition from SFM to FFDM has taken place over such a long period of time (from 2000 to 2011), we ended up doing a study where only a few FFDM units had been implemented in the program, and then comparing the dose level for these few FFDM units with SFM units operating in the program.

One of the arguments for changing from SFM to FFDM in the NBCSP has been that FFDMs provide lower radiation doses than SFM units. On the other hand, in digital imaging it is possible to obtain higher doses than with SFM, where signal saturation would occur, and it is therefore particularly important to monitor the doses. In 2003 Obenauer conducted a phantom study which showed that the FFDM unit provided lower doses than the SFM unit (155). Clinical studies have supported these findings (151, 153, 154, 245). Hermann et al. showed that a reduction in dose of 25% is possible (153). However, these studies were conducted on only one FFDM system, namely GE Senographe 2000D. In a review from 2006 of several studies it is claimed that a reduction of 50% is possible with

FFDM compared to SFM (119). Although, no references to what studies these results are based on are given. Hendrick et al. compared radiation doses from SFM and FFDM of different manufacture (SenoScan (Fischer Imaging), 5000D CR System (Fujifilm Medical Systems USA), GE Senographe 2000D, and Lorad/Hologic CCD (charge-coupled device) and Hologic Lorad Selenia) and found a 28% lower MGD for FFDM than for SFM for 18 GE Senographe 2000D units (121). Further, they found an 18.0-18.5% increase in MGD per view for Hologic Lorad Selenia. The increase was valid for the entire thickness range. When averaged over all digital manufacturers included in Hendrick et al.'s study, MGD per primary view was 22% lower for FFDM than for SFM, whereas the total MGD per woman was 17% lower for FFDM than SFM. Further, Hendrick et al. found for the GE Senographe 2000D that for thinner breasts the FFDM units did not provide lower doses than SFM, while for thicker breasts (>4 cm) GE Senographe 2000D provided lower doses than SFM (121). Philips uses the multislit scanning technology, which has been shown to perform as well as or better than SFM and provide lower doses than other systems (246-248). For the thicker compressed breast thicknesses (≥50 mm) the MGD per exposure was significantly smaller for FFDM than for SFM (247). In conclusion, from these studies it seems that for thicker breasts FFDM systems do provide a lower dose, but not all FFDM are capable of providing lower doses than SFM systems.

The results in Paper I showed that using FFDM does not guarantee a lower MGD per exposure than SFM. This is in agreement with earlier studies (119, 121, 151, 153, 154, 245-247). Two FFDM models (Hologic Lorad Selenia and GE Senographe 2000D) provided an average MGD higher than four of the SFM models in Paper II (Siemens Mammomat 300, Siemens Mammomat 3000, Instrumentarium Alpha and GE Senographe DMR). Our study seems to agree with Hendrick et al.´s study for Hologic Lorad Selenia, but not for GE Senographe 2000D (121). The difference between our study and Hendrick et al.´s study is that we only had one Hologic Lorad Selenia unit and one GE Senographe 2000D unit. We found an 18% higher MGD for GE Senographe 2000D compared to the average for all SFM units in our study (11% higher than for GE Senographe DMR (SFM)). For Hologic Lorad Selenia we found a 9% higher MGD than for the average of all SFM units in our study. A clinical study conducted by Hermann et al. found a MGD of 1.51 mGy (standard deviation: ±0.34) for a GE Senographe 2000D unit (153). This represented a 25% lower dose for FFDM compared to SFM, when comparing their results with a prior

study where an overall average MGD of 2.6 mGy (range: 1.3-2.6 mGy) was found for SFM units, (153, 249). For GE Senographe 2000D we found a MGD of 1.57±0.06 mGy, which is close to what Hermann et al. found, although the average SFM was lower in our study than in Hermann et al.´s, ending up with different conclusions regarding if FFDM provide higher or lower doses than SFM. Moran et al. found a MGD of 1.88±0.01 mGy for a GE Senographe 2000D unit (154). This is a higher MGD than what we found in our study. Moran et al. compared this dose to SFM units equipped with Mo/Mo target/filter combinations and two types of screen film systems, fast and slow (154). They found that for small and intermediate compressed breast thicknesses the dose values are similar for the FFDM unit and for the SFM unit with slow image receptors, but much higher if compared with SFM with fast image receptors. For larger compressed breast thicknesses dose values are similar for the FFDM system and SFM with fast image receptors. In other words, for fast image receptors the GE Senographe 2000D did not necessarily provide lower doses than SFM systems.

The FFDM system showed a 33% lower and a 32% higher than the third quartile of the entrance surface air kerma values for slow and fast screen film systems, respectively (154). This is in accordance with the findings in our study. Kodak Min-R 2000/Min-R 2190 is a faster screen film combination than Kodak Min-R EV/EV (133). In Paper I it was shown that even if the OD was not statistically different for the two screen film combinations Min-R 2000 and Min-R EV ($p = 0.844$), the average MGD for the systems using Min-R EV (CC: 1.22 ± 0.02 mGy, MLO: 1.32 ± 0.03 mGy) was significantly smaller (CC: $p = 0.001$, MLO: $p < 0.001$) than for the systems utilizing Min-R 2000 (CC: 1.22 ± 0.02 mGy, MLO: 1.32 ± 0.03 mGy)

6.2 Optimization of mammography units in screening

The ICRP have published three principles that are to be fulfilled in modern radiological protection (62). One of them is the principle of optimization. Optimization in digital

radiology means that only the dose level required for the medical imaging task should be used, and that one should refrain from using any additional dose beyond that level (250). A mammography unit needs to be optimized with respect to the applied target, filter and selected tube voltage. The selection of these exposure factors are often determined by an AEC termination device, and has been programmed through for instance lookup tables or are determined based on compressed breast thickness.

In Paper I it was shown that for Hologic Lorad Selenia and GE Senographe 2000D the applied target/filter combinations did not agree with what has been recommended in other studies (201, 230). Dance et al. recommends that Mo/Mo should only be applied for 2 cm compressed breast thicknesses (201). The systems that use Mo/Mo were Hologic Lorad Selenia and GE Senographe 2000D. The Hologic Lorad unit in this study applied the target/filter combination Mo/Mo up to compressed breast thicknesses of 59 mm, while the GE 2000D unit applied Mo/Mo up to 42 mm compressed breast thickness. The target/filter combination is in other words applied for thicknesses much higher than what is recommended by Dance et al. GE Senographe 2000D had the possibility of applying the target/filter combinations Mo/Rh and Rh/Rh for thicker breasts, while Hologic Lorad Selenia had the possibility of applying the target/filter combination Mo/Rh. The results in Paper I showed that Hologic Lorad Selenia applied the target/filter combination Mo/Rh for compressed breast thicknesses down to 53 mm. By applying Mo/Rh or Rh/Rh, a lower dose could have been achieved at the same contrast (87, 89). By applying the target/filter combination Mo/Mo the obtained doses were higher than what they could have been, increasing the overall MGD for the FFDM units.

For both Hologic Lorad Selenia and GE Senographe 2000D the optimal beam quality is Mo/Rh 27 kV, with the exception of the thickest and densest breasts where Rh/Rh and a higher kV should be used for GE Senographe 2000D and Mo/Rh 28 kV should be used for Hologic Lorad Selenia (230). Paper I shows that Hologic Lorad Selenia did not apply the target/filter combination Mo/Rh 27 kV at all (0% of the total number of exposures), while the target/filter combination Mo/Rh 28 kV, which is recommended for the thickest breasts for Hologic Lorad Selenia, was only applied once (out of 200 exposures) for a breast with thickness 72 mm. For the GE Senographe 2000D the target/filter combination Mo/Rh 27

kV (13.0% of the total number of exposures) was applied for thicknesses 41-76 mm, Rh/Rh 28-32 kV (53.5% of the total number of exposures) for compressed breast thicknesses 37-100 mm. In other words neither GE Senographe 2000D nor Hologic Lorad Selenia was at the time of our study using the optimal beam quality. In a clinical study it has been demonstrated that it is possible for the GE Senographe 2000D to lower the dose level, but at the same time obtain sufficient image quality (231). In conclusion, FFDM systems has the potential to provide lower doses, but needs to be optimized before being taken into use in an organized screening program.

The results in Paper I did reveal that not all FFDM units in use in the NBCSP at the time of the study were optimized before they were taken into use. Further, it was shown that some mammography screening units were not optimized and an optimization should have been conducted before the screening units were put into use in the NBCSP. This will affect the dose level. In Paper IV it was shown that the dose level varies for units of the same manufacture/model and that an optimization of the systems with doses far from the average for that manufacture/model would hopefully have managed to bring that unit closer to the average MGD for that manufacture/model. Based on the results in Paper I and Paper IV, it was shown that dose surveys do reveal the need for optimization. By conducting regular dose surveys for all units in a screening program, it is possible to discover such differences between different units of the same manufacture/model and conduct optimization schemes. Without dose surveys, the mammography units may be operated at a less than optimal level. Dose surveys are therefore an important supplement to annual technical quality controls, where the beam quality settings for a selection of compressed breast thicknesses are tested. AEC testing has been shown to be one of the most important procedures (251, 252). In conclusion, it suggests that more emphasis should be put on optimization in a technical quality control schema.

6.3 Factors that affect the accuracy of the MGD

The radiation dose is measured for several reasons: a) to assess the performance of mammographic imaging equipment, b) to compare imaging systems, c) to comply with regulations and techniques, d) in order to perform benefit-risk analysis, and e) to answer questions regarding dose level from patients and physicians (68, 69). National surveys of radiation dose were implemented in the late 1970s (253). Accurate estimation of MGD is important because these estimates are used to evaluate the risk of radiation-induced cancers, to compare imaging systems and techniques and to assess the performance of mammographic imaging equipment. Inaccurate dose estimates will lead to the wrong conclusions when it comes to the performance of imaging systems. Here I would like to discuss factors that affect the accuracy of MGD estimates.

The MGD is estimated according to equation (18) from the incident air kerma at the breast surface without backscatter and conversion factors (g, c and s). The incident air kerma is estimated from the point-to-(breast) surface distance, d_{FSD}, according to equation (19), and d_{FSD} relies on the compressed breast thickness. Uncertainties in the compressed breast thickness, as shown in Paper II, will result in uncertainties in incident air kerma. The g-factor relies on the compressed breast thickness and HVL, while the c-factor relies both on the mammographic density, the readout compressed breast thickness and HVL. Mammograms are used in order to estimate mammographic density (254-257). Further, the standardized mammographic density measurement for breast cancer risk analysis relies on accurate measurement of the compressed breast thickness (258). Inaccuracies in the compressed breast thickness will induce unacceptable errors in the estimation of mammographic density. In other words, thickness inaccuracies will lead to inaccuracies in the mammographic density, which will lead to inaccuracies in the c-factor. The s-factor relies upon choice of target/filter combination, which for some manufacturers (Instrumentarium, Siemens and Hologic) does rely upon compressed breast thickness. In conclusion, one parameter (c-factor) relies on mammographic density, two parameters

relies on HVL, while three or all parameters, depending on the type of mammography unit used in the examination, relies on the compressed breast thickness.

Uncertainties in the a) mammographic density, b) the readout thickness and c) the HVL will lead to uncertainties in the estimation of the MGD. But it seems that uncertainties in the compressed breast thickness will have the greatest impact, since so many of the parameters rely on the compressed breast thickness.

Readout thickness has been shown to be inaccurate, since compression paddles may deform/tilt during a mammographic examination (218, 219, 221, 258, 259). This can lead to differences between the readout and measured compressed breast thickness of the compressed breast. A maximum variation of 21.1 mm in the chest wall to nipple direction was found by Diffey et al. (219). Further, tilt during a mammographic examination will affect the volumetric breast density estimation (259). But mammography units were never designed to provide an accurate display of the compressed breast thickness. The compressed breast thickness uncertainty as specified by the manufacturers can be as large as ±10 mm (Table I, Paper II).

Methods have been proposed which provide a better estimate of the compressed breast thickness (218, 220-222). An accurate method using optical stereoscopic photogrammetry has been proposed by Tyson et al. (222). They found a variation in readout thickness with as much as 15 mm when compressing the same breast or phantom (222). However, the method developed by Tyson et al. (222) is labor intensive, being highly dependent on room lighting and also on image quality. In Paper II we came up with an easy method for measuring the compressed breast thickness, not requiring a lot of equipment. The variation between readout and measured compressed breast thickness seemed to vary between units of the same manufacture/model, urging the need to conduct corrections for each and every one of the units. Thus it does not seem sufficient to come up with a function for a given manufacture/model that would give the relation between compressed breast thickness and compression force for all units of the same manufacture/model. Mawdsley et al. proposed such functions, but from the results in our study it seems that they might only apply for one

specific unit (221). Our method is easy, although not as accurate as Tyson et al. (222), which is a weakness in the study. Also, if the compression changes over time, the measured compressed breast thickness will change.

Hemdal (260) found that if an ionisation chamber is used, the compression paddle should be in contact with the chamber, otherwise the air kerma and absorbed dose will be underestimated due to the forward-scattered radiation from the compression paddle to the dosemeter. The forward-scattered contribution to the air kerma was found to be 2-10%, and increased with increasing compression paddle thickness and HVL. When measuring the air kerma, the paddle was always in contact with the ionization chamber (RadCal), and based on Hemdal's work it should not be necessary to do any additional corrections.

By correcting for the discrepancy between measured (real) and displayed (readout) compressed breast thickness, a more accurate MGD can be achieved. Uncertainties in compressed breast thicknesses of approximately ±10 mm will result in uncertainties in the MGD of approximately ±10%. In Paper IV a range in MGDs for the compressed breast thickness range 55-65 mm was found for Siemens Mammomat Inspiration (range: 1.18-1.66 mGy) and GE Senographe Essential (range: 0.92-1.65 mGy). Since a correction of the displayed compressed breast thickness was not conducted the range in MGD could have been the result of a discrepancy in compressed breast thickness between the units, but taking a possible 10% uncertainty in the MGD into account, this does not result in the range in MGD as observed for Siemens Mammomat Inspiration and GE Senographe Essential. Since no correction in the displayed (readout) compressed breast thickness was conducted in Paper I and IV, it can be said that this is a weakness in these studies. However, it seems that a recent dose survey conducted in Ireland proceeded in the same manner as was conducted in Paper I and IV: they used the compressed breast thickness found in the Digital Imaging and Communications in Medicine (DICOM) header (44, 259). This does not gratify our approach of not correcting for the compressed breast thickness used for the different manufacture/models, but rather points to a problem in dose surveys. Namely, that it should be specified if a correction has been conducted or not for the compressed breast thickness, given the results in Paper II, where it was shown that there is a difference between measured (real) and displayed (readout) compressed breast thickness

for the different manufacture/model and even between units of the same manufacture/model. If such a correction is to be applied, it is important to specify what factor has been used. That said, since the compressed breast thickness is involved in determining so many of the parameters for the MGD, it would be of great help if the compressed breast thickness accuracy for the different manufacture/models was far more accurate than it actually is. That would be of tremendous help when conducting dose surveys where several units from different manufacture/models are included.

There is one known weakness in the study presented in Paper IV. Some of the HVLs and radiation outputs for some of the different radiation qualities (target/filter/kV) were measured a long time after the collection of the exposure parameters from the women. If we were to do the studies all over again, we would make sure that the measurements for the HVLs and radiation outputs would be conducted after the collection of the exposure factors, in order to make sure that all HVLs and radiation outputs would be measured as close in time to the collection of the exposure data as possible. Gregory et al. have listed the numerous error sources that contribute to the uncertainty of exposure-related quantities, such as HVL, AEC reproducibility, MGD, and radiation output rate (261). The error sources that affect the measurement uncertainty of the four quantities are: a) exposure meter model, b) exposure meter calibration type, c) x-ray unit output, d) attenuator purity, e) attenuator thickness, f) attenuator increment size, g) exposure meter positioning, h) beam collimation, i) beam angle, j) pressure, k) temperature, l) dose conversion factor (*g*), and m) off-axis exposure. While all of them affect the MGD, only a)-j) affect the HVL and only a)-c), g), j) and k) affect radiation output rate. For the HVL efforts to carefully position exposure meters and measure and correct for beam angulation did not reduce the uncertainty significantly. The uncertainties of the four exposure-related quantities were found to be ±1.6% (HVL), ±0.0008% (AEC reproducibility), ±2.3% (MGD), and ±2.1% (radiation output rate) for x-ray units applying Mo/Mo. This would then add to the uncertainties in Paper III as well. However, the numerous error sources that contribute to the uncertainty of exposure-related quantities contribute less as for instance uncertainty in the compressed breast thickness. Also, Gregory et al. conducted their studies on Mo/Mo x-ray beams, which are low energy. The unique error sources for these might not be the same as for FFDM units, for which the results in Paper I showed do apply target/filter

combinations of higher energy. It would be expected that the error sources would be smaller for higher energy.

6.4 Use of diagnostic reference level (DRL) as a tool in acceptance testing

The purpose of a DRL is to indicate abnormally high radiation doses and trigger the first step in the optimization of patient doses (226). The DRL has been and will continue to indicate the accepted dose level in mammographic examinations (230, 232, 262, 263). In general diagnostic radiology, the 75th percentile is applied for the DRL, while in mammography the 95th percentile has been used, arguing that the doses are much more optimized, and vary to a smaller extent (230). For SFM this may be true, as the detectors are similar and perhaps of the same manufacture (Kodak), but for FFDM different detector technology is available that leads to a difference in dose (Paper I).

In the NBCSP a shift from SFM to FFDM has taken place over a long period of time (Figure 8). A new DRL for FFDM was thus needed. In Paper IV the DRL for the FFDM units operating in the NBCSP in 2010-2011 was found. Data were collected for approximately 50 women, which is in the recommended range of 10-60 women (251). The 75th percentile is 1.4 mGy and the 95th percentile is 2.0 mGy for all units. The reason for estimating both the 75th and 95th percentile is that DRL is defined as the 75th percentile, but since a joint working group in the UK proposed using a percentile closer to the top end of the distribution (226), we have decided to estimate both percentiles. In a study in Belgium where the DRL was estimated for SFM units, the 95th percentile was applied, arguing that the doses were expected to be quite similar due to extensive quality assurance for mammography units (230, 231). In Paper IV we found that the average MGD for different manufacture/model (GE Senographe DS, GE Senographe Essential, Hologic Lorad Selenia, Hologic Selenia Dimensions, Philips L30 and Siemens Inspiration) ranges from 0.69 to 2.11 mGy, a range of 1.42 mGy, for the compressed breast thickness interval 55-65 mm. The highest MGD was 206% larger than the smallest MGD. This is quite a large

range, and due to the difference in technology, it might be a better idea to separate the manufacture/models from each other and evaluate the units within each category of manufacture/model. As national DRL the 95th percentile, 2.0 mGy, is proposed, but in order to identify the need for optimization, we propose a set of manufacture/technology specific DRLs based on the 75th percentile values of the respective dose distributions. This will take into consideration the difference in dose level between the manufacture/models and better identify those units that are in need of optimization for each manufacture/model. Only Siemens Mammomat Inspiration and GE Senographe Essential were represented with several units, and therefore it was only possible to establish technology specific DRLs based on the 75th percentile values for these two manufacture/models; the value for both being 1.4 mGy.

In the NBCSP there are multiple units from GE Senographe Essential and Siemens Inspiration, enabling a comparison of MGD and FOM between these units. A study has been conducted comparing GE Senographe DS and GE Senographe Essential detectors, finding that GE Senographe DS showed statistically significant poorer detection ability than GE Senographe Essential (264). Overall, for the FOM we also found that the GE Senographe DS unit provided a lower FOM than the GE Senographe Essential units. Further, the results in Paper IV showed that there is a large variation in FOM for the GE Senographe Essential units, compared to the Siemens Mammomat Inspiration units, for which the FOM seems to vary less for the different units. Such a large variation in FOM indicates that an optimization might be needed for some of the units. Based only on the DRL (either the 75^{th} or 95^{th} percentile) this was not so apparent. The results in Paper IV showed that three Siemens Mammomat Inspiration and two GE Senographe Essential had an average MGD above the 75^{th} percentile. Further, it was shown that one Siemens Mammomat Inspiration and one GE Senographe Essential had an average MGD above the 95^{th} percentile. Applying the 95^{th} percentile would then only indicate that one GE Senographe Essential was in need of optimization, while from the large difference in FOM for GE Senographe Essential units one might think that more of them were in need of optimization. Using only the DRL as a means of optimization criteria, one might miss out on the other units in need of optimization.

The results in Paper IV do indicate that the DRL is not sufficient as a tool to identify units in need of optimization. This is in agreement with Svahn et al., who have also shown that the radiation dose and performance (as described by the FOM) should not be evaluated independently (46). The FOM, defined as SDNR squared divided by the MGD, should be considered as well, because the results in Paper IV show that those units with high FOMs do not necessarily have low MGDs, and those units with low FOMs do not necessarily have high MGDs. Zdesar has published reference levels for image quality, in the form of contrast index values, where contrast index is defined as the difference in OD between 100% glandular and 100% fatty regions of a phantom image (265). The mammography units included were mainly SFM units. Zdesar ranged the units from worst to best contrast index, and the first quartile is used as a reference level (265). For the SFM units no correlation between contrast index and MGD was found. Zdesar conclude that this might be due to the fact that after the optimal mean OD is reached, contrast depends on other parameters than the dose (mainly on material and the film-developing process). It might be that one could establish reference levels for the FOM for the different manufacture/models, setting a minimum value for the FOM. Any unit having a lower FOM would have to go through optimization. This would combine a measurement for both the image quality and the MGD.

In Paper IV we included results from CDMAM tests conducted during the annual quality controls, which may only give a momentary view of the situation if the image quality measurements differ significantly from day to day. However, in an earlier study it has been shown that the measured threshold contrast values are reasonably stable (maximum: 10%), only with some random variations (266). This implies that the estimations are pretty stable, and that the results shown in Paper IV can be used to make general conclusions about each of the units.

6.5 Radiation doses in a dose-risk perspective

Mammography is associated with a small dose of ionizing radiation, which is seen as a disadvantage in mammography screening due to the potential risk of radiation-induced

cancer. In its 2007 recommendations ICRP increased the tissue weighting factor for breast from 0.05 to 0.12 in the light of recent epidemiological findings and the focus on cancer incidence in the detriment calculations (62, 195). Since the NBCSP are inviting asymptomatic women to screening, it is therefore particularly important to follow the ALARA principle. This is achieved with annual quality control and surveillance of the dose level. In order to evaluate the NBCSP as a whole one of the aspects that need to be evaluated is the dose level and the risk of radiation-induced breast cancers. In order to estimate absolute risks we need to apply the models that are currently used for estimating the dose. In Paper V an estimation of the risk of radiation-induced breast cancers, breast cancer deaths, the number of lives lost and lives saved has been conducted with Preston et al.`s model and a schema developed by Yaffe and Mainprize (180, 223). The uncertainty in the model is in the order of 40%. This is reflected in the width of the confidence intervals for risk estimates in Paper V. Here, the results in Paper V, the model in itself, and what is known from epidemiologic and cell studies for the dose level applied in mammography will be discussed.

When applying a model that assumes an LNT relationship, we found that one death (95% confidence interval: 0-2) in 100 000 women might be induced by radiation when the women were followed from age 50 to 85, exposed to a dose of 2.5 mGy, assuming a latency time of 10 years, and applying a DDREF of 1. Of approximately 7900 breast cancer incidences it is possible that 0.05–0.3% of the cases may be due to mammographic screening. One death per 100 000 has been categorized as a minimal risk (267). We therefore concluded that radiation doses in the NBCSP are of minimal risk to the women attending the NBCSP.

The latency time and DDREF are both factors that influences on the risk estimate. Earlier studies have applied a latency time of 10 years when assessing the breast cancer risk (208, 223), and we decided to apply a latency period of 5 and 10 years, which seemed to be consistent with earlier studies (171, 174, 201, 268). In attempting to estimate lifetime population risks it is important to predict how risk vary as a function of time after radiation exposure. In Paper V, for a dose of 2.5 mGy and a DDREF of 1, a latency time of 5 years resulted in a higher estimate for the number of radiation-induced breast cancers than a 10

year latency time did, 13 (range: 6-31) versus 10 (range: 4-25), respectively. A longer latency time, will result in fewer radiation-induced breast cancers. Further, we applied a DDREF of both 1 and 2, in consistency with UNSCEAR, although higher values for the DDREF has been found (174). Also, it has been suggested that the DDREF decreases with decreasing energy (269). But there are large uncertainties, and the choice of DDREF will influence the dose estimates: a shift to a higher DDREF will reduce the number of radiation-induced breast cancers.

In the cohort data that Preston et al. included in their analysis the mean age for the study population was 27 years (range: 13 – 44 years). This is substantially lower than the screening population in Norway, which is 50-69 years. Sensitivity to ionizing radiation is known to decrease with age (174). An overestimation of radiation-induced breast cancers and breast cancer deaths is therefore expected in our study.

Quantitative information on the risk of cancer in human populations exposed to ionising radiation comes largely from information available from groups exposed at intermediate and high doses and dose-rates (185). This is also the case for the model published by Preston et al. They established their model based on radiation doses 8-20 000 times (0.02-50 Gy) larger than the current MGD per examination (2.5 mGy) for women in the NBCSP (180). The doses in the cohort studies which Preston et al. based their model on were applied at low and high dose-rates. For radiation protection purposes, however, it is thus necessary to estimate the influence of low doses delivered at low dose-rates on cancer induction (185). However, mammography is considered to be a low dose (<100 mGy) and high dose-rate examination (>12 Gy/h (=3.33×10^{-3} Gy/s) (121, 212, 270, 271). In the NBCSP the dose-rate for the target/filter combination Mo/Mo and 28 kV for 27 screening units (16 Siemens Mammomat Inspiration, one GE Senographe DS and nine GE Senographe Essential) is found to be in the range 39-60 Gy/h (=$1.1\text{-}1.7\times10^{-2}$ Gy/s). Cancer induction in mammography, thus, has to be estimated based on the fact that mammography is a low dose and high dose-rate examination. A prior study has shown that for doses of 1 Gy or higher, in other words high doses, delivered at high dose-rates ($2.2\ 10^{-2}$ Gy/s (=78 Gy/h)) the frequency of chromosome aberrations with respect to the radiation dose is non-linear (272). When non-linearity is found for high doses and high dose-rates, there is

reason to question the validity of a linear model at low dose and high dose-rate. In other words, it might be suspected that non-linearity is present at low dose and high dose-rate.

Studying dose-risk relationship in an epidemiological approach is almost impossible due to the high number of persons exposed to ionizing radiation and the follow-up time needed (187, 201). A recent large population based study on CT scans shows the overall cancer incidence was 24% greater for exposed than for unexposed persons for all types of cancer (273). For all cancers, except brain cancers after brain CT the average effective dose per scan was approximately 5 mSv. For brain cancers after brain CT (brain exposures) the average brain dose per scan was approximately 40 mGy, while for leukaemias and myelodysplasias (all exposures) the average red bone marrow dose per scan was approximately 5 mGy. For breast cancer, however, no separate increase in the incidence rate ratio can be found (incidence rate ratio: 0.99 (95% CI: 0.83-1.17)) (273). This leads us to think that when doses in the range 5-40 mGy does not lead to an increased risk of breast cancer, it is not likely that doses below this range will imply an increased risk. Since mammography typically provides average doses of 2.5 mGy, which is below the range 5-50 mGy, it may be that there is no increased risk in this dose area.

For studies on laboratory animals, 64% of the 262 experiments reviewed did not show any linear dose relationship for doses 0.04 Gy-40 Gy (274). The dose-response curve was either J-shaped, hockey-stick-like, or with no discernible effect. Studies on cells are not conclusive in how cells respond to radiation, but it is known that the cellular responses at low doses differ from those at high doses (189, 213, 214, 275-277). Beyreuther et al. has found that for energies below 50 keV, which are typically relevant for mammography, increased chromosomal aberrations frequencies take place (278).

The use of the LNT model is controversial for low doses where the LNT model has lacked to show validity and the debate continues (279, 280). Deterministic effects has been observed for doses from 0.2 Gy and upwards, but below this dose there is not consistency in the data (279). By applying a model that assumes a LNT relationship an unwarranted fear about ionizing radiation may occur (280). A study has shown that 59% of doctors

identified fear as a major reason for their patients` refusal of mammography examinations (281). Based on the findings in Paper V and similar studies, such fear seems to lack support. It is important to inform the women that the risk is minimal, and that the radiation dose should not be considered as a reason for refraining from a mammography examination.

The model applied in Paper V has been applied by others when estimating the risk of radiation-induced breast cancers in mammography, and therefore it was decided to use this model in our estimations of the risk of radiation-induced breast cancers. However, the model is connected with large uncertainties: a) the assumption of linearity in a dose area for which data are missing and b) inherent uncertainty in the model due to statistical uncertainty in the data on which the model is based. In addition, there is increasing evidence of non-linear responses of biological systems to low radiation doses delivered at low dose-rates, resulting in doubts concerning extrapolations from high doses and high dose-rates as well (194). The topic of biological effects and risks of low doses of ionizing radiation is an on-going debate, and it has turned out to be the longest running debate in the radiation sciences. In other words, more research is needed in order to make any conclusions as to the effects at low doses. Until a new model for low doses and high dose-rates has been proposed it is difficult to make better estimations regarding the radiation-induced risk. The estimates in Paper V are to be considered as the best estimate that one is able to make with the current knowledge. The LNT model is used worldwide for radiation protection regulations. In ICRP Publication 99 it is stated that: “The report concludes that while existence of a low-dose threshold does not seem to be unlikely for radiation-related cancers of certain tissues, the evidence does not favour the existence of a universal threshold. The LNT hypothesis, combined with an uncertain DDREF for extrapolation from high doses, remains a prudent basis for radiation protection at low doses and low dose rates.” (282) This might result in an overestimation of the risk, but according to ICRP it is better to err on the safe side. It is important to use the estimates with caution, though. In order to make more accurate estimations, a new model must be founded on both epidemiological data and biological mechanisms (194).

6.6 Cost-benefit: An evaluation of the NBCSP

In order to legitimize a screening program the benefits needs to exceed the associated risks (283). This is the principle of justification (62). In an evaluation of the benefit-risk (or cost-benefit) the advantages and disadvantages of screening need to be weighed up against each other (54). Breast cancer screening has been shown to be cost-effective in Norway (284, 285). Given the results in Paper V we found the risk to be minimal. In the NBCSP one in every 5 women (20%) will be recalled for further assessment with a negative outcome. In comparison to other European screening programmes, where a pooled estimate 19.7% was found (286), this seems to be in the high end of this range. The interval cancer rate is 18.2 per 10 000 screens in the NBCSP (287), which is higher than recommended in the European Guidelines. The elevated rate in the second part of the interval may be explained by the definition, the use of the background incidence from an earlier time period without adjusting for temporal increases as discussed above, a somewhat low screening detection rate, and the possibility of opportunistic screening in the interval between two screening sessions in the NBCSP. No reliable estimates for overdiagnosis were available for the NBCSP (288). The unadjusted or incompletely adjusted estimates ranged from 37% to 54% in Norway. For other screening programs in Europe the most plausible estimates of overdiagnosis range from 1% to 10%. In conclusion, it might be that the numbers for false positives and interval cancers are in the high end compared to the rest of the screening programmes in Europe. Given that the estimates of overdiagnosis are undecided, and that the risk of radiation-induced breast cancer is minimal there are in other words two factors out of four that seems to be a great disadvantage for the NBCSP. On the other hand, recently a mortality reduction of 43% was reported from the NBCSP (21). This should be considered a large benefit in a screening program.

7 Conclusion

Previous studies have shown that FFDM systems are capable of producing lower doses compared with SFM systems, but the results in this thesis shows that using FFDM does not necessarily guarantee a lower MGD per exposure than SFM. FFDM do provide lower doses for larger compressed breast thicknesses, but for the thinner breasts no significant difference is found (Paper I).

Estimating the MGD depends on the compressed breast thickness. The difference in the readout thickness and the measured thickness varies between units for the same model and between manufacturers. Any corrections to compressed breast thickness need therefore to be performed for the unit in question (Paper II).

Difference between readout thickness and the measured thickness implies uncertainties in the estimation of the MGD. Uncertainties in thickness of approximately ±10 mm adds uncertainties in the MGD of approximately ±10% and uncertainty in the glandularity, due to uncertainty in the compressed breast thickness, of +/-10% will lead to an uncertainty in the MGD of -/+4% (Paper III).

The DRL does not seem sufficient as a tool to identify units in need of optimization. The image quality by means of FOM, defined here as SDNR squared divided by the MGD, should be considered as well, especially when new manufacture/models are introduced to the market (Paper IV).

For women screened according to the schema used in the NBCSP, the risk of radiation induced breast cancer and breast cancer death is minimal (Paper V).

Asymptomatic women are being screening, and it is therefore important to fulfil the ALARA principle. Radiation protection in the form of optimization with respect to dose and image quality will have an effect on the diagnostic outcome.

8 References

1. Parkin DM, Bray F, Ferlay J, Pisani P. Global cancer statistics, 2002. *CA: a cancer journal for clinicians* 2005;55(2):74-108.

2. Ferlay J, Shin HR, Bray F, Forman D, Mathers C, Parkin DM. Estimates of worldwide burden of cancer in 2008: GLOBOCAN 2008. *Int J Cancer* 2010.

3. Cancer Registry of Norway. Cancer in Norway 2011 - Cancer incidence, mortality, survival and prevalence in Norway. Oslo: Cancer Registry of Norway, 2013.

4. Cancer Registry of Norway. Cancer in Norway 2010 - Cancer incidence, mortality, survival and prevalence in Norway. Oslo: Cancer Registry of Norway, 2012.

5. Salomon A. Beiträge zur Pathologie und Klinik des Mammakarzinoms. *Arch Klin Chir* 1913;101:573-668.

6. Bassett LW, Gold RH, Kimme-Smith C. History of the Technical Development of Mammography. In: Haus AG, Yaffe MJ, editors. Syllabus: A Categorical Course in Physics Technical Aspects of Breast Imaging Third edition Presented at the 80th Scientific Assembly and Annual Meeting of the Radiological Society of North America, November 27-December 2, 1994. Oak Brook, IL, USA: RSNA Publications; 1994. p. 9-19.

7. Pisano ED, Yaffe MJ, Kuzmiak CM. Digital mammography. Philadelphia, PA, USA: Lippincott Williams & Wilkins; 2004.

8. Kopans DB. What is a useful adjunct to mammography? *Radiology* 1986;161(2):560-1.

9. Borretzen I, Lysdahl KB, Olerud HM. Diagnostic radiology in Norway trends in examination frequency and collective effective dose. *Radiat Prot Dosimetry* 2007;124(4):339-47.

10. Kopans DB, Monsees B, Feig SA. Screening for cancer: when is it valid?--Lessons from the mammography experience. *Radiology* 2003;229(2):319-27.

11. Hofvind S, Geller B, Vacek PM, Thoresen S, Skaane P. Using the European guidelines to evaluate the Norwegian Breast Cancer Screening Program. *Eur J Epidemiol* 2007;22(7):447-55.

12. Duffy SW, Hill C, Estève J. Quantitative methods for the evaluation of cancer screening. London, New York: Arnold ; Co-published in the United States of America by Oxford University Press; 2001.

13. Rothman KJ, Greenland S. Modern epidemiology. 2nd ed. Philadelphia, PA: Lippincott-Raven; 1998.

14. Vainio H, Bianchini Fe, editors. IARC Handbooks of Cancer Prevention Volume 7 Breast Cancer Screening. Lyon, France: IARCPress; 2002. Available from: http://www.iarc.fr/en/publications/pdfs-online/prev/handbook7/Handbook7_Breast.pdf, accessed 10.10.2013.

15. World Health Organization. National cancer control programmes : policies and managerial guidelines. 2nd ed. Geneva: World Health Organization; 2002.

16. Wilson JM, Jungner YG. [Principles and practice of mass screening for disease] Principios y metodos del examen colectivo para identificar enfermedades. *Boletin de la Oficina Sanitaria Panamericana Pan American Sanitary Bureau* 1968;65(4):281-393.

17. Hofvind S. The Norwegian Breast Cancer Screening Program: Selected Process Indicators and their Utilization in Epidemiological Research. Oslo, Norway: University of Oslo; 2005.

18. Schopper D, de Wolf C. How effective are breast cancer screening programmes by mammography? Review of the current evidence. *Eur J Cancer* 2009;45(11):1916-23.

19. Independent UK Panel on Breast Cancer Screening. The benefits and harms of breast cancer screening: an independent review. *Lancet* 2012;380(9855):1778-86.

20. Broeders M, Moss S, Nystrom L, Njor S, Jonsson H, Paap E*, et al.* The impact of mammographic screening on breast cancer mortality in Europe: a review of observational studies. *J Med Screen* 2012;19 Suppl 1:14-25.

21. Hofvind S, Ursin G, Tretli S, Sebuodegard S, Moller B. Breast cancer mortality in participants of the Norwegian Breast Cancer Screening Program. *Cancer* 2013;119(17):3106-12.

22. Humphrey LL, Helfand M, Chan BK, Woolf SH. Breast cancer screening: a summary of the evidence for the U.S. Preventive Services Task Force. *Ann Intern Med* 2002;137(5 Part 1):347-60.

23. Fletcher SW, Elmore JG. Clinical practice. Mammographic screening for breast cancer. *N Engl J Med* 2003;348(17):1672-80.

24. High M. Mammographic Quality Control: ACR-recommended Physicist's-level Testing. In: Haus AG, Yaffe MJ, editors. Syllabus: A Categorical Course in Physics Technical Aspects of Breast Imaging Third edition Presented at the 80th Scientific Assembly and Annual Meeting of the Radiological Society of North America, November 27-December 2, 1994. Oak Brook, IL, USA: RSNA Publications; 1994. p. 185-217.

25. Cancer Registry of Norway. Mammografiprogrammet. Kvalitetsmanual. [Quality assurance manual of the Norwegian Breast Cancer Screening Program (NBCSP). -In Norwegian] Ertzaas AKO, editor. Oslo, Norway: Cancer Registry of Norway; 2003. Available from: http://www.kreftregisteret.no/Global/Kvalitetsmanualer/kvalitetsmanual_mammografiprogrammet.pdf, accessed 10.10.2013.

26. Pedersen K, Bredholt K, Landmark ID, Istad TSJ, Almén A, Hauge IHR. Teknisk kvalitetskontroll – statuskontroller for digitale mammografisystemer. StrålevernRapport 2010:8. [Technical quality control – routine controls for digital mammography systems. -In Norwegian]. Østerås: Norwegian Radiation Protection Authority; 2010. Available from: http://www.nrpa.no/dav/181f92b655.pdf, accessed 10.10.2013.

27. Kirkpatrick A, Törnberg S, Thijssen MAO. European guidelines for quality assurance in mammography screening: final report. Luxembourg: Commission of the European Communities; 1993. Available from: http://bookshop.europa.eu/en/european-guidelines-for-quality-assurance-in-mammography-screening-pbCENA14821/?CatalogCategoryID=X74KABstxngAAAEjdpEY4e5L, accessed 11.10.2013.

28. Perry N, Broeders M, de Wolf C, Tornberg S, Holland R. European guidelines for quality assurance in breast cancer screening and diagnosis: European Communities: printed in Belgium; 2006. Available from: http://ec.europa.eu/health/archive/ph_projects/2002/cancer/fp_cancer_2002_ext_guid_01.pdf, accessed 11.10.2013.

29. Perry N, Schouten J, Europe against Cancer Programme, EUREF (Organization). European guidelines for quality assurance in mammography screening. 3rd ed. Luxembourg: Office for Official Publications of the European Communities; 2001. Available from: http://bookshop.europa.eu/en/european-guidelines-for-quality-assurance-in-mammography...-pbND3601540/, accessed 11.10.2013.

30. Nystrom L, Rutqvist LE, Wall S, Lindgren A, Lindqvist M, Ryden S*, et al.* Breast cancer screening with mammography: overview of Swedish randomised trials. *Lancet* 1993;341(8851):973-8.

31. Working group chaired by Sir Patrick Forrest. Breast Cancer Screening: Report to the health minister of England, Wales, Scotland and Northern Ireland. London: Her Majesty's Stationery Office1996.

32. Dodd GD. American Cancer Society Guidelines on Screening for Breast-Cancer. An Overview. *Cancer* 1992;69(7):2008-9.

33. Olerud HM, Widmark A. Kvalitetskontrollhåndbok mammografi: basert på anbefalinger gitt av de nordiske strålevernsmyndighetene. Versjon 02-91. Østerås: Statens Institutt for Strålehygiene; 1991.

34. Statens Institutt for Strålehygiene. Kvalitetssikring i mammografi. SIS-Råd 1992:1. Østerås: Statens Institutt for Strålehygiene, 1992.

35. Olerud HM, Widmark A. Kvalitetskontrollhåndbok i mammografi: Strålevernhefte 2. Østerås: Statens Institutt for Strålehygiene; 1994.

36. Fosmark H, Olerud HM, Widmark A, Sager EM. A Norwegian survey on mammography. *Radiat Prot Dosim* 1993;49(1/3):207-8.

37. Olsen JB, Skretting A, Widmark A. Assessment of image quality and total performance in Norwegian mammography laboratories. Findings in a national survey based on different phantoms and ROC methodology. *Acta Radiol* 1998;39(5):507-13.

38. Pedersen K, Landmark ID, Bredholt K, Hauge IHR. Teknisk kvalitetskontroll – konstanskontroller for digitale mammografisystemer. StrålevernRapport 2009:5. [Technical quality control - constancy controls for digital mammography systems. -In Norwegian]. Østerås: Norwegian Radiation Protection Authority, 2009. Available from: http://www.nrpa.no/dav/67e3d2a63b.pdf, accessed 10.10.2013.

39. ICRP. Recommendations of the ICRP. ICRP Publication 26. *Ann ICRP* 1977;1(3).

40. Pedersen K. Prøveprosjekt med mammografiscreening. Pasientdosemålinger. StrålevernRapport 1998:4. [Mammography screening trial project. Patient dose measurements. - In Norwegian]. Østerås, Norway: Norwegian Radiation Protection Authority; 1998. Available from: http://www.nrpa.no/dav/805e92e519.pdf, accessed 10.10.2013.

41. Dance DR. Monte Carlo calculation of conversion factors for the estimation of mean glandular breast dose. *Phys Med Biol* 1990;35(9):1211-9.

42. Dance DR, Skinner CL, Young KC, Beckett JR, Kotre CJ. Additional factors for the estimation of mean glandular breast dose using the UK mammography dosimetry protocol. *Phys Med Biol* 2000;45(11):3225-40.

43. Giordano L, von Karsa L, Tomatis M, Majek O, de Wolf C, Lancucki L*, et al.* Mammographic screening programmes in Europe: organization, coverage and participation. *J Med Screen* 2012;19 Suppl 1:72-82.

44. McCullagh JB, Baldelli P, Phelan N. Clinical dose performance of full field digital mammography in a breast screening programme. *Br J Radiol* 2011;84(1007):1027-33.

45. The Ministry of Health and Care Services. Forskrift om strålevern og bruk av stråling (strålevernforskriften) av 29. oktober 2010, nr. 1380. [Regulation No. 1380 of 29 October 2010 on Radiation Protection and Use of Radiation. -In Norwegian]. Available from: http://www.lovdata.no/cgi-wift/ldles?doc=/sf/sf/sf-20101029-1380.html, accessed 10.10.2013.

46. Svahn T, Hemdal B, Ruschin M, Chakraborty DP, Andersson I, Tingberg A*, et al.* Dose reduction and its influence on diagnostic accuracy and radiation risk in digital mammography: an observer performance study using an anthropomorphic breast phantom. *Br J Radiol* 2007;80(955):557-62.

47. Nystrom L, Andersson I, Bjurstam N, Frisell J, Nordenskjold B, Rutqvist LE. Long-term effects of mammography screening: updated overview of the Swedish randomised trials. *Lancet* 2002;359(9310):909-19.

48. Smith RA, Duffy SW, Gabe R, Tabar L, Yen AM, Chen TH. The randomized trials of breast cancer screening: what have we learned? *Radiol Clin North Am* 2004;42(5):793-806, v.

49. Paap E, Holland R, den Heeten GJ, van Schoor G, Botterweck AA, Verbeek AL*, et al.* A remarkable reduction of breast cancer deaths in screened versus unscreened women: a case-referent study. *Cancer Causes Control* 2010;21(10):1569-73.

50. Olsen AH, Njor SH, Vejborg I, Schwartz W, Dalgaard P, Jensen MB*, et al.* Breast cancer mortality in Copenhagen after introduction of mammography screening: cohort study. *BMJ* 2005;330(7485):220.

51. Kalager M, Haldorsen T, Bretthauer M, Hoff G, Thoresen SO, Adami HO. Improved breast cancer survival following introduction of an organized mammography screening program among both screened and unscreened women: a population-based cohort study. *Breast Cancer Res* 2009;11(4):R44.

52. Moss SM, Nystrom L, Jonsson H, Paci E, Lynge E, Njor S*, et al.* The impact of mammographic screening on breast cancer mortality in Europe: a review of trend studies. *J Med Screen* 2012;19 Suppl 1:26-32.

53. Cancer Registry of Norway. Cancer in Norway 2009. Special issue: Cancer screening in Norway. Oslo: Cancer registry of Norway, 2011.

54. Heywang-Kobrunner SH, Hacker A, Sedlacek S. Advantages and Disadvantages of Mammography Screening. *Breast care* 2011;6(3):199-207.

55. Boyd N, Martin L, Chavez S, Gunasekara A, Salleh A, Melnichouk O*, et al.* Breast-tissue composition and other risk factors for breast cancer in young women: a cross-sectional study. *The lancet oncology* 2009;10(6):569-80.

56. ICRU. Patient Dosimetry for X Rays used in Medical Imaging. Journal of the ICRU Vol 5 No 2. Report 74. Oxford: Oxford University Press: International Commission on Radiation Units and Measurements, 2005.

57. Carlsson CA, Carlsson GA. Dosimetry in diagnostic radiology and computerized tomography. In: Kase KR, Bjärngard BE, Attix FH, editors. The Dosimetry of ionizing radiation. III. Orlando: Academic Press; 1990. p. 183-94.

58. Boone JM. X-ray Production, Interaction, and Detection in Diagnostic Imaging. In: Beutel J, Kundel HL, Van Metter RL, editors. Handbook of Medical Imaging. Volume 1. Physics and Psychophysics. Bellingham, Washington, USA: SPIE Press; 2000. p. 1-78.

59. ICRU. Fundamental Quantities and Units for Ionizing Radiation. ICRU Report 60. Bethesda, MD, USA: International Commission on Radiation Units and Measurements, 1998.

60. Dance DR, Skinner CL, Carlsson GA. Breast dosimetry. *Applied radiation and isotopes : including data, instrumentation and methods for use in agriculture, industry and medicine* 1999;50(1):185-203.

61. ICRP. The Biological Basis for Dose Limitation in the Skin. ICRP Publication 59. *Ann ICRP* 1991;22(2).

62. ICRP. The 2007 Recommendations of the International Commission on Radiological Protection. ICRP Publication 103. *Ann ICRP* 2007;37(2-4).

63. Institute of Physical Sciences in Medicine (IPSM). The commisioning and routine testing of mammographic x-ray systems. Second ed. Law J, Dance DR, Faulkner K, Fitzgerald MC, Ramsdale ML, Robinson A, editors: Institute of Physical Sciences in Medicine; 1994.

64. O'Leary D, Rainford L. A comparison of mean glandular dose diagnostic reference levels within the all-digital Irish nationalbreast screening programme and the Irish symptomatic breast services. *Radiat Prot Dosimetry* 2013;153(3):300-8.

65. Al-Hajj M, Clarke MF. Self-renewal and solid tumor stem cells. *Oncogene* 2004;23(43):7274-82.

66. Klein R, Aichinger H, Dierker J, Jansen JT, Joite-Barfuss S, Sabel M*, et al.* Determination of average glandular dose with modern mammography units for two large groups of patients. *Phys Med Biol* 1997;42(4):651-71.

67. Hammerstein GR, Miller DW, White DR, Masterson ME, Woodard HQ, Laughlin JS. Absorbed radiation dose in mammography. *Radiology* 1979;130(2):485-91.

68. Rothenberg LN. AAPM tutorial. Patient dose in mammography. *Radiographics* 1990;10(4):739-46.

69. Rothenberg LN. Exposures and Doses in Mammography. In: Haus AG, Yaffe MJ, editors. Syllabus: A Categorical Course in Physics Technical Aspects of Breast Imaging Third edition Presented at the 80th Scientific Assembly and Annual Meeting of the Radiological Society of North America, November 27-December 2, 1994. Oak Brook, IL, USA: RSNA Publications; 1994. p. 113-9.

70. Dance DR, Young KC, van Engen RE. Further factors for the estimation of mean glandular dose using the United Kingdom, European and IAEA breast dosimetry protocols. *Physics in Medicine and Biology* 2009;54(14):4361-72.

71. Wu X, Gingold EL, Barnes GT, Tucker DM. Normalized average glandular dose in molybdenum target-rhodium filter and rhodium target-rhodium filter mammography. *Radiology* 1994;193(1):83-9.

72. Boone JM. Normalized glandular dose (DgN) coefficients for arbitrary X-ray spectra in mammography: computer-fit values of Monte Carlo derived data. *Med Phys* 2002;29(5):869-75.

73. Dance DR, Thilander AK, Sandborg M, Skinner CL, Castellano IA, Carlsson GA. Influence of anode/filter material and tube potential on contrast, signal-to-noise ratio and average absorbed dose in mammography: a Monte Carlo study. *Br J Radiol* 2000;73(874):1056-67.

74. Persliden J. A Monte Carlo program for photon transport using analogue sampling of scattering angle in coherent and incoherent scattering processes. *Computer programs in biomedicine* 1983;17(1-2):115-28.

75. Boone JM. Glandular breast dose for monoenergetic and high-energy X-ray beams: Monte Carlo assessment. *Radiology* 1999;213(1):23-37.

76. Wu X, Barnes GT, Tucker DM. Spectral dependence of glandular tissue dose in screen-film mammography. *Radiology* 1991;179(1):143-8.

77. Zoetelief J, Fitzgerald M, Leitz W, Säbel M. European protocol on dosimetry in mammography. Luxembourg: Office for Official Publication of the European Communities; 1996.

78. Dance DR, Young KC, van Engen RE. Estimation of mean glandular dose for breast tomosynthesis: factors for use with the UK, European and IAEA breast dosimetry protocols. *Phys Med Biol* 2011;56(2):453-71.

79. Hendrick RE. Standardization of image quality and radiation dose in mammography. *Radiology* 1990;174(3 Pt 1):648-54.

80. Dance DR, Persliden J, Carlsson GA. Calculation of dose and contrast for two mammographic grids. *Phys Med Biol* 1992;37(1):235-48.

81. Fryback DG, Thornbury JR. The efficacy of diagnostic imaging. *Medical decision making : an international journal of the Society for Medical Decision Making* 1991;11(2):88-94.

82. ICRU. Medical imaging - the assessment of image quality. ICRU Report 54. Bethesda, MD, USA: International Commission on Radiation Units and Measurements, 1996.

83. Krupinski EA, Jiang Y. Anniversary paper: evaluation of medical imaging systems. *Med Phys* 2008;35(2):645-59.

84. Yaffe MJ, Mainprize JG, Jong RA. Technical developments in mammography. *Health Phys* 2008;95(5):599-611.

85. Boone JM, Seibert JA. A comparison of mono- and poly-energetic x-ray beam performance for radiographic and fluoroscopic imaging. *Med Phys* 1994;21(12):1853-63.

86. Flower MA, Webb S. Webb's physics of medical imaging. Boca Raton, FL, USA: CRC Press; 2012.

87. Dowsett DJ, Kenny PA, Johnston RE. The physics of diagnostic imaging. London: Hodder Arnold; 2006.

88. Beaman SA, Lillicrap SC. Optimum x-ray spectra for mammography. *Phys Med Biol* 1982;27(10):1209-20.

89. Gros CM. Méthodologie: symposium sur le sein. *J Radiol Electrol Med Nucl* 1967;48:638-55.

90. Johns PC, Yaffe MJ. X-ray characterisation of normal and neoplastic breast tissues. *Phys Med Biol* 1987;32(6):675-95.

91. Marshall NW, Monnin P, Bosmans H, Bochud FO, Verdun FR. Image quality assessment in digital mammography: part I. Technical characterization of the systems. *Phys Med Biol* 2011;56(14):4201-20.

92. Yaffe MJ. Basic Physics of Digital Mammography. In: Bick U, Diekmann F, editors. Digital Mammography. Berlin Heidelberg: Springer-Verlag; 2010. p. 1-11.

93. Sharp PF, Metz CE, Wagner RF, Myers KJ, Burgess AE. Medical imaging : the assessment of image quality. Bethesda, Md.: International Commission on Radiation Units and Measurements; 1996.

94. Aslund M, Cederstrom B, Lundqvist M, Danielsson M. Scatter rejection in multislit digital mammography. *Med Phys* 2006;33(4):933-40.

95. Wolff SD, Balaban RS. Assessing contrast on MR images. *Radiology* 1997;202(1):25-9.

96. Sandborg M, Carlsson GA. Influence of X-ray energy spectrum, contrasting detail and detector on the signal-to-noise ratio (SNR) and detective quantum effciency (DQE) in projection radiography. *Phys Med Biol* 1992;37(6):1245-63.

97. Dobbins JT. Image quality Metrics for Digital Systems. In: Beutel J, Kundel HL, Van Metter RL, editors. Handbook of medical imaging. Volume 1. Physics and Psychophysics. Bellingham, Washington, USA: SPIE Press; 2000. p. 161-222.

98. Fujita H, Tsai DY, Itoh T, Doi K, Morishita J, Ueda K, *et al.* A simple method for determining the modulation transfer function in digital radiography. *IEEE Trans Med Imaging* 1992;11(1):34-9.

99. Jennings RJ, Quinn PW, Gagne RM, Fewell TR. Evaluation of x-ray sources for mammography. *Proc SPIE 1896, Medical Imaging 1993: Physics of Medical Imaging, 259 (September 14, 1993)* 1993.

100. Baldelli P, Taibi A, Tuffanelli A, Gilardoni MC, Gambaccini M. A prototype of a quasi-monochromatic system for mammography applications. *Phys Med Biol* 2005;50(10):2225-40.

101. Yaffe MJ, Jennings RJ, Fahrig R, Fewell TR. X-ray Spectral Considerations for Mammography. In: Haus AG, Yaffe MJ, editors. Syllabus: A Categorical Course in Physics Technical Aspects of Breast Imaging Third edition Presented at the 80th Scientific Assembly and Annual Meeting of the Radiological Society of North America, November 27-December 2, 1994. Oak Brook, IL, USA: RSNA Publications; 1994. p. 63-73.

102. Thilander-Klang AC, Ackerholm PH, Berlin IC, Bjurstam NG, Mattsson SL, Mansson LG, *et al.* Influence of anode-filter combinations on image quality and radiation dose in 965 women undergoing mammography. *Radiology* 1997;203(2):348-54.

103. Fahrig R, Yaffe MJ. Optimization of spectral shape in digital mammography: dependence on anode material, breast thickness, and lesion type. *Med Phys* 1994;21(9):1473-81.

104. Cunha DM, Tomal A, Poletti ME. Optimization of x-ray spectra in digital mammography through Monte Carlo simulations. *Phys Med Biol* 2012;57(7):1919-35.

105. Delis H, Spyrou G, Costaridou L, Tzanakos G, Panayiotakis G. Suitability of new anode materials in mammography: dose and subject contrast considerations using Monte Carlo simulation. *Med Phys* 2006;33(11):4221-35.

106. Gingold EL, Wu X, Barnes GT. Contrast and dose with Mo-Mo, Mo-Rh, and Rh-Rh target-filter combinations in mammography. *Radiology* 1995;195(3):639-44.

107. Jennings RJ, Eastgate RJ, Siedband MP, Ergun DL. Optimal x-ray spectra for screen-film mammography. *Med Phys* 1981;8(5):629-39.

108. Monticciolo DL, Sprawls P, Kruse BD, Peterson JE. Optimization of radiation dose and image quality in mammography: a clinical evaluation of rhodium versus molybdenum. *Southern medical journal* 1996;89(4):391-4.

109. Desponds L, Depeursinge C, Grecescu M, Hessler C, Samiri A, Valley JF. Influence of anode and filter material on image quality and glandular dose for screen-film mammography. *Phys Med Biol* 1991;36(9):1165-82.

110. Baldelli P, Phelan N, Egan G. Investigation of the effect of anode/filter materials on the dose and image quality of a digital mammography system based on an amorphous selenium flat panel detector. *Br J Radiol* 2010;83(988):290-5.

111. Thilander-Klang A, Dance DR, Sandborg M, Skinner C, Smith IC, Alm Carlsson G, *et al.* Influence of anode/filter material and tube potential on contrast, signal-to-noise ratio and mean absorbed dose in mammography: a Monte Carlo study. Göteborg University, Sweden, 1997.

112. van Engen R. European protocol for the quality control of the physical and tecnical aspects of mammography screening. 4th ed. Luxembourg: European Commission; 2006. Available from: http://www.euref.org/european-guidelines/physico-technical-protocol, accessed 11.02.2014.

113. van Engen R, Bosmans H, Heid P, Lazzari B, Schopphoven S, Thijssen M, *et al.* Supplement to the European Guidelines fourth edition 2011. Available from: http://www.euref.org/european-guidelines/physico-technical-protocol, accessed 11.02.2014.

114. Barnes GT, Brezovich IA. The intensity of scattered radiation in mammography. *Radiology* 1978;126(1):243-7.

115. Yester MV, Barnes GT, King MA. Experimental measurements of the scatter reduction obtained in mammography with a scanning multiple slit assembly. *Med Phys* 1981;8(2):158-62.

116. Wagner AJ. Contrast and grid performance in mammography. In: Barnes GT, Frey GD, editors. Screen film mammography : imaging considerations and medical physics responsibilities : proceedings of SEAAPM Spring Symposium, April 6, 1990, Columbia, South Carolina. Madison, Wis.: Medical Physics Publishing; 1991. p. 115-58.

117. Richter D, editor Evaluation of grid technique in mammography. Presented at the 20th Annual Meeting of American Association of Physicists in Medicine, San Francisco, CA, July 30-Aug 3, 1978; 1978.

118. Hendee WR. History and status of x-ray mammography. *Health Phys* 1995;69(5):636-48.

119. Fischer U, Hermann KP, Baum F. Digital mammography: current state and future aspects. *Eur Radiol* 2006;16(1):38-44.

120. Pisano ED, Yaffe MJ. Digital mammography. *Radiology* 2005;234(2):353-62.

121. Hendrick RE, Pisano ED, Averbukh A, Moran C, Berns EA, Yaffe MJ*, et al.* Comparison of acquisition parameters and breast dose in digital mammography and screen-film mammography in the American College of Radiology Imaging Network digital mammographic imaging screening trial. *AJR Am J Roentgenol* 2010;194(2):362-9.

122. Aslund M, Cederstrom B, Lundqvist M, Danielsson M. AEC for scanning digital mammography based on variation of scan velocity. *Med Phys* 2005;32(11):3367-74.

123. NHS Breast Screening Programme (NHSBSP). Quality assurance guidelines for mammography including radiographic quality control. Sheffield, UK: NHS Cancer Screening Programmes, 2006.

124. Kopans DB. Mammography equipment and basic physics. In: Kopans DB, editor. Breast imaging. 3rd ed. ed. Philadelphia, PA: Lippincott Williams and Wilkins; 2007. p. 255.

125. Poulos A, Rickard M. Compression in mammography and the perception of discomfort. *Australas Radiol* 1997;41(3):247-52.

126. Barnes GT. Mammography Equipment: Compression, Scatter Control, and Automatic Exposure Control. In: Haus AG, Yaffe MJ, editors. Syllabus: A Categorical Course in Physics Technical Aspects of Breast Imaging Third edition Presented at the 80th Scientific Assembly and Annual Meeting of the Radiological Society of North America, November 27-December 2, 1994. Oak Brook, IL, USA: RSNA Publications; 1994. p. 75-84.

127. Mercer CE, Hogg P, Lawson R, Diffey J, Denton ER. Practitioner compression force variability in mammography: a preliminary study. *Br J Radiol* 2013;86(1022):20110596.

128. Hogg P, Taylor M, Szczepura K, Mercer C, Denton E. Pressure and breast thickness in mammography--an exploratory calibration study. *Br J Radiol* 2013;86(1021):20120222.

129. Dustler M, Andersson I, Brorson H, Frojd P, Mattsson S, Tingberg A*, et al.* Breast compression in mammography: pressure distribution patterns. *Acta Radiol* 2012;53(9):973-80.

130. Haus AG. Screen-Film Image Receptors and Film Processing. In: Haus AG, Yaffe MJ, editors. Syllabus: A Categorical Course in Physics Technical Aspects of Breast Imaging

Third edition Presented at the 80th Scientific Assembly and Annual Meeting of the Radiological Society of North America, November 27-December 2, 1994. Oak Brook, IL, USA: RSNA Publications; 1994. p. 85-101.

131. Yaffe MJ. Digital Mammography. In: Haus AG, Yaffe MJ, editors. Syllabus: A Categorical Course in Physics Technical Aspects of Breast Imaging Third edition Presented at the 80th Scientific Assembly and Annual Meeting of the Radiological Society of North America, November 27-December 2, 1994. Oak Brook, IL, USA: RSNA Publications; 1994. p. 275-86.

132. Yaffe MJ. AAPM tutorial. Physics of mammography: image recording process. *Radiographics* 1990;10(2):341-63.

133. Monnin P, Gutierrez D, Bulling S, Lepori D, Valley JF, Verdun FR. A comparison of the performance of modern screen-film and digital mammography systems. *Phys Med Biol* 2005;50(11):2617-31.

134. Bunch PC. Advances in high-speed mammographic image quality. *Proc SPIE* 1999;3659:120–30.

135. Young KC. Recent developments in digital mammography. *Imaging* 2006;18(2):68-74.

136. Noel A, Thibault F. Digital detectors for mammography: the technical challenges. *Eur Radiol* 2004;14(11):1990-8.

137. Saunders RS, Jr., Samei E, Jesneck JL, Lo JY. Physical characterization of a prototype selenium-based full field digital mammography detector. *Med Phys* 2005;32(2):588-99.

138. Bick U, Diekmann F. Digital mammography: what do we and what don't we know? *Eur Radiol* 2007;17(8):1931-42.

139. Lundqvist M, Danielsson M, Cederström B, Chmillb V, Chuntonova A, Åslunda M, editors. Measurements on a full-field digital mammography system with a photon counting crystalline silicon detector. Medical imaging 2003: Physics of medical imaging Proceedings of SPIE; 2003; 16-18 February 2003, San Diego, California, USA: SPIE.

140. Aslund M, Cederstrom B, Lundqvist M, Danielsson M. Physical characterization of a scanning photon counting digital mammography system based on Si-strip detectors. *Med Phys* 2007;34(6):1918-25.

141. Cahn RN, Cederstrom B, Danielsson M, Hall A, Lundqvist M, Nygren D. Detective quantum efficiency dependence on x-ray energy weighting in mammography. *Med Phys* 1999;26(12):2680-3.

142. Van Ongeval C, Bosmans H, Van Steen A. Current status of digital mammography for screening and diagnosis of breast cancer. *Current opinion in oncology* 2006;18(6):547-54.

143. Skaane P. Studies comparing screen-film mammography and full-field digital mammography in breast cancer screening: updated review. *Acta Radiol* 2009;50(1):3-14.

144. Vinnicombe S, Pinto Pereira SM, McCormack VA, Shiel S, Perry N, Dos Santos Silva IM. Full-field digital versus screen-film mammography: comparison within the UK breast screening program and systematic review of published data. *Radiology* 2009;251(2):347-58.

145. Dershaw DD. Status of mammography after the Digital Mammography Imaging Screening Trial: digital versus film. *The breast journal* 2006;12(2):99-102.

146. Thierry-Chef I, Simon SL, Weinstock RM, Kwon D, Linet MS. Reconstruction of absorbed doses to fibroglandular tissue of the breast of women undergoing mammography (1960 to the present). *Radiat Res* 2012;177(1):92-108.

147. Karssemeijer N, Bluekens AM, Beijerinck D, Deurenberg JJ, Beekman M, Visser R*, et al.* Breast cancer screening results 5 years after introduction of digital mammography in a population-based screening program. *Radiology* 2009;253(2):353-8.

148. Sala M, Comas M, Macia F, Martinez J, Casamitjana M, Castells X. Implementation of digital mammography in a population-based breast cancer screening program: effect of screening round on recall rate and cancer detection. *Radiology* 2009;252(1):31-9.

149. Pisano ED, Gatsonis C, Hendrick E, Yaffe M, Baum JK, Acharyya S*, et al.* Diagnostic performance of digital versus film mammography for breast-cancer screening. *N Engl J Med* 2005;353(17):1773-83.

150. Cooper VN, 3rd, Oshiro T, Cagnon CH, Bassett LW, McLeod-Stockmann TM, Bezrukiy NV. Evaluation of detector dynamic range in the x-ray exposure domain in mammography: a comparison between film-screen and flat panel detector systems. *Med Phys* 2003;30(10):2614-21.

151. Gennaro G, di Maggio C. Dose comparison between screen/film and full-field digital mammography. *Eur Radiol* 2006;16(11):2559-66.

152. Berns EA, Hendrick RE, Cutter GR. Performance comparison of full-field digital mammography to screen-film mammography in clinical practice. *Med Phys* 2002;29(5):830-4.

153. Hermann KP, Obenauer S, Marten K, Kehbel S, Fischer U, Grabbe E. Average glandular dose with amorphous silicon full-field digital mammography - Clinical results. *Rofo* 2002;174(6):696-9.

154. Moran P, Chevalier M, Ten JI, Fernandez Soto JM, Vano E. A survey of patient dose and clinical factors in a full-field digital mammography system. *Radiat Prot Dosimetry* 2005;114(1-3):375-9.

155. Obenauer S, Hermann KP, Grabbe E. Dose reduction in full-field digital mammography: an anthropomorphic breast phantom study. *Br J Radiol* 2003;76(907):478-82.

156. Korner M, Weber CH, Wirth S, Pfeifer KJ, Reiser MF, Treitl M. Advances in digital radiography: physical principles and system overview. *Radiographics* 2007;27(3):675-86.

157. Chan HP, Helvie MA, Petrick N, Sahiner B, Adler DD, Paramagul C*, et al.* Digital mammography: observer performance study of the effects of pixel size on the characterization of malignant and benign microcalcifications. *Acad Radiol* 2001;8(6):454-66.

158. Diekmann S, Bick U, von Heyden H, Diekmann F. Visualisierung von Mikrokalzifikationen in digitaler Vollfeldmammographie im Vergleich zu konventioneller Film-Folien-Mammographie. [Visualization of microcalcifications on mammographies obtained by digital full-field mammography in comparison to conventional film-screen mammography. - In German]. *Rofo* 2003;175(6):775-9.

159. Fischer U, Baum F, Obenauer S, Luftner-Nagel S, von Heyden D, Vosshenrich R*, et al.* Comparative study in patients with microcalcifications: full-field digital mammography vs screen-film mammography. *Eur Radiol* 2002;12(11):2679-83.

160. Kim HH, Pisano ED, Cole EB, Jiroutek MR, Muller KE, Zheng Y*, et al.* Comparison of calcification specificity in digital mammography using soft-copy display versus screen-film mammography. *AJR Am J Roentgenol* 2006;187(1):47-50.

161. Krug KB, Stutzer H, Girnus R, Zahringer M, Gossmann A, Winnekendonk G*, et al.* Image quality of digital direct flat-panel mammography versus an analog screen-film technique using a phantom model. *AJR Am J Roentgenol* 2007;188(2):399-407.

162. Obenauer S, Luftner-Nagel S, von Heyden D, Munzel U, Baum F, Grabbe E. Screen film vs full-field digital mammography: image quality, detectability and characterization of lesions. *Eur Radiol* 2002;12(7):1697-702.

163. Suryanarayanan S, Karellas A, Vedantham S, Sechopoulos I, D'Orsi CJ. Detection of simulated microcalcifications in a phantom with digital mammography: effect of pixel size. *Radiology* 2007;244(1):130-7.

164. Skaane P, Balleyguier C, Diekmann F, Diekmann S, Piguet JC, Young K*, et al.* Breast lesion detection and classification: comparison of screen-film mammography and full-field digital mammography with soft-copy reading--observer performance study. *Radiology* 2005;237(1):37-44.

165. Souza FH, Wendland EM, Rosa MI, Polanczyk CA. Is full-field digital mammography more accurate than screen-film mammography in overall population screening? A systematic review and meta-analysis. *Breast* 2013.

166. Skaane P, Skjennald A. Screen-film mammography versus full-field digital mammography with soft-copy reading: randomized trial in a population-based screening program--the Oslo II Study. *Radiology* 2004;232(1):197-204.

167. Hall EJ, Giaccia AJ. Radiobiology for the radiologist. 6th ed. Philadelphia: Lippincott Williams & Wilkins; 2006.

168. Suzuki K, Yamashita S. Low-dose Radiation Exposure and Carcinogenesis. *Japanese journal of clinical oncology* 2012.

169. Hendee WR, Edwards FM. ALARA and an integrated approach to radiation protection. *Seminars in nuclear medicine* 1986;16(2):142-50.

170. Hendee WR, O'Connor MK. Radiation risks of medical imaging: separating fact from fantasy. *Radiology* 2012;264(2):312-21.

171. National Academy of Sciences. Health risks from exposure to low levels of ionizing radiation : BEIR VII, Phase 2. Washington, D.C.: National Academies Press; 2006. Available from: http://www.nap.edu/openbook.php?isbn=030909156X, accessed 11.10.2013.

172. United Nations Scientific Committee on the Effects of Atomic Radiation (UNSCEAR). Epidemiological studies of radiation and cancer. New York: United Nations: 2008.

173. Ozasa K, Shimizu Y, Suyama A, Kasagi F, Soda M, Grant EJ*, et al.* Studies of the Mortality of Atomic Bomb Survivors, report 14, 1950-2003: An Overview of Cancer and Noncancer Diseases. *Radiation Research* 2012;177(3):229-43.

174. United Nations Scientific Committee on the Effects of Atomic Radiation (UNSCEAR). Volume I: Report to the General Assembly. Scientific Annex A. Epidemiological studies of radiation and cancer. New York: United Nations: 2006. Available from: http://www.unscear.org/docs/reports/2006/07-82087_Report_Annex_A_2006_Web_corr.pdf, accessed 11.10.2013.

175. Kellerer AM, Walsh L, Nekolla EA. Risk coefficient for gamma-rays with regard to solid cancer. *Radiat Environ Biophys* 2002;41(2):113-23.

176. Balonov MI, Shrimpton PC. Effective dose and risks from medical X-ray procedures. *Ann ICRP* 2012;41(3-4):129-41.

177. Ronckers CM, Doody MM, Lonstein JE, Stovall M, Land CE. Multiple diagnostic X-rays for spine deformities and risk of breast cancer. *Cancer Epidemiol Biomarkers Prev* 2008;17(3):605-13.

178. Mettler FA. Medical effects and risks of exposure to ionising radiation. *J Radiol Prot* 2012;32(1):N9-N13.

179. Berrington de Gonzalez A. Estimates of the potential risk of radiation-related cancer from screening in the UK. *J Med Screen* 2011;18(4):163-4.

180. Preston DL, Mattsson A, Holmberg E, Shore R, Hildreth NG, Boice JD, Jr. Radiation effects on breast cancer risk: a pooled analysis of eight cohorts. *Radiat Res* 2002;158(2):220-35.

181. Lundell M, Mattsson A, Hakulinen T, Holm LE. Breast cancer after radiotherapy for skin hemangioma in infancy. *Radiat Res* 1996;145(2):225-30.

182. Hildreth NG, Shore RE, Dvoretsky PM. The risk of breast cancer after irradiation of the thymus in infancy. *N Engl J Med* 1989;321(19):1281-4.

183. Darby SC, Doll R, Gill SK, Smith PG. Long term mortality after a single treatment course with X-rays in patients treated for ankylosing spondylitis. *Br J Cancer* 1987;55(2):179-90.

184. Hoffman DA, Lonstein JE, Morin MM, Visscher W, Harris BS, 3rd, Boice JD, Jr. Breast cancer in women with scoliosis exposed to multiple diagnostic x rays. *J Natl Cancer Inst* 1989;81(17):1307-12.

185. National Radiological Protection Board. Board statement on diagnostic medical exposures to ionising radiation during pregnancy and estimates of late radiation risks to the UK population. Chilton: NRPB: Documents of the NRPB; 1993.

186. Aurengo A, Averbeck D, Bonnin A, LeGuen B, Masse R, Monier R*, et al.* Dose-effect relationships and estimation of the carcinogenic effects of low doses of ionizing radiation. Paris: Medicine Academy of Sciences-National Academy of Medicine; 2005.

187. Brenner DJ, Doll R, Goodhead DT, Hall EJ, Land CE, Little JB*, et al.* Cancer risks attributable to low doses of ionizing radiation: assessing what we really know. *Proc Natl Acad Sci U S A* 2003;100(24):13761-6.

188. Redpath JL. Health risks of low photon energy imaging. *Radiat Prot Dosimetry* 2006;122(1-4):528-33.

189. Dauer LT, Brooks AL, Hoel DG, Morgan WF, Stram D, Tran P. Review and evaluation of updated research on the health effects associated with low-dose ionising radiation. *Radiat Prot Dosimetry* 2010;140(2):103-36.

190. Wakeford R. Cancer risk modelling and radiological protection. *J Radiol Prot* 2012;32(1):N89-93.

191. United Nations Scientific Committee on the Effects of Atomic Radiation (UNSCEAR). Effects of ionizing radiation: UNSCEAR 2006 Report to the General Assembly, with scientific annexes, vol. 1. United Nations, New York: 2009.

192. Scott BR. Low-dose radiation risk extrapolation fallacy associated with the linear-no-threshold model. *Human & experimental toxicology* 2008;27(2):163-8.

193. Scott BR. It's time for a new low-dose-radiation risk assessment paradigm--one that acknowledges hormesis. *Dose-response : a publication of International Hormesis Society* 2008;6(4):333-51.

194. Ulsh BA. The new radiobiology: returning to our roots. *Dose-response : a publication of International Hormesis Society* 2012;10(4):593-609.

195. Wrixon AD. New ICRP recommendations. *J Radiol Prot* 2008;28(2):161-8.

196. Kathren RL. Pathway to a paradigm: the linear nonthreshold dose-response model in historical context. The American Academy of Health Physics 1995 Radiology Centennial Hartman Oration. *Health Phys* 1996;70(5):621-35.

197. Calabrese EJ. The road to linearity: why linearity at low doses became the basis for carcinogen risk assessment. *Archives of toxicology* 2009;83(3):203-25.

198. Tao Z, Akiba S, Zha Y, Sun Q, Zou J, Li J*, et al.* Cancer and non-cancer mortality among Inhabitants in the high background radiation area of Yangjiang, China (1979-1998). *Health Phys* 2012;102(2):173-81.

199. Nair RR, Rajan B, Akiba S, Jayalekshmi P, Nair MK, Gangadharan P*, et al.* Background radiation and cancer incidence in Kerala, India-Karanagappally cohort study. *Health Phys* 2009;96(1):55-66.

200. Pochin EE. Problems involved in detecting increased malignancy rates in areas of high natural radiation background. *Health Phys* 1976;31(2):148-51.

201. Land CE. Estimating cancer risks from low doses of ionizing radiation. *Science* 1980;209(4462):1197-203.

202. Hauge IHR, Pedersen K. Stråledose til screena kvinner i Mammografiprogrammet. StrålevernRapport 2005:12. [Radiation doses to screened women in the Norwegian Breast Cancer Screening Program. -In Norwegian]. Østerås, Norway: Norwegian Radiation Protection Authority, 2005. Available from: http://www.nrpa.no/dav/7522f8df5d.pdf, accessed 10.10.2013.

203. Hauge IHR, Bredholt K, Pedersen K. Stråledose til screena kvinner i Mammograf iprogrammet i 2005 og 2006. StrålevernRapport 2007:6. [Radiation doses to screened women in the Norwegian Breast Cancer Screening Program in 2005 and 2006. -In Norwegian]. Østerås: Norwegian Radiation Protection Authority, 2007. Available from: http://www.nrpa.no/dav/7cb07ea3bf.pdf, accessed 10.10.2013.

204. Shore RE, Hildreth N, Woodard E, Dvoretsky P, Hempelmann L, Pasternack B. Breast cancer among women given X-ray therapy for acute postpartum mastitis. *J Natl Cancer Inst* 1986;77(3):689-96.

205. Lindberg S, Karlsson P, Arvidsson B, Holmberg E, Lunberg LM, Wallgren A. Cancer incidence after radiotherapy for skin haemangioma during infancy. *Acta Oncol* 1995;34(6):735-40.

206. Mattsson A, Ruden BI, Hall P, Wilking N, Rutqvist LE. Radiation-induced breast cancer: long-term follow-up of radiation therapy for benign breast disease. *J Natl Cancer Inst* 1993;85(20):1679-85.

207. Thompson DE, Mabuchi K, Ron E, Soda M, Tokunaga M, Ochikubo S*, et al.* Cancer incidence in atomic bomb survivors. Part II: Solid tumors, 1958-1987. *Radiat Res* 1994;137(2 Suppl):S17-67.

208. Boice JD, Jr., Preston D, Davis FG, Monson RR. Frequent chest X-ray fluoroscopy and breast cancer incidence among tuberculosis patients in Massachusetts. *Radiat Res* 1991;125(2):214-22.

209. Howe GR, McLaughlin J. Breast cancer mortality between 1950 and 1987 after exposure to fractionated moderate-dose-rate ionizing radiation in the Canadian fluoroscopy cohort study and a comparison with breast cancer mortality in the atomic bomb survivors study. *Radiat Res* 1996;145(6):694-707.

210. Lundell M, Mattsson A, Karlsson P, Holmberg E, Gustafsson A, Holm LE. Breast cancer risk after radiotherapy in infancy: a pooled analysis of two Swedish cohorts of 17,202 infants. *Radiat Res* 1999;151(5):626-32.

211. Depuydt J, Baert A, Vandersickel V, Thierens H, Vral A. Relative biological effectiveness of mammography X-rays at the level of DNA and chromosomes in lymphocytes. *International journal of radiation biology* 2013;89(7):532-8.

212. Heyes GJ, Mill AJ, Charles MW. Mammography-oncogenecity at low doses. *J Radiol Prot* 2009;29(2A):A123-32.

213. Heyes GJ, Mill AJ. The neoplastic transformation potential of mammography X rays and atomic bomb spectrum radiation. *Radiat Res* 2004;162(2):120-7.

214. Heyes GJ, Mill AJ, Charles MW. Enhanced biological effectiveness of low energy X-rays and implications for the UK breast screening programme. *Br J Radiol* 2006;79(939):195-200.

215. Law J, Faulkner K, Young KC. RBE for mammographic X-ray energies. *Br J Radiol* 2006;79(946):851-2; author reply 2-4.

216. Miller AB, Howe GR, Sherman GJ, Lindsay JP, Yaffe MJ, Dinner PJ*, et al.* Mortality from breast cancer after irradiation during fluoroscopic examinations in patients being treated for tuberculosis. *N Engl J Med* 1989;321(19):1285-9.

217. Menzel HG, Harrison J. Effective dose: a radiation protection quantity. *Ann ICRP* 2012;41(3-4):117-23.

218. Burch A, Law J. A method for estimating compressed breast thickness during mammography. *Br J Radiol* 1995;68(808):394-9.

219. Diffey J, Hufton A, Beeston C, Smith J, Marchant T, Astley S. Quantifying Breast Thickness for Density Measurement. In: Krupinski EA, editor. Digital Mammography, 9th International Workshop, IWDM 2008, July 20-23, 2008, Tucson, AZ, USA: Springer-Verlag; 2008. p. 651-8.

220. Highnam RP, Brady JM, Shepstone BJ. Estimation of compressed breast thickness during mammography. *Br J Radiol* 1998;71(846):646-53.

221. Mawdsley GE, Tyson AH, Peressotti CL, Jong RA, Yaffe MJ. Accurate estimation of compressed breast thickness in mammography. *Med Phys* 2009;36(2):577-86.

222. Tyson AH, Mawdsley GE, Yaffe MJ. Measurement of compressed breast thickness by optical stereoscopic photogrammetry. *Med Phys* 2009;36(2):569-76.

223. Yaffe MJ, Mainprize JG. Risk of radiation-induced breast cancer from mammographic screening. *Radiology* 2011;258(1):98-105.

224. Jansen JT, Veldkamp WJ, Thijssen MA, van Woudenberg S, Zoetelief J. Method for determination of the mean fraction of glandular tissue in individual female breasts using mammography. *Phys Med Biol* 2005;50(24):5953-67.

225. European Communities. Guidance on Diagnostic Reference Levels (DRLs) for Medical Exposures. Luxembourg: Office for Official Publications of the European Communities; 1999.

226. The Institute of Physics and Engineering in Medicine (IPEM). Guidance on the establishment and use of diagnostic reference levels for medical x-ray examinations. IPEM Report No. 88. York: Institute of Physics and Engineering in Medicine; 2004.

227. European Commission. Council Directive 97/43/EURATOM of 30 June 1997 on health protection of individuals against the dangers of ionising radiation in relation to medical exposure. Luxembourg: Official Journal of the European Communities; 1997.

228. ICRP. Radiological Protection and Safety in Medicine. ICRP Publication 73. *Ann ICRP* 1996;26(2).

229. Moores BM. Radiation dose measurement and optimization. *Br J Radiol* 2005;78(933):866-8.

230. Smans K, Bosmans H, Xiao M, Carton AK, Marchal G. Towards a proposition of a diagnostic (dose) reference level for mammographic acquisitions in breast screening measurements in Belgium. *Radiat Prot Dosimetry* 2005;117(1-3):321-6.

231. Michielsen K, Jacobs J, Lemmens K, Nens J, Zoetelief J, Faulkner K*, et al.* Results of a European dose survey for mammography. *Radiat Prot Dosimetry* 2008;129(1-3):199-203.

232. Baldelli P, McCullagh J, Phelan N, Flanagan F. Comprehensive dose survey of breast screening in Ireland. *Radiat Prot Dosimetry* 2011;145(1):52-60.

233. Kulama E, Burch A, Castellano IA, Lawinski CP, Marshall N, Young KC. Commissioning and Routine Testing of Full Field Digital Mammography Systems. Sheffield, UK: National Health Service Cancer Screening Programmes, 2009.

234. Sisini F, Zanca F, Marshall NW, Taibi A, Cardarelli P, Bosmans H. Comparison of signal to noise ratios from spatial and frequency domain formulations of nonprewhitening model observers in digital mammography. *Med Phys* 2012;39(9):5652-63.

235. Thierens H, Bosmans H, Buls N, Bacher K, De Hauwere A, Jacobs J*, et al.* Typetesting of physical characteristics of digital mammography systems: first experiences within the Flemish breast cancer screening programme. *JBR-BTR* 2007;90(3):159-62.

236. Bosmans H, Carton AK, Rogge F, Zanca F, Jacobs J, Van Ongeval C*, et al.* Image quality measurements and metrics in full field digital mammography: an overview. *Radiat Prot Dosimetry* 2005;117(1-3):120-30.

237. Young KC, Alsager A, Oduko JM, Bosmans H, Verbrugge B, Geertse T*, et al.*, editors. Evaluation of software for reading images of the CDMAM test object to assess digital mammography systems. Proc SPIE: Medical Imaging 2008: Physics of Medical Imaging; 2008; San Diego, CA, USA.

238. Karssemeijer N, Thijssen MAO. Determination of contrast-detail curves of mammography systems by automated image analysis. In: Doi K, Nishikawa RG, Schmidt RA, editors. Digital Mammography '96: Proceedings of the 3rd International Workshop on Digital Mammography; 9-12 June; Chicago. Amsterdam: Elsevier Science; 1996. p. 155-60.

239. Veldkamp WJ, Thijssen MA, Karssemeijer N. The value of scatter removal by a grid in full field digital mammography. *Med Phys* 2003;30(7):1712-8.

240. European Reference Organisation for Quality Assured Breast Screening and Diagnostic Services (EUREF), www.euref.org, accessed 10.10.2013.

241. Artinis Medical Systems B.V., http://www.artinis.com/product/cdmam_34, accessed 05.02.2014.

242. Preston DL. Errata. *Radiation Research* 2002;158(5):666.

243. Feig SA, Hendrick RE. Radiation risk from screening mammography of women aged 40-49 years. *J Natl Cancer Inst Monogr* 1997(22):119-24.

244. de Gelder R, Draisma G, Heijnsdijk EA, de Koning HJ. Population-based mammography screening below age 50: balancing radiation-induced vs prevented breast cancer deaths. *Br J Cancer* 2011;104(7):1214-20.

245. Gennaro G, Baldelli P, Taibi A, Di Maggio C, Gambaccini M. Patient dose in full-field digital mammography: an Italian survey. *Eur Radiol* 2004;14(4):645-52.

246. Hemdal B, Herrnsdorf L, Andersson I, Bengtsson G, Heddson B, Olsson M. Average glandular dose in routine mammography screening using a Sectra MicroDose Mammography unit. *Radiat Prot Dosimetry* 2005;114(1-3):436-43.

247. Oduko JM, Young KC, Burch A. A Survey of Patient Doses from Digital Mammography Systems in the UK in 2007 to 2009. In: Martí J, editor. In: Proceedings of the 2010 International Workshop on Digital Mammography; June 16-18; Girona, Spain. Heidelberg: Springer-Verlag Berlin; 2010. p. 365-70.

248. Heddson B, Ronnow K, Olsson M, Miller D. Digital versus screen-film mammography: a retrospective comparison in a population-based screening program. *Eur J Radiol* 2007;64(3):419-25.

249. Kruger RL, Schueler BA. A survey of clinical factors and patient dose in mammography. *Med Phys* 2001;28(7):1449-54.

250. ICRP. Managing patient dose in digital radiology. ICRP Publication 93. *Ann ICRP* 2004;34(1).

251. Reis C, Pascoal A, Sakellaris T, Koutalonis M. Quality assurance and quality control in mammography: a review of available guidance worldwide. *Insights into imaging* 2013;4(5):539-53.

252. Meeson S, Young KC, Hollaway PB, Wallis MG. Procedure for quantitatively assessing automatic exposure control in mammography: a study of the GE Senographe 600 TS. *Br J Radiol* 2001;74(883):615-20.

253. Rothenberg LN, Kirch RL, Snyder RE. Patient exposures from film and xeroradiographic mammographic techniques. *Radiology* 1975;117(3 Pt 1):701-3.

254. van Engeland S, Snoeren PR, Huisman H, Boetes C, Karssemeijer N. Volumetric breast density estimation from full-field digital mammograms. *IEEE Trans Med Imaging* 2006;25(3):273-82.

255. Jeffreys M, Warren R, Highnam R, Smith GD. Initial experiences of using an automated volumetric measure of breast density: the standard mammogram form. *Br J Radiol* 2006;79(941):378-82.

256. Highnam R, Jeffreys M, McCormack V, Warren R, Davey Smith G, Brady M. Comparing measurements of breast density. *Phys Med Biol* 2007;52(19):5881-95.

257. Kaufhold J, Thomas JA, Eberhard JW, Galbo CE, Trotter DE. A calibration approach to glandular tissue composition estimation in digital mammography. *Med Phys* 2002;29(8):1867-80.

258. Heine JJ, Cao K, Thomas JA. Effective radiation attenuation calibration for breast density: compression thickness influences and correction. *Biomed Eng Online* 2010;9:73.

259. Kallenberg MG, van Gils CH, Lokate M, den Heeten GJ, Karssemeijer N. Effect of compression paddle tilt correction on volumetric breast density estimation. *Phys Med Biol* 2012;57(16):5155-68.

260. Hemdal B. Forward-scattered radiation from the compression paddle should be considered in glandular dose estimations. *Radiat Prot Dosimetry* 2011;147(1-2):196-201.

261. Gregory KJ, Pattison JE, Bibbo G. Uncertainties of exposure-related quantities in mammographic x-ray unit quality control. *Med Phys* 2006;33(3):687-98.

262. Bahreyni Toossi MT, Zare H, Bayani Roodi S, Hashemi M, Akbari F, Malekzadeh M. Towards Proposition of a Diagnostic Reference Level for Mammographic Examination in the Greater Khorasan Province, Iran. *Radiat Prot Dosimetry* 2012.

263. Young KC, Burch A, Oduko JM. Radiation doses received in the UK Breast Screening Programme in 2001 and 2002. *Br J Radiol* 2005;78(927):207-18.

264. Ghetti C, Borrini A, Ortenzia O, Rossi R, Ordonez PL. Physical characteristics of GE Senographe Essential and DS digital mammography detectors. *Med Phys* 2008;35(2):456-63.

265. Zdesar U. Reference levels for image quality in mammography. *Radiat Prot Dosimetry* 2008;129(1-3):170-2.

266. Young KC, Oduko JM. Long-Term Stability of Image Quality Measurements for Two Digital Mammography Systems. In: Maidment AD, Bakic PR, Gavenonis S, editors. International Workshop on Breast Imaging (IWDM); Philadelphia, PA, USA. Berlin Heidelberg: Springer-Verlag 2012.

267. Wall BF, Haylock R, Jansen JTM, Hillier MC, Hart D, Shrimpton PC. HPA-CRCE-028 - Radiation Risks from Medical X-ray Examinations as a Function of the Age and Sex of the Patient. Public Health England, 2011.

268. Weiss HA, Darby SC, Doll R. Cancer mortality following X-ray treatment for ankylosing spondylitis. *Int J Cancer* 1994;59(3):327-38.

269. Trabalka JR, Kocher DC. Energy dependence of dose and dose-rate effectiveness factor for low-let radiations: potential importance to estimation of cancer risks and relationship to biological effectiveness. *Health Phys* 2007;93(1):17-27.

270. Wakeford R, Tawn EJ. The meaning of low dose and low dose-rate. *J Radiol Prot* 2010;30(1):1-3.

271. United Nations. Summary of Low-dose Radiation Effects on Health. United Nations Scientific Committee on the Effects of Atomic Radiation, 2010 Report to the General Assembly. New York: United Nations: 2011.

272. Loucas BD, Cornforth MN. Complex chromosome exchanges induced by gamma rays in human lymphocytes: an mFISH study. *Radiat Res* 2001;155(5):660-71.

273. Mathews JD, Forsythe AV, Brady Z, Butler MW, Goergen SK, Byrnes GB*, et al.* Cancer risk in 680 000 people exposed to computed tomography scans in childhood or adolescence: data linkage study of 11 million Australians. *BMJ* 2013;346:f2360.

274. Duport P, Jiang H, Shilnikova NS, Krewski D, Zielinski JM. Database of radiogenic cancer in experimental animals exposed to low doses of ionizing radiation. *Journal of toxicology and environmental health Part B, Critical reviews* 2012;15(3):186-209.

275. Averbeck D. Does scientific evidence support a change from the LNT model for low-dose radiation risk extrapolation? *Health Phys* 2009;97(5):493-504.

276. Colin C, Devic C, Noel A, Rabilloud M, Zabot MT, Pinet-Isaac S*, et al.* DNA double-strand breaks induced by mammographic screening procedures in human mammary epithelial cells. *International journal of radiation biology* 2011;87(11):1103-12.

277. Collis SJ, Schwaninger JM, Ntambi AJ, Keller TW, Nelson WG, Dillehay LE*, et al.* Evasion of early cellular response mechanisms following low level radiation-induced DNA damage. *J Biol Chem* 2004;279(48):49624-32.

278. Beyreuther E, Dorr W, Lehnert A, Lessmann E, Pawelke J. FISH-based analysis of 10- and 25-kV soft X-ray-induced DNA damage in 184A1 human mammary epithelial cells. *Radiat Environ Biophys* 2012;51(1):33-42.

279. Aleta CR. Regulatory implications of a linear non-threshold (LNT) dose-based risks. *Applied radiation and isotopes : including data, instrumentation and methods for use in agriculture, industry and medicine* 2009;67(7-8):1290-8.

280. Mossman KL. The LNT Debate in Radiation Protection: Science vs. Policy. *Dose-response : a publication of International Hormesis Society* 2012;10(2):190-202.

281. Albanes D, Weinberg GB, Boss L, Taylor PR. A survey of physicians' breast cancer early detection practices. *Prev Med* 1988;17(5):643-52.

282. ICRP. Low-dose Extrapolation of Radiation-related Cancer Risk. ICRP Publication 99. *Ann ICRP* 2005;35(4).

283. Law J, Faulkner K, Young KC. Risk factors for induction of breast cancer by X-rays and their implications for breast screening. *Br J Radiol* 2007;80(952):261-6.

284. Yoo KB, Kwon JA, Cho E, Kang MH, Nam JM, Choi KS*, et al.* Is mammography for breast cancer screening cost-effective in both Western and asian countries?: results of a systematic review. *Asian Pac J Cancer Prev* 2013;14(7):4141-9.

285. Wang H, Karesen R, Hervik A, Thoresen SO. Mammography screening in Norway: results from the first screening round in four counties and cost-effectiveness of a modeled nationwide screening. *Cancer Causes Control* 2001;12(1):39-45.

286. Hofvind S, Ponti A, Patnick J, Ascunce N, Njor S, Broeders M*, et al.* False-positive results in mammographic screening for breast cancer in Europe: a literature review and survey of service screening programmes. *J Med Screen* 2012;19 Suppl 1:57-66.

287. Hofvind S, Geller B, Vacek PM, Thoresen S, Skaane P. Using the European guidelines to evaluate the Norwegian Breast Cancer Screening Program. *European Journal of Epidemiology* 2007;22(7):447-55.

288. Puliti D, Duffy SW, Miccinesi G, de Koning H, Lynge E, Zappa M*, et al.* Overdiagnosis in mammographic screening for breast cancer in Europe: a literature review. *J Med Screen* 2012;19(Suppl.):42-56.

9 Papers I-V

I

II

III

IV

The risk of radiation-induced breast cancers due to biennial mammographic screening in women aged 50-69 years is minimal

Ingrid Helen Ryste Hauge (corresponding author) (MSc) [1, 2, 3], Kristin Pedersen (MSc) [2], Hilde Merete Olerud (PhD) [2, 3], Eli Olaug Hole (Professor, PhD) [3], Solveig Hofvind (Professor, PhD) [1, 4]

E-mail: ingrid.helen.ryste.hauge@nrpa.no

[1]Oslo and Akershus University College of Applied Sciences, Faculty of Health Sciences, Department of Radiography and Dental Technology, P. O. Box 4 St. Olavs plass, NO-0130 Oslo, Norway

[2]Norwegian Radiation Protection Authority, P. O. Box 55, NO-1332 Østerås, Norway

[3]Department of Physics, University of Oslo, P.O. Box 1048 Blindern, NO-0316 Oslo, Norway

[4]Cancer Registry of Norway, P.O. box 5313 Majorstuen, NO-0304 Oslo, Norway

Correspondence to

Ingrid Helen Ryste Hauge
Mailing address:
Norwegian Radiation Protection Authority
P. O. Box 55
NO-1332 Østerås
Norway
Telephone: +47 67 16 25 58

Abstract

Background: The main aim of mammographic screening is to reduce the mortality from breast cancer. However, use of ionizing radiation is considered a potential harm due to the possible risk of inducing cancer in healthy women.

Purpose: To estimate the potential number of radiation-induced breast cancers, radiation-induced breast cancer deaths, and lives saved due to implementation of organized mammographic screening as performed in Norway.

Material and Methods: We used a previously published excess absolute risk model which assumes a linear no-threshold dose-response. The estimates were calculated for 100 000 women aged 50-69 years, a screening interval of two years, and with an assumed follow-up until age 85 or 105 years. Radiation doses of 0.7, 2.5, and 5.7 mGy per screening examination, a latency time of 5 or 10 years, and a dose and dose-rate effectiveness factor (DDREF) of 1 or 2 were applied.

Results: The total lifetime risk of radiation-induced breast cancers per 100 000 women was 10 (95% CI: 4-25) if the women were followed from age 50 to 85, for a dose of 2.5 mGy, a latency time of 10 years, and a DDREF of 1. For the same parameter values the number of radiation-induced breast cancer death was 1 (95% CI: 0-2). The assumed number of lives saved is approximately 350.

Conclusion: The risk of radiation-induced breast cancer and breast cancer death due to mammographic screening is minimal. Women should not be discouraged from attending screening due to fear of radiation-induced breast cancer death.

Keywords

Breast, Mammography, Screening, Adults, Radiation Safety, Radiation Effect

Introduction

Mammographic screening is proved to reduce mortality from breast cancer (1). However, it is still debated whether the benefits outweigh the harms. Use of ionizing radiation is considered a potential harm due to the possible risk of inducing cancer in healthy women (2-4).

It is generally agreed that ionizing radiation at high doses (>100 milligray (mGy)) and high dose-rate (>0.1 mGy/min) has the potential to induce cancer (5, 6). Mammography is considered a low dose and high dose-rate examination (7). Radiation risk at low doses is commonly extrapolated from the risk at high doses (8). Extrapolation from high to low doses can be performed by a linear extrapolation (linear no-threshold (LNT) model), with a downward or upward curving line/pointing curve, with a threshold linear model, or with a hormetic model (8, 9). In 2002 Preston et al. analyzed data from eight cohorts of irradiated women (3, 10). The radiation doses included in the analysis ranged from 0.2 to 5.8 Gy delivered both at low and high dose-rates. For both the region where Preston et al. had data, and for the low dose region where data was missing, they stated that their analysis did not provide evidence against a linear dose-response model. Their excess absolute risk (EAR) model has subsequently been widely used to estimate the risk of radiation-induced breast cancer due to mammography and mammographic screening (2, 4, 11).

In 2011 Yaffe and Mainprize described a model for estimating the risk of radiation-induced breast cancers, breast cancer deaths, the number of lives lost, and lives saved for a variety of mammography screening scenarios (2). However, biennial screening for the age group 50-69 years, as recommended by the European guidelines for breast cancer screening and diagnosis, was not included in their estimates.

The Norwegian Breast Cancer Screening Program (NBCSP) is a population based screening program offering women aged 50-69 years two-view mammography every two year (12). The program started as a pilot in four counties in 1996 and became nationwide in 2005. It is run according to the European guidelines. We wanted to apply the model developed by Yaffe and Mainprize on data collected as a part of the quality assurance of the NBCSP to estimate the potential number of radiation-induced breast cancers, radiation-induced breast cancer deaths, and lives saved due to implementation of the NBCSP.

Materials and method

Dose data collected in the NBCSP was used in the study (13). The program started in four counties in 1996 and became nationwide in 2005. The NBCSP offers women aged 50-69 biennial mammography screening. No ethical committee approval was necessary since we used aggregate data without linkage to the individual women.

We adopted the model of Yaffe and Mainprize (2) and estimated the expected number of radiation-induced incidences, radiation-induced deaths, and number of lives saved per 100 000 women in a scenario where the women started to undergo mammographic screening at age 50 years and received a total of ten screening examinations at two-year intervals. The women were followed for radiation-induced breast cancer and breast cancer death until age 85 and 105 years, which are the expected average age and maximum age of death for women in Norway in 2011, respectively (14)..

The parameters a) radiation dose per examination, b) the latency period for developing breast cancer, and c) dose and dose-rate effectiveness factor (DDREF) were input values in the model (2). Three different dose values were chosen for estimation of lifetime risks; 0.7, 2.5, and 5.7 mGy. The specific values were chosen as a result of a previous study from the NBCSP where an average mean glandular dose (MGD) for full-field digital mammography was found to be 2.5 mGy (range: 0.7 - 5.7 mGy) per screening examination (13). Latency times of 5 and 10 years were applied (5).

The DDREF is applied to correct for possible reduction in risk of radiation-induced cancers at low dose or low dose-rate compared to high dose and high dose-rate exposure (15). A value equal to 1 implies no correction, while a value larger than 1 implies a lower risk. The National Academy of Sciences (NAS) Biological Effects of Ionizing Radiation (BEIR) report, NAS

BEIR VII, recommends a value of 1.5 (15), while the International Committee on Radiation Protection (ICRP) considers a value of 2 to be appropriate (9). In the present study, a DDREF of 1 and 2 were applied.

Number of radiation-induced breast cancer cases

The number of radiation-induced breast cancers, $N_C(A)$, was estimated as (2):

$$N_C(A) = M(A_B, A) \sum_{A_X=A_B}^{A_E} EAR(A_X, A, D)$$

$M(A_B, A)$ is a life-table correction which provides the probability that a woman alive at age A_B, the age at which screening starts, is still alive at age A_x, the age at which the woman is exposed to radiation (here: 50-69 years), is able to participate in the screening program, and is alive at age A, the age at which the radiation-induced breast cancer develops (16). The life-table correction for women is used to account for deaths (*D*) due to other causes than radiation-induced breast cancer.

The excess absolute risk (EAR) per year of developing a radiation-induced breast cancer per 10 000 woman years (WY) per radiation dose (Gy) for women at age A (50 years and older) was estimated as (3, 10):

$$\frac{EAR}{10\,000 WY\ Gy} = 10e^{-0.05(A_x-25)}(\frac{A}{50})$$

The maximum value for *A* was either 85 or 105 years. The total lifetime risk was estimated for women aged 50-69 years who attended biennial screening, i.e. ten examinations, by summing the values for each of the A_x values in the stated range.

Number of radiation-induced breast cancer deaths

The number of deaths from radiation-induced breast cancer, $N_D(A_D)$, at age of death A_D, was estimated as (2):

$$N_D(A_D) = \sum_{A=A_B+L}^{A_D} N_C(A)M(A,A_D)[S(A,\Delta-1)][S(A,\Delta-1)-S(A,\Delta)]$$

$N_C(A)$ is the number of radiation-induced breast cancers. $M(A,A_D)$ is a life-table correction, which provides the probability that a woman alive at age A is alive until age A_D. $S(A,\Delta)$ is the probability of surviving a number of years, Δ, after detection of breast cancer at age A, where Δ=(A_D- A). $S(A,\Delta-1)$ is the probability that a woman will survive until A_D minus one year after the cancer is detected, but not to age A_D (2). For S, adjusted survival-rates for women screened in the NBCSP from 1996 to 2009, provided by the Cancer Registry of Norway, were used. $N_C(A)$ and $N_D(A_D)$ are estimated with 95% confidence intervals as described by Yaffe and Mainprize (2).

Number of lives saved

The expected number of breast cancer deaths without screening is estimated from the breast cancer incidence (Table 1) by making a life-table correction and summing the numbers that arise each year (16). The life-table correction takes into account the number of expected deaths. The estimation was conducted with cut offs at 85 and 105 years. The estimation of the breast cancer mortality without screening is conducted in the same manner as the estimation of radiation-induced breast cancer deaths, except that a survival curve for an unscreened population is applied.

The number of lives saved is estimated as the difference between the expected number of breast cancer deaths with ($N_{D,with}$) and without ($N_{D,without}$) screening (2). The expected number of breast cancer deaths with screening is estimated as the expected number without screening, multiplied with the expected mortality reduction, M_{red}, due to screening. We applied a mortality reduction of 43% as reported recently from the NBCSP (17). The number of lives saved is expressed as:

$$Number\ of\ lives\ saved = N_{D,without} - N_{D,with} = N_{D,without} - \left(N_{D,without} \times M_{red}\right)$$

Results

Lifetime risk of radiation-induced breast cancer for the various combinations of the input parameters (dose, latency time, and DDREF) used in the model has been estimated (Table 2). The estimates are based on biennial mammographic screening in women aged 50-69 years if followed until age 85 or 105 years. The lifetime risk of radiation-induced breast cancers per 100 000 women was 10 (95% CI: 4 - 25) when a radiation dose of 2.5 mGy, a latency time of 10 years, and a DDREF of 1 were used (Table 2). If followed until 105 years, the risk is 13 (95% CI: 5 - 34).

For the same parameter values, the lifetime risk for radiation-induced breast cancer deaths per 100 000 women was estimated to be 0.8 and 1.0 (range: 0.3-2.7) if followed until age 85 and 105 years, respectively.

The expected number of breast cancer deaths without screening, is found by applying the breast cancer incidence from 2010 (in other words while the NBCSP was running). A 43% reduction in breast cancer mortality is applied, as found as an effect of attending the NBCSP (17). Lives saved are found to be 395 and 415 if women aged 50 years are followed until age 85 and 105 years, respectively. Using the breast cancer incidence from 1995 (before the NBCSP started) resulted in 339 and 362 lives saved with a cut-off at 85 and 105 years, respectively.

Discussion

Depending on the parameter values (radiation dose, latency time, DDREF), we estimated between 1 and 30 breast cancers to be induced by ionizing radiation if 100 000 women aged 50-69 years were screened biennially ten times for breast cancer and if they were followed until age 85 years. The number of radiation-induced breast cancer deaths was estimated to range from zero to 3 for the same parameter values and same cohort of women. In accordance with the Health Protection Agency in the United Kingdom risk of this order of size is considered to be minimal (18).

In 1995, before the NBCSP started, 1548 breast cancers were detected among the 703 122 women aged 50-85 years residing in Norway, i.e. a breast cancer-rate of 220 per 100 000. If we assume an incidence rate of 220/100 000 during a time-span of 36 years (from age 50 to 85 years) we will have 7920 breast cancer cases (220 × 36) among 100 000 women. The number of radiation-induced breast cancers in our calculations for the same time-span was 0.13% (10/7920) of the estimated breast cancer cases diagnosed for this group of women in the described scenario. The percentage of radiation-induced breast cancer deaths is even smaller.

Yaffe and Mainprize estimated 86 radiation-induced breast cancers and 11 breast cancer deaths in women aged 40-74 years, while de Gelder et al. estimated 8 breast cancers and 2 breast cancer deaths in women aged 50-74 years (2, 4). We applied a similar model as Yaffe and Mainprize and de Gelder et al., but the outcome in our study differed from their estimates. These discrepancies were expected due to different screening intervals, age groups, and parameter values used in the estimations.

However, these estimates have several limitations and only represent a rough estimate. The expected number of breast cancer cases is probably underestimated, which will result in an overestimation of the percentage of radiation-induced breast cancer cases and deaths.

In addition, the LNT hypothesis assumes linearity of the dose-response relationship for cancer induction in general, even at low doses (19). This implies that even a small dose of radiation is assumed to represent an increased risk of cancer in humans (15, 20). Because the dose-response curve could not be determined at low dose level, the LNT model was originally used to provide an upper limit of risk, with zero as the smallest risk value for low dose levels (21). The LNT model has several limitations and its validity is debated (2, 3, 20, 22-25). A protective effect at low doses, hormesis, is even suggested (22, 25). Significant fluctuations are shown in the estimated risk of induced cancers in studies with low ionizing radiation doses (20, 26-28). Studies are not conclusive in how cells respond to ionizing radiation, but it is known that the cellular responses to low doses differ from those that to high doses (20, 29, 30). In practice it is impossible to draw conclusions regarding the shape of the curve describing the dose-risk relationship with the knowledge available today.

The LNT model is considered to be the "best practical approach to managing risk" from a radiation protection point of view, despite of its known limitations (8, 9, 29). The "better safe than sorry" approach is debated (26, 31, 32), but scientific committees like the ICRP maintain that it is better to err on the side of caution (9). This approach is also supported in a report by BEIR VII (15). On the other hand, the French National Academies of Science and Medicine concluded that the LNT model lacks justification for doses from 0.2 to 5 Gy (33).

The EAR model used in this study has an inherent uncertainty of about 40% (3). The model was based on a pooled analysis of eight cohorts. Only one of the cohorts showed significantly increased risk of breast cancer for doses lower than 0.02 Gy. In addition, the mean age for the

study population was 27 years (range 13 – 44 years), which is substantially lower than the screening population in Norway. Sensitivity to ionizing radiation is known to decrease with age (15, 18, 34). The latter factor make us expect an overestimation rather than an underestimation of the number of radiation-induced breast cancers and breast cancer deaths in our study (32, 34).

In conclusion, using the LNT-model resulted in 30 or less radiation-induced breast cancers if 100 000 women aged 50-69 years were screened biennially ten times and if they were followed for breast cancer until age 85 years. The estimated number of radiation-induced breast cancer deaths was 3 or less, compared to the assumed number of lives saved of approximately 350. It should thus be safe to conclude that the risk of radiation-induced breast cancer and breast cancer death as a result of organized screening is considered minimal when applying a screening program according to the European guidelines.

Table 1: Numbers and crude rates of breast cancer cases in Norway, 1995 and 2010 by age (35, 36).

Age (years)	Breast cancer cases			
	1995		2010	
	n	Rate per 100 000 women	n	Rate per 100 000 women
50-59	359	160.8	683	224.3
60-69	419	224.7	770	296.7
50-69	778	189.9	1 453	257.6

Table 2: Estimated lifetime risk of radiation-induced breast cancer cases and deaths for a latency time of 5 and 10 years, different dose levels (0.7, 2.5, and 5.7 mGy) and a dose and dose-rate effectiveness factor (DDREF) of 1 (no correction) and 2, and a lifetime risk until age 85 and 105 years.

Latency time (years)	Dose (mGy)	DDREF	50-85 years[1]		50-105 years[2]	
			No. of radiation-induced breast cancers per 100 000[1,3] (95% confidence interval)	No. of radiation-induced breast cancer deaths per 100 000[1,3] (95% confidence interval)	No. of radiation-induced breast cancers per 100 000 [2,3] (95% confidence interval)	No. of radiation-induced breast cancer deaths per 100 000[2,3] (95% confidence interval)
10	2.5 (mean)	1	10.2 (4.1-25.2)	0.8 (0.3-2.1)	13.0 (5.0-34.3)	1.0 (0.4-2.7)
		2	5.1 (2.1-12.6)	0.4 (0.2-1.0)	6.5 (2.5-17.1)	0.5 (0.2-1.3)
	0.7 (lowest)	1	2.8 (1.2-7.0)	0.2 (0.1-0.6)	3.6 (1.4-9.6)	0.3 (0.1-0.8)
		2	1.4 (0.6-3.5)	0.1 (0.0-0.3)	1.8 (0.7-4.8)	0.1 (0.1-0.4)
	5.7 (highest)	1	23.2 (9.5-57.4)	1.9 (0.7-4.7)	29.7 (11.5-78.1)	2.3 (0.9-6.1)
		2	11.6 (4.7-28.7)	0.9 (0.4-2.4)	14.8 (5.7-39.1)	1.2 (0.4-3.1)
5	2.5	1	13.0 (5.5-30.7)	1.1 (0.3-1.5)	15.8 (6.4-39.7)	1.4 (0.5-2.7)
		2	6.5 (2.8-15.4)	0.6 (0.2-0.8)	7.9 (3.2-19.9)	0.7 (0.2-1.3)
	0.7	1	3.6 (1.6-8.6)	0.3 (0.1-0.4)	4.4 (1.8-11.1)	0.4 (0.1-0.7)
		2	1.8 (0.8-4.3)	0.2 (0.0-0.2)	2.2 (0.9-5.6)	0.2 (0.1-0.4)
	5.7	1	29.5 (12.6-70.1)	2.6 (0.7-3.5)	36.0 (14.7-90.6)	3.1 (1.1-6.3)
		2	14.8 (6.3-35.0)	1.3 (0.4-1.7)	18.0 (7.3-45.3)	1.5 (0.6-3.2)

[1]: Lifetime: average age at which radiation-induced cancer occurs is 85 years.

[2]: Lifetime: average age at which radiation-induced cancer occurs is 105 years.

[3]: The estimated values are based on a model valid for the dose range 0.02-50 Gy, and an LNT model is assumed for the low doses.

References

1. Independent UK Panel on Breast Cancer Screening. The benefits and harms of breast cancer screening: an independent review. Lancet 2012;**380**:1778-86.
2. Yaffe MJ, Mainprize JG. Risk of radiation-induced breast cancer from mammographic screening. Radiology 2011;**258**:98-105.
3. Preston DL, Mattsson A, Holmberg E*, et al.* Radiation effects on breast cancer risk: a pooled analysis of eight cohorts. Radiat Res 2002;**158**:220-35.
4. de Gelder R, Draisma G, Heijnsdijk EA*, et al.* Population-based mammography screening below age 50: balancing radiation-induced vs prevented breast cancer deaths. Br J Cancer 2011;**104**:1214-20.
5. United Nations Scientific Committee on the Effects of Atomic Radiation (UNSCEAR). Volume I: Report to the General Assembly. Scientific Annex A. Epidemiological studies of radiation and cancer. New York: United Nations: 2006. Available from: http://www.unscear.org/docs/reports/2006/07-82087_Report_Annex_A_2006_Web_corr.pdf, accessed 11.10.2013.
6. United Nations Scientific Committee on the Effects of Atomic Radiation (UNSCEAR). Biological mechanisms of radiation actions at low doses. UNSCEAR website (www.unscear.org): United Nations; 2012. Available from: http://www.unscear.org/docs/reports/Biological_mechanisms_WP_12-57831.pdf, accessed 11.10.2013.
7. Heyes GJ, Mill AJ, Charles MW. Mammography-oncogenecity at low doses. J Radiol Prot 2009;**29**:A123-32.
8. Brenner DJ, Doll R, Goodhead DT*, et al.* Cancer risks attributable to low doses of ionizing radiation: assessing what we really know. Proc Natl Acad Sci U S A 2003;**100**:13761-6.
9. ICRP. The 2007 Recommendations of the International Commission on Radiological Protection. ICRP Publication 103. Ann ICRP 2007;**37**.
10. Preston DL. Errata. Radiation Research 2002;**158**:666.

11. Feig SA, Hendrick RE. Radiation risk from screening mammography of women aged 40-49 years. J Natl Cancer Inst Monogr 1997:119-24.

12. Hofvind S, Geller B, Vacek PM, *et al.* Using the European guidelines to evaluate the Norwegian Breast Cancer Screening Program. European Journal of Epidemiology 2007;**22**:447-55.

13. Hauge IH, Pedersen K, Sanderud A, *et al.* Patient doses from screen-film and full-field digital mammography in a population-based screening programme. Radiat Prot Dosimetry 2012;**148**:65-73.

14. Statistics Norway. Statistisk årbok 2013. 2013. Available from: http://www.ssb.no/befolkning/artikler-og-publikasjoner/_attachment/140702?_ts=1415a7ca078, accessed 11.10.2013.

15. National Academy of Sciences. Health risks from exposure to low levels of ionizing radiation : BEIR VII, Phase 2. Washington, D.C.: National Academies Press; 2006. Available from: http://www.nap.edu/openbook.php?isbn=030909156X, accessed 11.10.2013.

16. Statistics Norway. Dødelighetstabeller 2011. Available from: http://www.ssb.no/a/kortnavn/dode/tab-2012-04-19-05.html, accessed 11.10.2013.

17. Hofvind S, Ursin G, Tretli S, *et al.* Breast cancer mortality in participants of the Norwegian Breast Cancer Screening Program. Cancer 2013;**119**:3106-12.

18. Wall BF, Haylock R, Jansen JTM, *et al.* HPA-CRCE-028 - Radiation Risks from Medical X-ray Examinations as a Function of the Age and Sex of the Patient. Public Health England, 2011.

19. ICRP. Low-dose Extrapolation of Radiation-related Cancer Risk. ICRP Publication 99. Ann ICRP 2005;**35**.

20. Dauer LT, Brooks AL, Hoel DG, *et al.* Review and evaluation of updated research on the health effects associated with low-dose ionising radiation. Radiat Prot Dosimetry 2010;**140**:103-36.

21. Kathren RL. Pathway to a paradigm: the linear nonthreshold dose-response model in historical context. The American Academy of Health Physics 1995 Radiology Centennial Hartman Oration. Health Phys 1996;**70**:621-35.

22. Scott BR. Low-dose radiation risk extrapolation fallacy associated with the linear-no-threshold model. Human & experimental toxicology 2008;**27**:163-8.

23. Tubiana M, Feinendegen LE, Yang C*, et al.* The linear no-threshold relationship is inconsistent with radiation biologic and experimental data. Radiology 2009;**251**:13-22.

24. Brenner DJ, Sawant SG, Hande MP*, et al.* Routine screening mammography: how important is the radiation-risk side of the benefit-risk equation? International journal of radiation biology 2002;**78**:1065-7.

25. Scott BR. It's time for a new low-dose-radiation risk assessment paradigm--one that acknowledges hormesis. Dose-response : a publication of International Hormesis Society 2008;**6**:333-51.

26. Wakeford R. Cancer risk modelling and radiological protection. J Radiol Prot 2012;**32**:N89-93.

27. Shore RE. Low-dose radiation epidemiology studies: status and issues. Health Phys 2009;**97**:481-6.

28. Preston DL, Shimizu Y, Pierce DA*, et al.* Studies of mortality of atomic bomb survivors. Report 13: Solid cancer and noncancer disease mortality: 1950-1997. Radiat Res 2003;**160**:381-407.

29. Averbeck D. Does scientific evidence support a change from the LNT model for low-dose radiation risk extrapolation? Health Phys 2009;**97**:493-504.

30. Heyes GJ, Mill AJ, Charles MW. Enhanced biological effectiveness of low energy X-rays and implications for the UK breast screening programme. Br J Radiol 2006;**79**:195-200.

31. Tubiana M. Dose-effect relationship and estimation of the carcinogenic effects of low doses of ionizing radiation: the joint report of the Academie des Sciences (Paris) and of the Academie Nationale de Medecine. Int J Radiat Oncol Biol Phys 2005;**63**:317-9.

32. Hendee WR, O'Connor MK. Radiation risks of medical imaging: separating fact from fantasy. Radiology 2012;**264**:312-21.

33. Aurengo A, Averbeck D, Bonnin A*, et al.* Dose-effect relationships and estimation of the carcinogenic effects of low doses of ionizing radiation. Paris: Medicine Academy of Sciences-National Academy of Medicine; 2005.

34. Mathews JD, Forsythe AV, Brady Z*, et al.* Cancer risk in 680 000 people exposed to computed tomography scans in childhood or adolescence: data linkage study of 11 million Australians. BMJ 2013;**346**:f2360.

35. Engholm G, Ferlay J, Christensen N*, et al.* NORDCAN--a Nordic tool for cancer information, planning, quality control and research. Acta Oncol 2010;**49**:725-36.

36. Engholm G, Ferlay J, Christensen N*, et al.* NORDCAN: Cancer Incidence, Mortality, Prevalence and Survival in the Nordic Countries, Version 5.3 (25.04.2013). Association of the Nordic Cancer Registries. Danish Cancer Society Available from: http://www.ancr.nu, accessed on 11.10.2013.